UNIVERSITÉ LIBRE DE BRUXELLES

BRUFACE BRUSSELS FACULTY OF ENGINEERING

VRIJE UNIVERSITEIT BRUSSEL

Graduation thesis submitted in partial fulfilment of the requirements for the degree of engineering sciences: Architectural Engineering

Computational Study of the Feasibility of Baubotanical Structures

Pierre-Marie Bernard Guillemot

Master thesis submitted under the supervision of
Prof. Peter Z. Berke

Academic year
2023-2024

In order to be awarded the Master's programme in
Architectural Engineering

Abstract

This master's thesis investigates the feasibility of using living plants as load-bearing structures through computational simulation using the finite element method. The main objective is to assess whether Baubotanical structures can withstand loads for serviceability purposes and to develop a methodology for designing with living plants. Foundational data on plant biomechanics and growth evolution were initially gathered to build simplified growth and structural parametric models focused on three plant species: Phyllostachis edulis, Salix alba L., and Hedera helix L. These models were subsequently applied in distinct projects for each plant. The analysis of differences among the plants and their applications led to the conclusion that constructing with living plants is feasible from a structural strength and stiffness perspective. However, compared to traditional construction methods, these structures require a longer implementation period, have a shorter service life, and demand extensive maintenance. Despite these challenges, their contribution to sustainability — particularly their capacity to absorb CO2 from the atmosphere, although modest — justifies further research in this area.

Keywords:
Living architecture - Baubotanik
Plant biomechanics
Plant growth
Finite Element Method
Parametric design

Acknowledgements

First, I would like to express my sincere gratitude to my promotor, Prof. Peter Z. Berke. The support, guidance and insightful feedback I received through the year have truly helped me complete this master's thesis. Also I am deeply grateful to my professor for accepting the topic I proposed, despite it's not being his area of expertise.
I extend my gratitude to Prof. Pierre J. Meerts for his support and generosity in dedicating his time and expertise towards enriching this research endeavor.
Finally, I would like to express my gratitude to my family and friends that much needed support throughout my studies.

Contents

Chapter 1

Introduction

Planet Earth formed around 4.5 billion years ago, the first hominids appeared between 6 and 7 million years ago, and Homo sapiens, our species, emerged a mere 200000 years ago. Thus, our existence is insignificant compared to that of our planet, yet our impact extends to every corner of the world. While Earth will continue on its course regardless, we may not be so immune. Climate change serves as a stark warning; the results of our actions could spell disaster for our species.

With a global warming of 1.1°C compared to the pre-industrial averages, we are already witnessing the changes around the world. The past year saw record-shattering global temperatures [1]. People around the world have experienced extreme heat events, agricultural and ecological droughts, fire-prone weather conditions, sea level rise, ocean acidification, heavy precipitation events, flooding, and various other phenomena. These phenomena have the potential to cause a severe loss of biodiversity and make the Earth a more inhospitable place for humans. It is estimated by the UN environment program (UNEP), that the current commitments under the Paris Agreement would results in a temperature increase of 2.5-2.9°C above pre-industrial levels by the end of the century [2]. According to the IPCC [3], "between half to three-quarters of the human population could be exposed to periods of life threatening climatic conditions arising from coupled impacts of extreme heat and humidity by 2100".

Cities can sustain livability as long as global warming is limited to 1.5°C [1]. To achieve this, global greenhouse gas (GHG) emissions need to be halved by 2030 and reach net zero emissions by the middle of the century [4]. This collective effort necessitates the involvement of all sectors and individuals.

The construction industry currently stands as one of the primary consumers of energy and raw materials globally. It has been estimated in 2016 to contribute to 32% of global energy consumption, 25% of CO2 emissions, 12% of water usage, 40% of mass-produced waste, and 40% of materials employed [5]. In 2023 the UNEP estimated the construction sectors to represent 37% of greenhouse gas emissions [6].

The construction sector has taken steps forward by integrating bioclimatic designs, optimizing material usage, exploring new biomaterials... But there is still much to be done to achieve the set objectives. An alternative approach to traditional design with inert materials like steel, concrete,

or wood is to incorporate living plants as building structures. In contrast to traditional structures, a living structure would function as a carbon sink by absorbing CO_2 from the atmosphere through photosynthesis, thereby resulting in a positive carbon footprint.

$$6\,CO_2 + 6\,H_2O + \text{sun} \xrightarrow{\text{photosyn.}} C_6H_{12}O_6 + 6\,O_2 \tag{1.1}$$

The use of trees or plants in construction provides numerous benefits, including enhancing air quality in cities where pollution levels are high due to dense human activities. Trees play a crucial role in mitigating the urban heat island effect by providing shade and cooling the surrounding air through evapotranspiration. Additionally, trees help reduce the risk of flooding in cities by capturing rainfall with their leaves. It is estimated that urban trees can retain an average of 18.3% of rainfall, with a maximum retention of 43.7% [7]. Moreover, plants promote biodiversity by offering shelter and food for various insects and animals, enriching local ecosystems. Integrating living plants into design not only enhances aesthetic appeal but also creates opportunities for urban farming within buildings.

Plants exhibit remarkable capabilities. For instance, Hyperion, the tallest tree on record, reaches a height of 115.5 meters. The stoutest trunk belongs to the Arbol del Tule, boasting a diameter exceeding 9 meters. Thimmamma Marrimanu boasts the world's largest single tree canopy, spanning over 19000 square meters. Additionally, Pando holds the title of the oldest clonal tree, estimated to be between 8000 and 12000 years old [8]. Bamboo showcases remarkable properties; not only is it among the strongest materials, surpassing steel in weight-to-strength ratio, but it also holds the record for growing over 1 meter in a single day. Additionally, bamboo has demonstrated extraordinary resilience, as evidenced by its survival of the atomic bomb in Hiroshima [9, 10]. When looking at nature there is no doubt it is of great interest to investigate using living plants for construction.

The Baubotanik research group [11] is at the forefront of research in living architecture, pioneering efforts to establish design principles for constructing with living plants. Their work focuses on addressing the challenges inherent in this type of construction, with an emphasis on experimental research. As far as the author is aware, there isn't a comprehensive model tailored specifically for designers of structures incorporating living plants. A model designed for architects or civil engineers, who may not have botanical expertise, should prioritize simplicity and straightforwardness for designing purposes. It should incorporate essential elements such as plant growth and structural behavior to enable effective design implementation.

This brief introduction highlights numerous reasons, alongside my personal interest in the subject, for undertaking research on construction design with living plants through a computational modeling approach.

1.1 Research goals, methodology and original contribution

This thesis studies the feasibility of using living plants as load bearing structures through computational simulation. It is important to note at this stage that this is a multidisciplinary topic,

comprising civil engineering, architecture but also biology, botanic, horticulture and arboriculture. As this thesis is written as part of the civil architectural engineering master program, the approach is oriented in consequence. Three living plant structures are designed using three different plant species, namely common ivy, Moso bamboo and white willow.

Before starting the design process, a review of the literature is conducted. This serves two purposes: first, to understand what has already been accomplished in the domain of living structures, and second, to identify the gaps and questions that need to be addressed to develop feasible Baubotanical design. These questions are essential, as their answers form the basis for the models. Data from the literature is collected to answer these questions, and assumptions are made when data is either unavailable or too complex to integrate into the first simple models developed here.

Once the foundations are established, two interconnected models are developed. A growth model is created for each plant to capture changes in plant geometry over time. Based on these growth models, structural models using the finite element method is proposed for each plant to analyze its structural behavior over time. The three plants are compared to understand their differences and their potential strengths or weaknesses for specific applications. Subsequently, an application is proposed for each plant: an ice cream pavilion made of bamboo, a replica of the Kupla observation tower made of willow, and a footbridge made of ivy. These applications lead to a discussion on feasibility, and a critical comparison of different designs.

Although the primary objective of this work is to evaluate the feasibility of Baubotanical structures through three applications, it also endeavors to serve as guidelines for designing living plant-based structures.

Original personal contributions

1. Review existing literature on Baubotanical design, identifying current knowledge and research gaps.
2. Develop simple growth and structural models for three specific plant species: Moso bamboo, white willow, and ivy.
3. Propose three real life inspired living plant projects employing the developed models.
4. Evaluate and compare the limitations of each application to assess the overall feasibility of Baubotanical structures.
5. Propose a methodology for designers interested in constructing load bearing structures with living plants.

Tools used

This manuscript was written using the Overleaf platform. Translations were conducted using ChatGPT 3.5 and DeepL. ChatGPT was additionally utilized for assistance in formulating certain sections of the text. MyBib was employed to compile the bibliography. Rhino3D software, along with the Grasshopper plugin, was utilized to build parametric numerical models. Finite element simulations were conducted using Karamba.

1.2 Structure of the manuscript

This thesis commences with a literature review (Chapter 2) to gather existing data on designing structures with living plants and to pinpoint gaps requiring attention for the development of a growth-structural model. Following this, Chapter 3 delves into addressing the identified gaps from the literature review. In Chapter 4, a comprehensive compilation of various properties—such as growth dynamics, mechanical behavior, and environmental interactions—pertaining to Moso bamboo, white willow, and ivy are undertaken. Chapter 5 then formulates assumptions based on the findings of the previous chapter for the implementation of desired models. In Chapter 6, a growth model and a structural model are developed for each plant species. These models are applied to three design proposals: a bamboo pavilion, an observation tower constructed with white willow, and a footbridge utilizing ivy plants. A discussion follows to evaluate and compare the limitations of each application and assess the overall feasibility of Baubotanical structures. Finally, Chapter 7 presents the main conclusions and potential future work of interest.

Part I

Foundations and Framework

Chapter 2

Living Architecture - Baubotanik Concepts and Applications

2.1 An Overview of Living Architecture

Using living plants as structural elements for design purposes is not a new concept. Through history many examples show how humans tried to control the growth process of trees to establish living structures.

In the early 20th century, well before our sustainability concerns, Arthur Wiechula, a German engineer for Culture an Horticulture, displayed an interest in designing living buildings, as evidenced by his imaginary drawings. He articulated, "If it were possible to grow wood in such a way that it already constituted walls during growth, walls which could be cultivated to make buildings, we could save on this lengthy process and would be able to use very young wood for construction". He devised a series of patents aimed at incorporating living elements into construction practices, including innovations for expediting the approach grafting of trees, manufacturing prefabricated wall panels, creating living walls, and constructing living fences. While he did not construct a living home, he did cultivate a 120-meter living wall designed to shield a section of train track from snow accumulation. Wiechula was a pioneer and a genuine source of inspiration for numerous individuals interested in this field [12, 13].

The manipulation of living plants extends beyond the construction field, holding significant interest for various domains such as crop development, art, and gardening, among others. An early example in cropping development is the cultivation of fruit trees, particularly apple and pear trees, which were trained into espaliers. This technique involved shaping the trees into a flat plane to maximize space utilization and ease harvesting [14]. In term of art, shaping plants was used by many artists. Peter Cook and Richard Reames were both arborsculpture artists who directed the growth of plants to shape them into furniture pieces like chairs. Cook preferred to keep the plants alive, allowing them to grow and mature naturally while taking on the desired form. On the other hand, Reames opted to prune the trunks of the plants, allowing them to be used as functional chairs within a house [15, 16]. Diana Scherer is a German artist who shapes plant root growth into three-dimensional objects by strategically placing obstacles. Her innovative approach to art has spurred material studies exploring the potential of using plant roots as a medium for bio-design applications [17, 18]. In gardening, shaping plants serves both

aesthetic and functional purposes. It is utilized for various applications such as creating living fences, pergolas, sculptures, providing shading, organizing spaces, and much more [19, 20].

Living plants have also been utilized in the construction of buildings, with numerous examples existing. For instance, there's Konstantin Kirsh's Ash Dome house (1989), constructed using 1350 bare root ash trees. Additionally, Kirsh has a park featuring various living structures open for visits. Marcel Kalberer's Willow Palace (1998) is a notable example, built using the traditional Mudhif construction technique. Giuliano Mauri's Tree Cathedral (2010) is an arboretum arranged to mimic the architectural elements of a medieval cathedral, such as the nave, choir, and transepts. The Patient Gardener (2011), conceived by a professor from the Politecnico di Milano and his students, is a project expected to span 80 years, aimed at challenging the fast-paced lifestyle's impact on ecology and environmental issues in architecture. Additionally, there's a ficus hut located in the Bio Park on Okinawa Island, serving as decorative art in the park while showcasing a distinctive aesthetic [13].

This brief overview highlights the diverse range of uses for shaped plants, with countless examples found across the globe. The array of constructed examples underscores the flexibility of and actual interest in such structures.

2.2 Living Root Bridges

A remarkable example of living architecture are the Living Root Bridges (LRBs) crafted by the Khasi and Jaintia communities residing in the Indian state of Meghalaya. LRBs serve as vital connectors between isolated villages in the region, bridging the gaps created by monsoon-swelled rivers. Nowadays LRBs not only serve as connector but also as tourist attractions. These traditional structures are a unique example of living architecture grown without the aid of contemporary engineering knowledge.

(a) Double-decker root bridge in Cheerapunji [21]

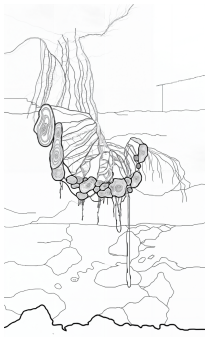

(b) cross-section [22]

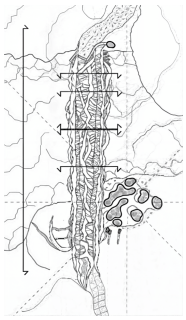

(c) plan [22]

Figure 2.1: Living root bridges

Local communities harness the mechanical strength of Ficus elastica's aerial roots and their innate propensity for anastomosis (vascular connection) to create the LRBs. These structures entail the weaving together of Ficus elastica's aerial roots, strategically planted on opposite sides of a gap or ditch. Sustaining such a structure necessitates ongoing efforts, including consistent maintenance. Villagers undertake regular tasks to ensure the integrity of the LRBs, such as

clearing moss and epiphytes accumulation, pruning and tying roots, creating the path with stone and earth, reinforcing vulnerable segments, and repairing any damaged sections.

There is no precise timeline for the construction and maturation of LRBs to attain full functionality. It is generally estimated that a minimum of 15 years is required for the roots to develop the necessary strength to support people crossing it. However, the variability inherent in these structures is evident in cases like the Siej bridge, where construction began 66 years ago and yet it remains not fully functional.

LRBs boast an impressive longevity, with the oldest registered among them estimated to have a life span of more than two centuries, and much more according to local people. They also exhibit remarkable spans, with the longest recorded LRB extending approximately 53 meters [22, 23, 24, 25].

2.3 Baubotanik

The term "Baubotanik", a German neologism which can be translated as "Living Plant Constructions" was coined by the Research Group Baubotanik, established in 2007 at the Institute for Architectural Theory and Design (IGMA) at the university of Stuttgart [26]. Baubotanik represents a fundamental engineering approach within a multidisciplinary field that combines architecture, engineering and biology. It leverages plants for load-bearing purposes within architectural structures. This approach results in the creation of hybrid structures that integrate both living and non-living elements. Individual living plants are interconnected, typically through inosculation (natural grafting), forming a single physiological organism with strong junctions [27]. Unlike the conventional linear construction approach, designing and building with living plants necessitates an iterative process. Designers need to monitor the plant growth and make continuous adaptations to the initial design, on a regular basis (typically every 1-3 years) [14].

One of the pioneering research efforts in the field of Baubotanik was conducted by the architect Ludwig Ferdinand, as part of his PhD study titled "The Botanical Fundamentals of Baubotanik and their Application in Design," completed in 2012. In this research, it is noted that despite numerous examples of living structures, there is a notable absence of a systematic survey regarding the contemporary state of research and technology in botanical and horticultural sciences. The two objectives set for his research were: developing Baubotanik building techniques and compiling a botanical base for design. The investigation included studying the inosculation of plant stems, assessing the feasibility of plant addition, optimizing greenhouse-grown control plants, all aimed at establishing design rules for living plant constructions. Through cultivation tests and biomechanical experiments, a series of plants were identified to be suitable for baubotanical applications. It was determined that the London Plane was the most suitable due to its ability for efficient and rapid inosculation. To conduct his research, Ferdinand constructed an experimental building known as the "Baubotanik tower." For this structure, White Willow (Salix Alba) was utilized due to site conditions. The tower comprised regular rhomboids initially supported by a scaffold, with the goal of constructing an 8-meter tower with a 2.8-meter square footprint (Fig.2.2). Three key topics were identified as relevant for Baubotanik design processes: **competitive conditions**, meaning that plants compete with each other for resources offered by their environment; **gravimorphism**, representing the plant's response to gravitational forces; and **transport processes**, ensuring the adequate distribution of nutrients through the plant's vascular system to sustain all its parts. Although mechanical stimulation, the response to external

loading (such as when a platform is attached to a plant), might seem important for Baubotanical design, it is not considered significant in practice [28].

(a) (b) (c)

Figure 2.2: Baubotanik tower [26]: (a) projected structure, (b) after completion in 2009, (c) second growth

The "Office for Living Architecture" (OLA) [29] is a German planning firm where this botanical-constructive approach is applied at architectural, urban planning, and landscape architecture levels. Some projects are realized, while others are presented for competition. Several of these projects have been awarded, demonstrating the current societal interest in this type of innovative projects. Here are some standout Baubotanical projects: Baubotanik footbridge (experimental structure, 2005), Bird Watching Station Waldkirchen (design and realization, 2007), Baubotanik Tower (experimental structure, 2007), House of the Future (competition - 3rd prize, 2012), Pratum in Caelo (competion - 2nd prize, 2016), Neighborhood square with green classroom (competition - 1st prize, 2017-2019) [30].

The research to establish Baubotanical design rules is still ongoing. The Baubotanik research group takes a highly experimental approach, investing time in growing plants to draw conclusions. While the research group proposes design applications from their research, they do not propose a comprehensive design methodology that designers could utilize to create living plant constructions (in the author's best knowledge). This paper aims at, among other objectives, constructing such a model. To begin, we must outline the key questions that need addressing, which will form the foundation for constructing these models.

2.4 Fundational inquiries

Given that the construction of the models relies on data extracted from the literature, an exploratory phase is imperative. This exploration involves a process of inquiry aimed at addressing the central question: How can we develop a simplified numerical model capable of representing the temporal evolution of the growth and structural performance of living plant structures that could be used for their design? The models are tailored for a non-specialized audience in botany, necessitating the inclusion of fundamental explanations for the comprehension of the results and

hypotheses derived from the collected data. Conventional construction serves as a solid foundation for developing a Baubotanical design process. Four main phases can be applied to living plant constructions: I Design, II Execution, III Maintenance, and IV Deconstruction and life-cycle analysis. From this perspective, the following non-exhaustive list of questions emerges:

I Design

1. Are there universally applicable principles governing plant growth?
2. What are the factors influencing the growth mechanics of a plant?
3. How does a plant interact with its environment? How does it affect it growth/mechanical properties?
4. What are the mechanical properties of living plant elements (stem, branches) and their evolution with time?
5. What tools, models, or design guidelines currently exist for the purpose of living architecture design?
6. Should roots be considered as an independent system? If so, the questions above should also be addressed for roots.

II Execution

7. What are the essential requirements for sustaining plant life and tailoring growth?

III Maintenance

8. What maintenance programming is required for such structures?

IV Deconstruction and life-cycle analysis

9. What is the living span of a plant and how does the structure behave mechanically beyond this?
10. What are the ecological impacts and benefits of living plants structures? (treated simply in the discussion)

All the questions in this series can be condensed into two coupled overarching questions: How does a plant function and how can it be tailored to structural use? Delving into the intricacies of living plants aids in formulating effective assumptions to streamline design guidelines and develop design tools. However, comprehensively understanding plant functioning exceeds the scope of this research's goal. Therefore, this work narrows its focus to specific questions pertinent to Baubotanical design. The following chapter aims to explore the most relevant and immediate questions (1,4,5, highlighted earlier) in detail.

Chapter 3

Laying the Foundations: Answering Key Questions for Growth-to-Structural Plant Modeling

This chapter aims to lay the foundations for creating growth-structural models based on the finite element method for Baubotanical design purposes. It is divided into two sections. The first section (3.1) explores plant growth principles and their incorporation into Baubotanik. It presents a fundamental understanding of plant anatomy, plant growth dynamics, plant tropisms (growth response to external stimuli), plant allometric rules (relationships between the growth of different plant organs), competition for resources among plants, the inosculation technique (grafting), the *plant addition principle* which allows the creation of Baubotanical structures by merging plants, and a series of rules from which a criterion is derived to ensure the viability of living plant structures from a vascular perspective. The second section (3.2) focuses on understanding the mechanical properties of living plants. It characterizes the mechanical properties of plant tissues, provides a correlation between different mechanical properties and plant density, and offers insights into the complexity of failure in living plants.

FEM for plant structural-growth modeling

The **Finite Element Method** (FEM) is frequently employed in structural plant analysis. This method is known for its robustness in analyzing complex geometries, making it well-suited for plant analysis. However, certain models prove too complex [31, 32], while others are overly specific to particular problems or plant types [33, 34], making them unsuitable for generic Baubotanical Design.

In the existing literature, a diverse array of studies delves into various aspects of Finite Element Modeling (FEM) applied to plants. These investigations range from detailed examinations of plant properties and morphogenesis at the microstructural level [31, 32, 35], such as cell behavior, to broader inquiries into growth dynamics within plants [36, 37, 38, 39] and other more general within living organisms [40, 41, 42].

Certain studies focus on specific plant structures like roots [43, 44, 45, 46], exploring their interactions with soil [47, 48, 49] and mechanisms of anchorage. Others investigate the influence of environmental factors like wind [50, 51, 52] on plant biomechanics. Additionally, there are endeavors employing advanced imaging techniques such as CT-scans to assess wood properties [53, 54, 55] or terrestrial laser scanning to analyze the behavior of trees under wind loads [56]. Inosculation, remains a domain with relatively sparse research coverage within the literature. The study of Middleton et al. [57] employing 3D FEM stands out as a pioneering exploration in this area.

The model proposed by Fourcaud and Lac [39] is of particular interest for Baubotanic. The model explores how the growth of plants relates to their mechanical behavior when subjected to internal or external loads. Growth is modeled as the incremental addition of new layers of material onto the existing structure, thereby simulating both primary and secondary growth processes.

A unique study was found regarding the application of FEM for inosculation nodes analysis. This research emphasizes that making appropriate assumptions or simplifications would lead to greater improvements in results compared to enhancing either geometric precision or material characterization. For example, using orthotropic materials or fine meshing may increase model complexity but result in only marginal improvements to the outcomes [57].

Note that the accuracy of structural analysis is deeply linked to the proper representation of geometry. Finite element analysis can be performed from highly precise 3D models to simplified 1D models. However, the complexity of the model directly impacts the computational load. Therefore, representing living plants for design purposes requires striking a balance between accuracy and computational efficiency.

In this work, an approach centered on constructing a **simplified structural-growth model using Finite Element Method for Baubotanical design applications is developed employing beam FE.** This model is fed by a geometry obtained from a plant growth model and the mechanical properties of living plant material. As such, this chapter serves as the cornerstone for developing and implementing the proposed approach.

3.1 Plant growth principles

3.1.1 Plant Growth Dynamics

Relevancy for Baubotanical design: Plant growth dynamics lie at the core of Baubotanik design. Longitudinal growth primarily occurs at the tips of plants. Consequently, if two plants are connected together (through inosculation), the connection node should remain stationary in space (or in a position compatible with the growth of both plants). Secondary growth (growth in diameter) follows longitudinal growth, enabling the plant to strengthen, especially in areas where it experiences greater stress.

Plant growth is deeply related to meristem tissues and the hormone auxin.

A **meristem** is a specialized type of tissue in plants responsible for cell division and growth. It is primarily located in the growing tips of roots and shoots, as well as in the buds of shoots. Meristematic cells are undifferentiated, meaning they haven't yet specialized into specific cell

types, and they possess the ability to continuously divide throughout the plant's life. There are several types of meristems [58, 59]:

- **Apical meristem**: Located at the tips of roots and shoots, apical meristems drive primary growth, contributing to the lengthening of roots and stems. They're responsible for the plant's primary growth in height.
- **Lateral meristem**: Also called the cambium, lateral meristems reside in the vascular tissue of stems and roots. They're accountable for secondary growth, leading to the increase in girth or thickness of stems and roots. Lateral meristems produce secondary xylem (wood) and secondary phloem.
- **Intercalary meristem**: Situated at the base of leaves and internodes in certain plants, intercalary meristems promote growth in length between nodes. They're commonly found in grasses and help these plants quickly recover from grazing or cutting.

Meristematic cells continually divide to produce new cells, which then undergo differentiation to form various specialized tissues such as vascular tissue, epidermis, and ground tissue. This process of cell division and differentiation enables plants to grow and develop throughout their life cycle [58, 59].

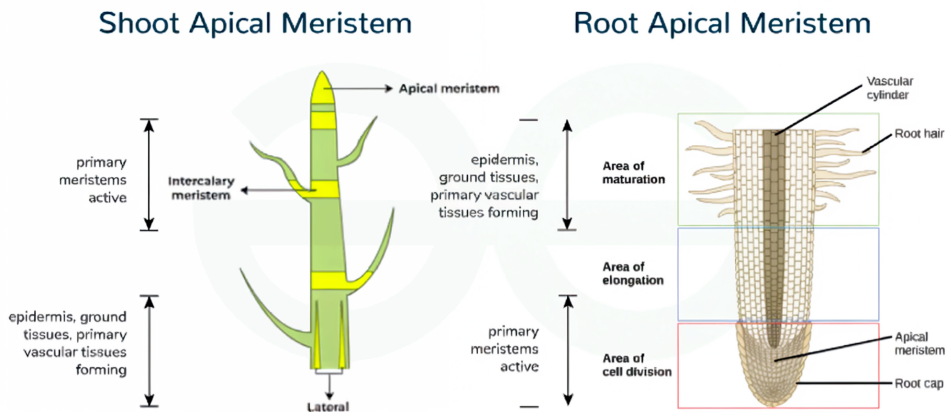

Figure 3.1: Plant growth through apical meristem [58]

Auxin is a category of plant hormones that serve for the regulation of diverse aspects of plant growth and development, including cell elongation, root growth, apical dominance and fruit development. Unlike meristem, which is a physical tissue, auxin acts as a chemical signal produced by certain cells in the plant. Synthesized primarily in the shoot apical meristem and young leaves, auxin is then transported throughout the plant to exert its effects. One of the key roles of auxin is to promote cell elongation, which contributes to primary growth and the elongation of stems and roots [60, 61].

Primary vs Secondary Growth

Primary growth in plants refers to the increase in length or height of the plant. This type of growth primarily occurs at the apical meristems, found at the tips of roots and shoots. Apical meristems are responsible for producing primary tissues, including primary xylem and phloem,

crucial for transporting water, nutrients, and sugars throughout the plant. In roots, primary growth involves the elongation of root cells and the development of root hairs, which help plants for water and mineral absorption. In shoots, primary growth results in the elongation of stem cells and the development of leaves and buds. Primary growth enables plants to establish themselves in the soil and reach towards sunlight for photosynthesis [62, 63].

Secondary growth, on the other hand, refers to the radial increase (thickening) of the plant. This type of growth primarily occurs at lateral meristems, such as the vascular cambium and cork cambium. A secondary phloem and a secondary xylem (wood) are produced during this phase. Secondary growth enhances the structural support of the plant and leads to the development of a woody or more rigid structure [62, 63].

Primary growth facilitates vertical growth and the establishment of plants, while secondary growth contributes to the thickening of stems and roots, providing structural support and protection. Both types of growth are essential for the overall development and survival of plants.

Adaptive growth in thickness

To meet the diverse demands placed upon them, trees possess an extraordinary ability to **adapt their growth in thickness**. They exhibit a remarkable responsiveness to mechanical stresses, concentrating their growth where stresses are highest. This adaptive response ensures that the structural integrity of the tree is maintained, allowing it to bear its own weight and resist external forces effectively [64, 65].

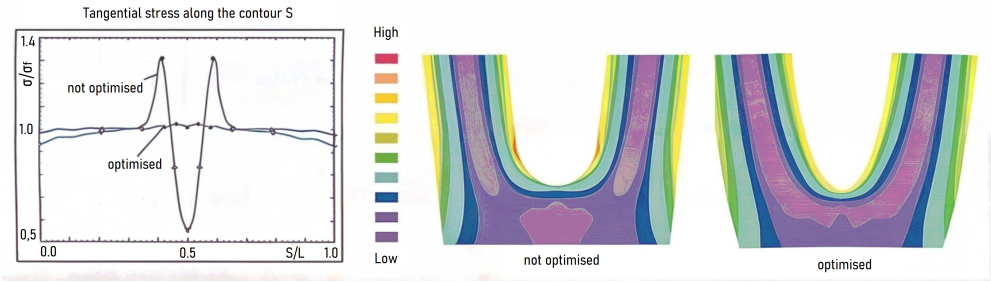

Figure 3.2: Adaptive Growth. The left graph illustrates stress smoothing due to secondary growth. The right drawings show how secondary growth occurs in high-stress zones (adapted to English) [26]

Moreover, trees prioritize growth in regions where efficient water transport is required, allocating resources to areas with high demand for water conduction. Interestingly, the leaves, which are the main destination for water and the main surfaces exposed to wind, represent hubs of high mechanical stress. Consequently, the optimization process in naturally grown trees often leads to a balanced distribution of stress throughout the plant, while simultaneously optimizing the efficiency of water transport [26].

A possible extension of Baubotanical computational design tools developed in this work could be their coupling to optimization with objective functions that are inspired from these observations (e.g. stress homogeneity).

3.1.2 Tropisms

Relevancy for Baubotanical design: Tropisms provide valuable insights into the interactions between plants and their environment, making them a potential input for Baubotanical design.

Tropism refers to a directional growth in response to an external stimulus. A positive tropism is a growth in the direction of the stimulus while a negative tropism is a growth in the opposite direction. There are various types of tropism, with four main ones standing out [66, 67]:

- **Phototropism**: The plant's growth response to light. For instance, when a plant bends towards a light source to maximize light absorption for photosynthesis.
- **Gravitropism** (or Geotropism): The response to gravity. Roots demonstrate positive gravitropism, growing downwards into the soil, while stems exhibit negative gravitropism, growing upward against the pull of gravity.
- **Thigmotropism**: Growth response to touch or contact with solid objects. For instance, vines winding around a support or tendrils coiling around a structure for support.
- **Hydrotropism**: Growth response to water. Roots might grow towards areas with higher moisture content in the soil.

Tropisms are linked to auxin hormones. Phototropism is a clear illustration. Auxin is sensitive to light, especially ultraviolet (UV) radiation. Prolonged exposure to sunlight, particularly UV light, can break down auxin molecules. Consequently, the stem exposed to sunlight contains less auxin, leading to reduced growth compared to the shaded part. This imbalance prompts the stem to bend toward the sun [68].

While these tropisms are not incorporated in the design tool set up in Ch.6, awareness of them is essential, since they can be harvested in real life to shape a plant to the target geometry.

3.1.3 Plant allometry

Relevancy for Baubotanical design: Plant allometry establishes proportional relationships between the growth of different plant organs. It is a key ingredient to set up growth models in Ch.6

A plant's natural shape is determined by its genes, referred to as its **genotype**, which can be influenced by the environment in which it thrives. This environmental influence results in the observable characteristics of the plant, known as its **phenotype** [69]. Describing plant growth can be complex due to numerous factors at play. However, there are basic **allometric rules** established to help model it [70].

Allometry, a concept originated by Julian Huxley and Georges Teissier in 1936, is a branch of biology that deals with the study of the relative growth of a part of an organism in relation to the growth of the whole organism or to the growth of a different part [71]. The mathematical relationship between the growth rate of two plant organs, having dimensions denoted as x and y, can be expressed as follows [72]:

$$y = ax^{\alpha} \tag{3.1}$$

Where a is a scaling constant which depends on the plant analyzed; α is the scaling exponent, determining the type of relationship (linear, quadratic...) between x and y. Depending on whether α is greater than, less than, or equal to 1, the relationship can be classified as positive allometry, negative allometry, or isometry, respectively [7].

Primary allometric relationships can be established between various organs of a plant and then combined to discover new connections. For example, there might be a relationship between the stem and leaves, and another between the stem and roots. By combining these, we can derive a relationship between the roots and leaves. An example that illustrates these relationships is the fundamental link between the mass of a plant m and its leaf area la, expressed as: $la \propto m^{3/4}$ [73]. This implies that as the plant's mass increases, its leaf area also increases, but not in direct proportion. This exponent of 3/4 is attributed to the necessity for larger vascular tubes to accommodate the increased leaf surface area and ensure efficient vascular transport [74].

The Allometric Partitioning Theory (APT) operates based on the assumption of consistent and universal allometric relationships for the ideal allometric plant[75]. Rötzer et al. [7] compiled several primary allometric rules into Tab.3.1. These tools are essential and are used for establishing and estimating unknown geometrical parameters in the growth models developed in Chapter 6.

Allometry	**Exponent**	**Dependent variable**	**Independent variable**
$h \propto d^{2/3}$	$\alpha_{h,d} = 2/3$	Tree height, h	Stem diameter, d
$v \propto d^{8/3}$	$\alpha_{v,d} = 8/3$	Stem volume, v	Stem diameter, d
$cr \propto d^{2/3}$	$\alpha_{cr,d} = 2/3$	Crown radius, cr	Stem diameter, d
$cpa \propto d^{4/3}$	$\alpha_{cpa,d} = 4/3$	Crown projection area, cpa	Stem diameter, d
$cv \propto v^{3/4}$	$\alpha_{cv,v} = 3/4$	Crown volume, cv	Stem volume, v
$la \propto d^{2}$	$\alpha_{la,d} = 2$	Leaf area, la	Stem diameter, d
$la \propto m^{3/4}$	$\alpha_{la,m} = 3/4$	Leaf area, la	Stem mass, m
$ms \propto mr$	$\alpha_{ms,mr} = 1$	Shoot mass, ms	Root mass, mr
$v_q \propto N^{-3/4}$	$\alpha_{v_q,N} = -3/4$	Volume mean stem, vq	Tree number, N
$N \propto d_q^{-2}$	$\alpha_{N,d_q} = 2/3$	Tree number, N	Mean stem diameter, d_q

Table 3.1: Primary Allometric Relationships in the Ideal Allometric Partitioning Theory [7]

In contrast to the APT, the **Optimal Partitioning Theory** (OPT) suggests that plants distribute resources in a way that optimizes their fitness, considering factors like environmental conditions and developmental constraints [76]. For example, in poor soil nutrient conditions, plants may allocate more resources to root growth to enhance nutrient uptake, even at the expense of aboveground growth. Similarly, in low sunlight conditions, plants may allocate more resources to leaf production to capture as much light as possible for photosynthesis [77]. The OPT provides more complex inputs that could be used to integrate plant interactions with their environment into the models. However, for the sake of simplicity, **the APT is used in this work**.

In ideal conditions, a plant follows its anticipated allometric path, but in less favorable environments, it adjusts its trajectory accordingly. When environmental conditions diverge significantly from what the species necessitates, the plant may deviate from its anticipated growth parameters. This can lead to failure and ultimately result in the plant dropping out from the population. Morphological flexibility enables plants to adapt to diverse spatial or temporal growth condi-

tions. Through a loop involving resource availability and absorption, allocation of growth, plant structure, and so on, the plant can thrive in unconventional growth environments [7]. In the field of Baubotanik, this flexibility provides a safety margin, as plants can adapt slightly if the models are not entirely accurate. Considering the use of APT in the developed models in this work, this is not accounted for, falling outside of the scope of this work. Awareness of these mechanisms and the ones in Sec.3.1.4 is however required to form a picture of plant growth complexity.

3.1.4 Competition - Self-thinning rule

Relevancy for Baubotanical design: Plant competition and self-thinning rule must be considered in Baubotanical design for plant viability. However, no specific rules or equations are used in the developed models; instead, an intuitive understanding is applied.

Competition among plants is a fundamental aspect of ecological dynamics, driven by the limited accessibility to essential resources as water, nutrients, light, and space within an ecosystem. This competition occurs both within and between plant species, influencing population dynamics, community structure, and ecosystem functioning. Plants within a population or stand compete for resources to support growth, reproduction, and survival. As plant density increases, competition intensifies, leading to a reduction in the availability of resources for individual plants. In response to this heightened competition, individual plants may experience mortality (die-off) and reduced growth rates [78].

The **self-thinning rule**, also known as density-dependent mortality, describes this phenomenon. According to this ecological principle, as plant density increases, average individual plant size or biomass decreases according to a predictable negative power-law relationship. Essentially, as some plants die off due to competition, others grow larger to compensate, maintaining a relatively stable total biomass within the population or stand [78].

This self-thinning process helps to regulate population density and structure, promoting ecological balance and sustainability within plant communities. It has practical applications in forestry, agriculture, and ecology, guiding management practices related to spacing, thinning, and competition control in planted forests, crops, and natural ecosystems [78].

Understanding the dynamics of competition among plants and the self-thinning rule should be integrated for enhanced and complex Baubotanical design to avoid consequences such as those observed in the Baubotanik footbridge, where many diagonal elements died due to competition. These are not accounted for in the simple models developed in this work .

3.1.5 Inosculation

Relevancy for Baubotanical design: Inosculation is a technique used to merge different plants together. An advantage of inosculation, where plants merge vascular systems, reduces competition by creating a unified entity. This cohesion enables efficient resource sharing, promoting collective growth and resilience within the plant community.

Grafting is "the act of placing the portion of one plant (scion or bud) into or on a stem, root, or branch of another (stock) in such a way that a union will be formed, and the partners will continue to grow" [79]. A successful and compatible graft has the potential to result in tissue merging, seamless vascular connection, and the creation of a physiologically and mechanically

unified entity. Pressure is exerted at the injured point of contact between two grafting partners [80].

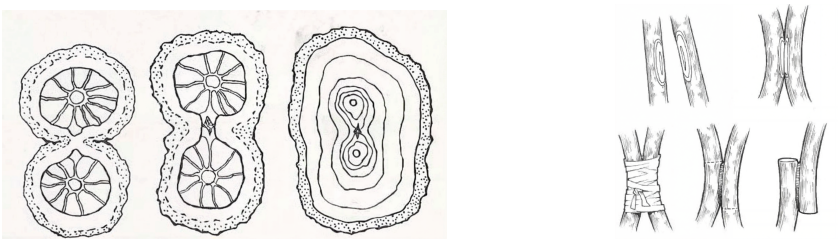

(a) (b)

Figure 3.3: Grafting: (a) natural grafting process [81], (b) approach graft [81]

Inosculation, employed in Baubotanik, describe a similar natural phenomenon where the joining of two partners does not require the cutting of bark. Inosculation originates from the Latin term "inosculari", signifying "to kiss", "to touch closely", or "to unite" [82].

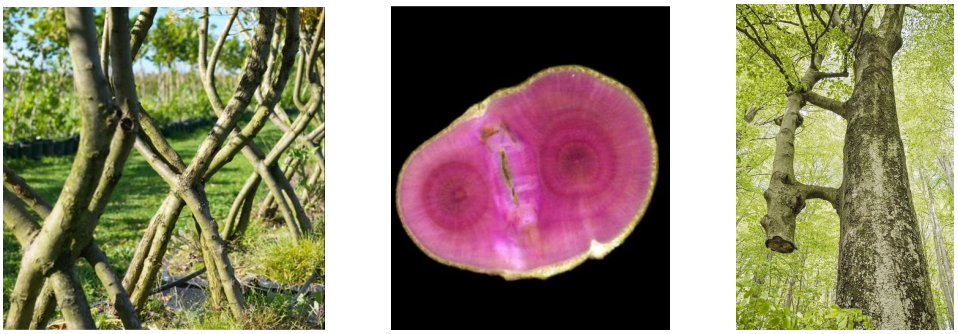

(a) (b) (c)

Figure 3.4: Inosculation: (a) experimental inosculation in field grown trees [26], (b) inosculated cross section [29], (c) natural inosculation @RebeccaH2030

In a recent study on inosculation across various species, it was observed that a successful inosculation shows similarities with natural branches. The study states that the mechanical behavior of an inosculation resembles that of natural branches due to the analogous cross-sectional patterns. Hence such connections will be **considered as rigid nodes in the structural models** in Ch.6. The study elaborates on the inosculation process, showing that there are no discernible differences in the quality of merging among various connection types (crosswise or bending) or fastening methods (rope or screw) [82]. However, the ease of inosculation process can vary depending on the species utilized. Robust plants with strong wound-healing capabilities and thin barks with low fiber content are better suited for inosculation [28].

3.1.6 Plant addition principle

Relevancy for Baubotanical design: This innovative method describes how to use inosculation (see Section 3.1.5) to enable the creation of living structures reaching the size of fully grown

trees.

The ***plant addition principle*** in Baubotanik harnesses the phenomenon of inosculation, where trees merge to form new physiological units [30]. This principle capitalizes on tree's capacity to compensate for organ loss by the generation of new organs in similar or different locations. By merging multiple plants into one organism through inosculations, redundant organs such as roots or leaves can be removed, provided the overall structure can maintain balance.

The technique involves arranging young plants spatially above and adjacent to each other, connecting them to form a truss-like structure. Only the lowest plants are planted in the ground, while others root in special containers supplied continuously with water and nutrients. Roots in the ground receive more space and resources, leading them to grow more extensively compared to those in the artificial containers.

Once inosculations develop, water and nutrients can be transported from ground roots to upper leaves, rendering container roots obsolete. These container roots can be gradually removed, eliminating the need for the watering system and scaffolding initially used for support. This approach transforms plants from mere saplings growing into trees to living construction elements integrated with technical construction elements, forming unified living structures.

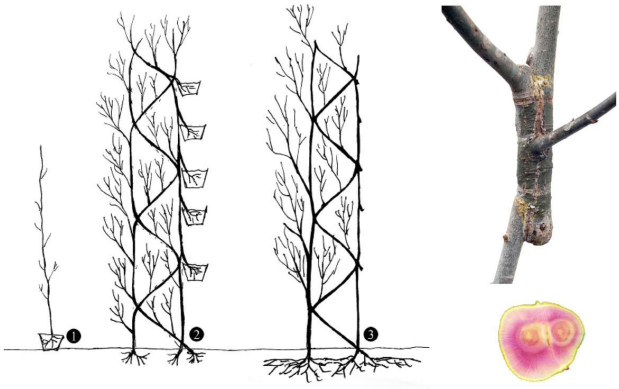

Figure 3.5: Plant addition principle [29]

This technique forms the basis for two project applications (the Willow Observatory Tower and the Ivy Footbridge) developed in Ch.6.

3.1.7 Corner's rules, pipe model theory and the resistance model

Relevancy for Baubotanical design: A series of rules are outlined to formulate a criterion (see Section 5) that ensures the viability of plant addition from a vascular perspective. In the projects, trigger times (the time when each plant is planted) are introduced to meet this criterion, ensuring that grafted plants have a cross-section lower than the stocking plant.

Plants present a remarkable diversity, finely tuned to their respective environments. **E.J.H. Corner**, a pioneering botanist, formulated a set of rules that help explain these structural adaptations. The Corner's rules consist of two principles governing plant architecture that were

established during the mid-20th century [83, 84, 85].

The axial conformity: "the stouter, or more massive, the axis in a given species, the larger and more complicated are its appendages." [85]

The diminution on ramification: "the greater the ramification the smaller become the branches and their appendages." [85]

These rules are quite rudimentary. To complement them, it was stated that plant density and shape should be taken as additional factors [85].

The **pipe model theory** somehow encapsulates these two Corner's rules, providing a more precise and practical framework for design purposes. It was first established in 1964 by Shinozaki. The model can be summarized as "a unit amount of leaves is provided with a pipe whose thickness or cross-sectional area is constant. The pipe serves both as the vascular passage and as the mechanical support and runs from the leaves to the stem base through all of the intervening strata" [86, 87].

Lehnebach et al. [88] caution that while the pipe model offers a valuable framework, it is essential to approach it cautiously as it is a universal model. It is recommended to adapt it to each plant specifics to establish a more robust model. 5 rules can be derived from this model:

1. **Sapwood area and leaves area/mass are proportional**: at a specific height in the stem, there exists a proportional relationship between the stem sapwood (SW) area and the mass of leaves above.
2. **Non-scalability**: the ratio of leaf-to-wood/mass remains consistent regardless of seasonal changes, growth stages, or different environmental conditions observed within a specific species.
3. **Area preserving rule**: the conductive area of the stem's (SW) at a specific height is equal to the combined basal area of its daughter branches located above that height
4. **Hydraulic sectoriality**: no lateral transport of water and mineral between pipes.
5. **Operating time of pipes**: In evergreen species, only the most recent growth ring of wood is conductive, as leaves are renewed annually and secondary growth occurs each year. Consequently, the conductive (SW) corresponds to the number of growth rings matching the lifespan of the leaves.

These five rules appear applicable to Baubotanik design. However, the third rule stands out as particularly interesting, as it ensures the conservation of vascularity throughout the plant.

Another approach, the **resistance model** proposes an analogy between the water transport system in plants and an electric circuit. Here, water flow parallels electric current, and segments of the plant stem act as electric resistors. The "water potential difference" between soil and air functions as the "voltage source", driving water absorption by roots, transport through the plant, and release via leaves, all without the plant expending energy for pumping. Similar to an electric circuit with multiple resistors in parallel, water flow in the plant network divides such that it predominantly travels through segments with the least resistance [89, 90, 91].

When combining the **resistance model** with the **Pipe-Model theory**, it becomes possible to determine where growth in thickness occurs, primarily in areas with high water flow, such as direct connections between roots and leaves, as detours are less efficient and experience less growth [26].

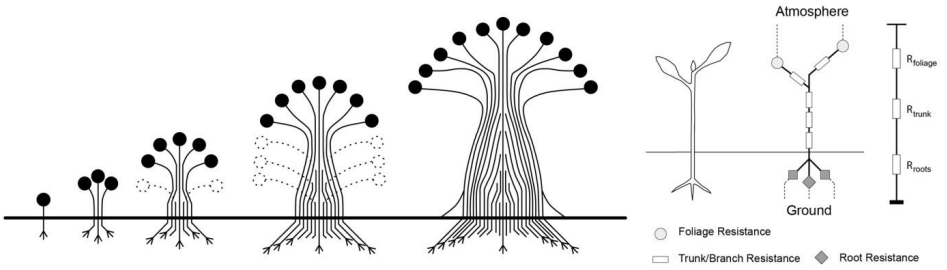

Figure 3.6: Left: plant representation according to the pipe model theory [86]. Right: plant representation according to the resistance model [90]. Image from [26].

The findings of a recent study on inosculation [82] serve as a complement to these principles. It emphasizes that the cumulative cross-sectional area above a node ought to be less than the combined cross-sectional area below that node. This study offers a qualitative assertion without introducing a reduction scale factor that could be used as a parameter in the models. To ensure vascular integrity, cross-sectional reduction is implemented in setting up the models in Ch.6.

3.2 Mechanical properties of living plants

Ideally, existing databases should provide the mechanical characteristics of a plant. Various online databases, such as TryDB [92], Plants For A Future [93], and TRID [94], offer access to extensive datasets. However, it's important to note that the data found in these databases may sometimes be contradictory or lacking. In such cases, alternative methods may be necessary to determine the mechanical properties of plants.

Since in general there are important differences between the root system and the shoot system, it can be more convenient to model them separately [95]. In the current work the focus is set entirely on the stems as structural load bearing elements and roots aren't represented, keeping in mind that their flexibility and strength may be considered in a future, more elaborate model (see research on roots in Appendix F).

The majority of existing studies on wood mechanical properties have been conducted on dried wood with a moisture content of less than 12%. This is primarily due to the significance of such properties for the construction industry. However, this approach limits the understanding of plants in their natural states, where moisture content can be significant, and mechanical properties decline with higher moisture content [96].

The cross-section of a plant typically consists of different tissues with varying mechanical characteristics. The layering of these tissues generally leads plants to have orthotropic properties with a different stiffness in the longitudinal direction, radial direction and circumferential direction

[55]. For the sake of simplicity, **plant material will be considered elastic homogeneous isotropic** in the models set up in this work.

Kretschmann [97] gathered measurements of the Young's modulus for both dry wood and green wood across a series of plants. Utilizing this dataset, Middleton et al. [98] established the following **correlation between the Young's modulus in the longitudinal direction for dry wood $E_{L,dry}$ and its counterpart in green wood $E_{L,green}$:**

$$E_{L,\text{green}} \sim 0.73 \cdot E_{L,\text{dry}} + 775\,\text{MPa} \tag{3.2}$$

Computed tomography intensity data can be utilized to establish the spatial variation of Young's modulus within a dried plant cross-section. This method is unsuitable for green plants due to the high water content, which absorbs X-rays excessively, resulting in inaccurate data [54]. The most rigorous approach involves mapping the various tissues onto a model and assigning their respective mechanical properties. Wolff-Vorbeck et al. simplified the geometries of cross sections into artificial representations, focusing solely on the principal tissues, which streamline the modeling process. Additionally, they compiled the Young's modulus of each tissue into a single table [99]:

Tissue	**E [MPa]**	**References**
sclerenchyma	24 500 - 45 000	[96, 100, 101]
wood (sec. xylem)	2600 - 16 000	[100]
phloem	xxxx - 3500	[96]
collenchyma	1000 - 2600	[96, 100, 102]
vascular bundles	30 - 840	[96, 100, 103]
epidermis + periderm	350 - 500	[104]
epidermis	3 - 250	[100, 103, 105]
parenchyma (non-lignified)	5 - 100	[100]

Table 3.2: Elastic modulus (E) of individual plant tissues derived from the literature. Taken from [99] and completed

Each plant species possesses a unique structure, making it challenging to establish universal properties applicable to all plants. Nonetheless, several studies have indicated a **correlation between tissue density and the mechanical properties of plants** [96, 106, 107].

Niklas and Spatz [108] established a correlation between plant tissue density (ρ) and its mechanical properties. They underscored this link through a brief mathematical development. First, the flexural stiffness (EI) and the critical bending moment (M_{crit}) for a stem (tubular section) are determined:

$$EI = E\frac{\pi}{4}r^4 \tag{3.3}$$

$$M_{\text{crit}} = \sigma_{\text{crit}}\frac{I}{r} = \sigma_{\text{crit}}\frac{\pi}{4}r^3 \tag{3.4}$$

Where E represents the Young modulus, I the moment of inertia, r the stem radius, M_{crit} the critical bending moment, and σ_{crit} the critical peak stress. From these, equations for the relative resistance to bending (RRB) and for the relative strength (RS) can be derived:

$$RRB = \frac{EI}{\frac{m}{l}} = \frac{r^2 E}{4\rho} \tag{3.5}$$

$$RS = \frac{M_{\text{crit}}}{\frac{m}{l}} = \frac{r\sigma_{\text{crit}}}{4\rho} \tag{3.6}$$

With $\frac{m}{l}$ the mass per unit length. These equations highlight the influence of density (ρ) on mechanical properties.

Furthermore, from a dataset comprising over 200 species, Niklas and Spatz established a statistical correlation between density ρ and four primary mechanical properties in green woods: the Young's modulus E, the tensile strength σ_t, the compressive strength σ_c, and the shear strength σ_s.

An ordinary least squares regression (OLS) was performed to determine the relations between density (x) and corresponding mechanical properties (y). The following formula was used:

$$\log y = \log \beta + \eta \log x \tag{3.7}$$

Where y represents one of the four mechanical properties in question, x the green plant tissue property, β serves as a scaling factor determining the starting point of y when $x = 1$, and η represents the scaling exponent defining the relationship type between x and y (linear, quadratic, etc.). The following table compiles the results of this study.

log y vs. log x	**n**	α	**log** β	r^2
All species				
E vs. ρ	175	1.00	1.09	0.745
σ_t vs. ρ	174	1.24	-1.76	0.877
σ_s vs. ρ	165	1.19	-2.50	0.843
σ_c vs. ρ	176	1.33	-2.33	0.84
Conifer species				
E vs. ρ	38	1.00	1.08	0.569
σ_t vs. ρ	37	1.14	-1.52	0.802
σ_s vs. ρ	37	0.96	-1.88	0.711
σ_c vs. ρ	39	1.10	-1.73	0.745
Angiosperm species				
E vs. ρ	137	1.02	1.02	0.737
σ_t vs. ρ	137	1.18	-1.57	0.859
σ_s vs. ρ	128	1.15	-2.36	0.812
σ_c vs. ρ	137	1.28	-2.17	0.812

Table 3.3: Statistical relationship between green plant tissue density and its mechanical properties [108]

The correlations established in Tab.3.3 are useful as a first estimate for various plants and could be utilized in cases where data on mechanical properties is unavailable. It was employed in this work to determine the compressive an tensile strength of Hedera helix L.

When green wood is loaded in bending beyond its strength, failure takes place. The failure type of green wood is closely linked to its ontogenesis. As mentioned in Section 3.1.3, plant growth

responds to external stimuli, leading to significant variability in cross-sectional properties. Light appears to be particularly influential on the mechanical behavior of living plants. Light-grown plants exhibit characteristics akin to solid wooden cylinders, with a tendency towards brittle failure. Conversely, shaded-grown plants display greater flexibility and behave more like hollow pipes [109]. This serves as additional information to illustrate the complexity of green wood mechanical behaviour, but it is not accounted for in the models for the sake of simplicity and to keep focus on their elastic behavior for their design.

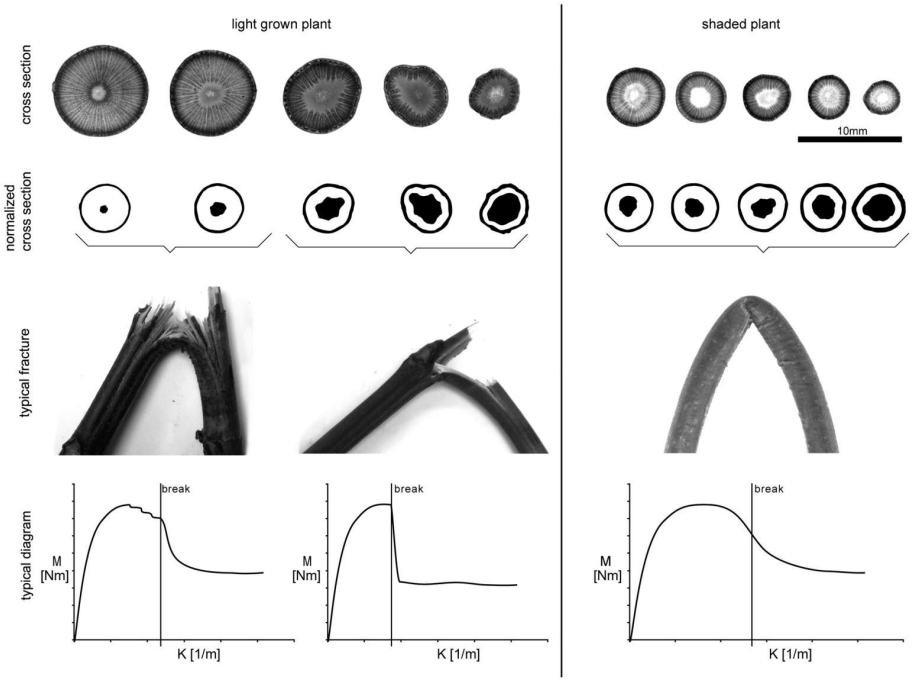

Figure 3.7: Plant failure for light grown plants vs shaded grown plants [109] - M the bending moment and K the curvature

Chapter 4

Dataset Assessment: Moso Bamboo,White Willow and Ivy

Designing a Baubotanical structure requires comprehensive data (i.e. mechanical properties, growth characteristics, environmental interactions) on the plants involved to create an accurate growth-structural model. This chapter is dedicated to collecting essential information for three specific plant species: Moso bamboo (Phyllostachys edulis), white willow (Salix alba L.), and ivy (Hedera helix L.), that are used in the projects developed in Ch.6. Bamboo was selected due to its rapid growth and excellent mechanical characteristics, while white willow was chosen as it's the primary plant utilized by the Baubotanical Research Group in their experiments. Ivy was selected for its widespread presence in Europe and its geometrical flexibility, offering potential for different applications.

4.1 Moso Bamboo - *Phyllostachys edulis*

Phyllostachys edulis, commonly known as Moso bamboo, is a monocarpic perennial plant belonging to the Poaceae (grass) family [110]. Bamboo originates from Asia, where approximately 80% of the world's bamboo species are found [111]. It naturally thrives in tropical and subtropical regions, spanning latitudes between 46°N and 47°S, ideally with sunny and humid conditions [112]. It can survive in cooler climates, as evidenced by various bamboo plantations in Belgium [113, 114]. It demonstrates resilience even in cooler climates, with the ability to withstand temperatures as low as -17.7°C, although its growth may be more rapid in its native regions [115]. Bamboo is one of the oldest construction material used, and is renowned for its exceptional material properties in construction, earning it the nickname "green steel" [116]. Some authors advance that it "has a higher strength-to-weight ratio than steel and concrete" [10]. Primarily utilized as a construction material in Asia [112], it is also employed to construct impressive scaffolding that can exceed 100 meters in height [117]. It is also one of the fastest growing plant in the world [118]: during its active growth phase, bamboo shoots can exhibit remarkable growth rates, with an extension of approximately 500 cm in a week and reaching a maximum daily growth of up to 100 cm [119]. Under favorable conditions, these shoots can exceed a height of 20 meters in only two months [120].

Moso Bamboo is a monocarpic plant, meaning that it flowers once during its life and then dies. This phenomenon that is to be considered for estimating the Baubotanical structure constructed

from Moso bamboo lifetime, is not well understood yet [121]. While some studies have documented flowering cycles ranging from 48 to 67 years [122, 123], others have observed cycles lasting more than a hundred years [124].

There is a lack of literature regarding bamboo's ability or inability for grafting (or inosculation), caution should be exercised when considering bamboo for Baubotanical design. This explains why in the project using this plant in Ch.6 rather mechanical joints are envisioned to connect each plant.

Moso bamboo allometry

Most of the available literature on Moso bamboo originates from Asia, obtaining precise data on bamboo growth in Belgium presents challenges due to the differences in environmental conditions. The extraordinary high growth rates mentioned earlier, are unlikely to occur in Belgium. At maturity, Moso bamboo can reach heights over than 20 meters [120, 125, 126, 127]. Its outer diameter and thickness decrease with height [127]. At breast height, the diameter of the hollow tube stem typically ranges from 8.5 cm to 17 cm [125, 127, 128, 129, 126], with a measured average wall thickness of 1.2 cm [129]. The dimensions observed in a bamboo plantation in Bretagne, France, at maturity are consistent with the earlier descriptions. However, it's important to highlight that maturity is attained at a slower rate in this climate, where it typically requires 10 to 15 years to reach maturity [126].

A study has shown the potential for applying the Logistic growth model to analyze the evolving growth patterns of Moso bamboo in China [130]:

$$h(t) = \frac{H}{1 + Te^{-ct}} \tag{4.1}$$

With h representing the plant height (in centimeters), t the time (in days), H the height reached at maturity (in centimeters), T the time needed to reach maturity (in days), and c a growth parameter. For Moso bamboo in China $H = 1553.94$ cm, $T = 142.43$ days, and $c = 0.135$; which predicts a growth of 15.45 m in 60 days.

The logistic model can be adjusted to Belgium to achieve a height of 20 meters within 10-15 years by manipulating its parameters (adaptation made in Section 6.1.1). Note that this may not accurately represent long-term growth, since the model is primarily designed to forecast the rapid initial growth stages.

Bamboo consists of a series of nodes and internodes, with growth resembling a telescopic pattern. Each node grows independently, with lower nodes growing earlier. A study conducted in China revealed that, on average, bamboo internodes attain a length of approximately 30 cm within approximately one month [131]. The elongation process can be divided into 6 phases (see Figure 4.1c): S1 - Slow Growth: $<$ 2.5 cm (15 days); S2 - Early Fast Growth: 2.5-5 cm (3 days); S3 - Active Fast Growth: 5-10 cm (3 days); S4 - Fastest Growth: 10-20 cm (6 days); S5 - Growth Decrease: 20-29 cm (9 days); S6 - Growth Cease: 29-30 cm.

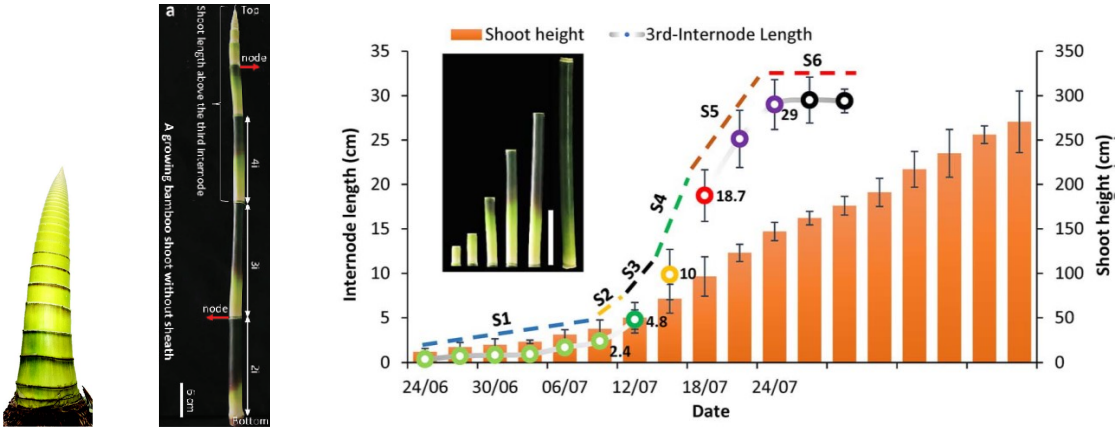

(a) (b) (c)

Figure 4.1: Moso bamboo growth. (a) Young shoot [132], (b) Growing shoot without sheath [131], (c) Growth Stages of an Internode: S1 (Slow Growth), S2 (Early Fast Growth), S3 (Active Fast Growth), S4 (Fastest Growth), S5 (Growth Decrease), and S6 (Growth Cease). [131]

This telescopic growth is utilized in Section 6.1 to predict when bamboo will stop growing at a desired height where a platform is intended to be attached to the living plant structure.

Moso bamboo mechanical properties

Bamboo has been extensively researched, but like many other plants, most studies have focused on dried samples [133]. Sanchez et al. [134] conducted a statistical study that included green Moso bamboo. They found the following average values: compressive strength of **42.7** MPa, tensile strength of **77.1** MPa, and Young's Modulus of **16.1** GPa. Although there is a notable difference in mechanical properties between dry and green bamboo ($\sigma_{c,dry} \sim 54.1$ MPa ; $\sigma_{t,dry} \sim 153.6$ MPa), the strength values remain significant.

Like many plants, bamboo is a composite material composed of various tissues. It can be seen as a natural fibre-reinforced composite, consisting of robust unidirectional fibers and conductive vessels enclosed within a matrix of parenchyma ground tissue [133]. These vessels decrease in size as they are located towards the outer regions of the cross-section, resulting in higher density at the outer part compared to the inner part [135]. A study revealed a dry density from 336 kg/m^3 in the inner part to 1283 kg/m^3 in the outer part [136]. As other plants, bamboo presents different properties in radial, longitudinal and tangential direction. Nevertheless, for the sake of simplicity, many studies assume a uniform density. Reported dry densities range from **464** to **1287** kg/m^3 [133].

Moso bamboo summary

Data	Value	Reference
Geographical location	tropical and subtropical regions 46°N-47°S	[111]
Natural conditions	sunny and humid	[112]
Hardniness	-17.7 °C	[115]
Living span	48-67 years	[122, 123]
Graftability (inosculation)	-	-
Max height	20-25 m	[120, 125, 126, 127]
Longitudinal growth rate	maturity = 10-15 years*	[126]
Maximum diameter	> 17 cm	[126, 129]
Radial growth rate	maturity = 10-15 years*	[126]
Max thickness	> 1.2 cm	[129]
Green Young's modulus E_{green}	16100 MPa	[134]
Density ρ	850 kg/m3	[133, 136]
Tensile strength σ_s	77.1 MPa	[134]
Compressive strength σ_c	42.7 MPa	[134]

Table 4.1: Moso bamboo properties, used in the simulations

*growth rate should be adjusted for Belgium, where maturity is typically reached in around 10-15 years (adaptation made in Section 6.1.1)

4.2 White Willow - *Salix alba*

Salix alba Linnaeus, commonly known as white willow, is a species of willow tree native to Europe and western and central Asia. It belongs to the family Salicaceae and the genus Salix [137]. While it is known for its rapid growth, this species does not have a long lifespan, generally lasting between 20 and 30 years. Under favorable conditions, this tree has the potential to live for more than a hundred years [137, 138]. Thriving in temperate climates, this species prefers abundant sunlight and well-hydrated soil for an optimal growing [139]. It ideally thrives in temperatures ranging from 0 to 32°C, but it can withstand temperatures ranging from -35 to 35°C [138, 140]. The Baubotanik research group uses this species for its rapid growth capabilities as well as its natural propensity for grafting (inosculation) [28, 57, 82].

Salix alba L. - allometry

Salix alba L. stands as one of the largest among willow species, capable of reaching heights up to 30 meters and boasting a maximum diameter of 1 meter or more [138, 141]. The growth rates of Salix babylonicae, a similar species, were estimated to be of 0.75 to 1 meter in height per year and 0.8 cm radially per year [142]. Slightly lower growth rates have been reported for Salix alba. A growth rate of 0.6 meters in height was reported [143]. Ludwig reported a diameter of 8 cm reached within 8 years [28], corresponding to an average radial growth rate of 0.5 cm per year.

Due to insufficient data, allometric rules cannot be applied to establish a growth model for Salix alba L.. Consequently, a linear growth model is proposed for this plant in Section 6.2. It's worth noting that with additional data, a more accurate model could be developed.

Salix alba L. - mechanical properties

Niklas and Spatz [108] conducted a study examining the mechanical properties of various green woods, with willow being one of the species investigated . The reported mechanical properties include a density of **529** kg/m^3, tensile strength of **36** MPa, compressive strength of **14.7** MPa, and a Young's modulus of **4800** MPa. These values were also taken in the application in Section 6.2.

Salix alba L. - summary

Data	Value	Reference
Geographical location	Europe, western and central Asia	[137]
Natural conditions	temperate, abundant sunlight, humid soil	[139]
Hardiness	-35°C	[138, 140]
Living span	20-30 years	[137, 138]
Graftability (inosculation)	yes	[28, 82, 57]
Max height	30 m	[138, 141]
Longitudinal growth rate	$>$ 60 cm/year	[142, 143]
Maximum diameter	100 cm	[138, 141]
Radial growth rate	0.5 cm/year	[142, 28]
Green Young's modulus E_{green}	4800 MPa	[108]
Density ρ	529 kg/m^3	[108]
Tensile strength σ_s	36 MPa	[108]
Compressive strength σ_c	14.7 MPa	[108]

Table 4.2: Salix alba L. properties, used in the simulations

4.3 Ivy - *Hedera helix L.*

Hedera helix L., also known as Ivy, English Ivy, common Ivy, European Ivy or lierre commun, is a woody, perennial evergreen plant from the Araliaceae family [144]. It is a woody climbing plant with a perennial stem, thus a vine [145]. Native ivy's home is ranging from southern Scandinavia to the Mediterranean area [146], approximately between 10° E and 25° E longitude and 35°N and 60° N latitude [147]. Ivy exhibits optimal growth conditions at around 21°C [148]. It can tolerate drops in temperature, surviving temperatures as low as -25°C [144], however at -8°C the plants photosynthetic apparatus may begin to sustain damage [149]. Although ivy exhibits a remarkable tolerance for a wide range of light conditions, it is not clearly stated which is its ideal growing environment. While Strelau et al. [146, 150] states that it does prefer to grow in areas exposed to direct sunlight, Okerman [145] claims "it prefers shade, damp soils, and a moist, cool environment". Young shoots, in particular, tend to thrive in lower light levels, although they demonstrate a heightened photosynthetic rate when exposed to strong light [151]. This plant is characterized by its ability to creep horizontally along the ground or ascend vertical

structures (seeking maximum light exposure) like trees or walls, using attachment roots that grow along its stem [152]. In its juvenile form, it appears as a woody vine needing structural support for growth. As it matures, it transforms into a shrub or can even develop into a tree [146].

An essential point to note is that ivy is not a parasitic plant in the conventional sense. Its above-ground roots primarily function to structurally support the plant, and it does not absorb nutrients from host trees. On the contrary, ivy often serves as a beneficial companion to host trees [153]. It offers protection from winter cold and certain parasites. Additionally, it contributes positively to biodiversity; by retaining its leaves throughout winter, it provides refuge for insects and birds. Moreover, the fruits it produces serve as a food source for numerous animals. However, in regions where these plants are not native, such as the USA, ivy is regarded as an invasive species that can disrupt the natural environment [154]. Since ivy doesn't require a tree as a host, it is indeed suitable for Baubotanical purposes as a single entity. Given that Europe is its native habitat, incorporating ivy into such designs could potentially enhance the local environment and contribute to ecological restoration efforts. In addition to other benefits of using ivy for Baubotanical designs, there is its remarkable flexibility, capable of adapting to nearly any desired shape; and its natural capacity for grafting (inosculation), a phenomenon studied in detail by Millner [155].

Hedera helix L. allometry

Typically, old Hedera helix L. vines can reach 30 m height and 30 cm in diameter [146, 156, 157]. But in extreme cases it can go far higher up to 90 m [154], and far wider with a diameter of 60 cm measured on a 433 year old plant [158]. In forests along the Rhine River in France, the oldest English ivy vines at one site were recorded to be 50 years old, while at another site, the oldest vines were found to be at least 66 years old [159]. There is no evidence found to determine whether the 433-year-old ivy stand was an exception or a normal occurrence. There are non academical sources discussing lifespans of English ivy that exceed 1000 years [160], and even 4000 years [161]. There exists substantial variation in growth patterns both among different sites and even within the same site. However, a positive correlation was identified between the height and diameter of ivy and the circumference of its host tree [162]. It was hypothesized that this difference stemmed from the limited surface area available on the hosting trees, causing the ivy's stems to compete with each other [163]. In southern Italy, a mean annual radial increment of 0.94 mm was observed [164]. In France, another study recorded a radial growth rate ranging from 0.5 mm to 2.06 mm per year [157]. Academic literature lacks information on the longitudinal growth rate of Hedera helix L. However, gardening websites suggest a growth rate ranging from 0.5 m [165] to 1.5 m [166] per year.

Mechanical properties

The wood of Hedera Helix is typically soft, with a density of **530** kg/m^3 [144]. A study on plant cuticle mechanics [167] measured the Hedera Helix cuticles to have a Young's modulus of 640 MPa and a breaking stress of 15 MPa. Another study on structural attachment measured the rootlets (above ground) to have a Young's modulus of 220 MPa and a tensile strength of 38 MPa [152]. Wisteria and grape vine, the two other main European vines have a Young's modulus respectiviely of 892 MPa and 1378 Mpa [168]. These mechanical characteristics, although not specific to the Hedera Helix or to its stem, offer an initial insight into its capabilities, especially considering the limited literature available on this subject.

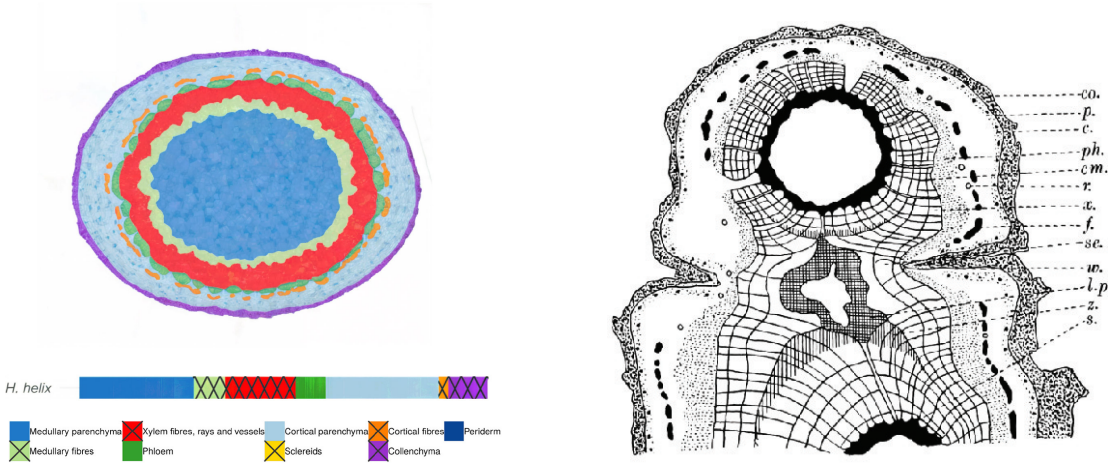

(a) Hedera helix cross-section [169]

(b) inosculation drawing [155]

Figure 4.2: Hedera Helix anatomical organisation

A study covered the mechanical properties of searcher shoots in climbing plants. From the given data it is possible to establish a range starting from 1200 MPa to 2800 MPa for the ivy's Young's modulus [169]. From the same study a cross section and the proportion of each tissues layer are given (see Figure 4.2a). With the mechanical properties compiled in Table 3.2, it is possible to determine an equivalent Young's modulus for the whole cross section with the following formula:

$$E_{\text{eq}} = \sum f_i \cdot E_i \tag{4.2}$$

With E_{eq} the equivalent Young's modulus, f_i the area fraction of each tissue in the cross section and E_i the Young's modulus of each tissue.

Proceeding this way, a Young's modulus of approximately **2122** MPa is found (63.5% parenchyma, 11.9% collenchyma, 17.5% phloem, 7.1% xylem). This result aligns with the range of values reported in the literature.

Regarding ivy's strength, no specific data was found. However, the correlation between green wood density and its strength: $\log y = \log \beta + \eta \log x$, established in Section 3.2 with the values for angiosperm species compiled in Table 3.2 could potentially be utilized to estimate its strength. Following this approach, a tensile strength of **44.12 MPa** and a compressive strength of **22.75 MPa** are estimated.

Hedera helix L. summary

Data	Value	Reference
Geographical location	southern Europe 10°-25°E and 35°-60°N	[146, 147]
Natural conditions	all kind of shading/moisture	[146, 150, 29]
Hardiness	-8°C	[149]
Living span	>100 years	[158, 160, 161]
Graftability (inosculation)	yes	[155]
Max height	30 m	[146, 156, 157]
Longitudinal growth rate	1 m/year	[165, 166]
Maximum diameter	60 cm	[158]
Radial growth rate	1.5 mm/year	[164, 157]
Green Young's modulus E_{green}	2100 MPa	[169]
Density ρ	530 kg/m3	[144]
Tensile strength σ_s	44.12 MPa	-
Compressive strength σ_c	22.75 MPa	-

Table 4.3: Hedera helix L. properties, used in simulations

4.4 Baubotanical Insights on Selected Plants

Ivy and willow are discussed together as they are both common species in Europe. They possess similar mechanical properties, with ivy slightly stronger than willow, but willow being stiffer. In terms of growth, ivy exhibits almost double the longitudinal growth rate but has a considerably lower radial growth rate compared to willow. The main challenge with willow is its short lifespan, while this doesn't seem to be a concern for ivy. Both plants are graftable and therefore suitable for Baubotanical applications following the *plant addition principle*.

On the other hand, bamboo is not native to Europe. Modeling its characteristics requires adapting data from Asian climates. However, it boasts excellent mechanical properties and vigorous growth. Its main limitation lies in its inability to graft, rendering it unsuitable for plant addition. Nevertheless, its exceptional properties continue to make it a highly interesting plant for living structures. A detailed comparison between the three plant species is discussed in Section 6.4

Since **bamboo** cannot graft, all plants must be planted individually. Hence, a sufficiently simple application is needed to meet this geometrical condition, and an **ice cream pavilion** (see Section 6.1) appears to be a suitable choice. **Willow** will be used to replicate an existing project, the **Kupla observatory tower** (see Section 6.2). Its rapid growth, strength, and ability to inosculate make it suitable for various projects. This application will serve as a test to determine if Baubotanical design can reproduce an existing project. Finally, the flexibility of **ivy** and its high longitudinal growth rate compared to its radial growth rate make it a suitable choice for a **footbridge** (see Section 6.3). Typically, creating a footbridge would require a large temporary installation (such as scaffolding) with other plants to support the growing phase, but with ivy, it is possible to use lighter installations.

Part II

Structural Design and Implementation

Chapter 5

Simplifying assumptions

Based on the information gathered in Chapters 3 and 4, the following assumptions are made to build growth-to-structural models for the three chosen plant species. These assumptions ease the implementation of models.

- The apical meristem (see Section 3.1.1) is considered to be fully located at the tips of the plant. As a result, the existing part of the stem stops elongating in length when tip is cut. It only undergoes expansion in diameter through secondary growth, facilitated by the lateral meristem. This hypothesis ensures that the nodes remain fixed and do not shift after inosculation.
- Only plant stems are modeled due to insufficient data, and attempting to model other elements such as branches and leaves would introduce excessive complexity. Note that the branching considered after *plant addition* consists of stems.
- The pipe model, combined with the resistance model (see Section 3.1.7) are utilized to ensure vascular viability within the plant. The following criterion must be fulfilled:

$$S_T \leq \sum S_i \tag{5.1}$$

  With S_T representing the basal stem area and S_i representing the combined area of all branches connected to the basal stem.

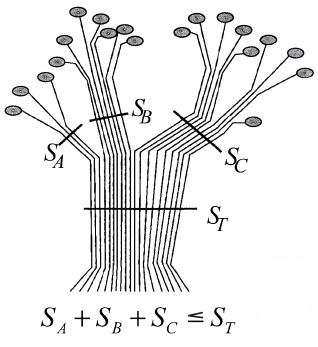

Figure 5.1: Vascular hypothesis, adapted from [89].

To ensure compliance with this rule, the diameter of the top of the plant stem will be considered to be 80% (reduction factor) of the diameter of the basal stem. Each plant has its own allometry, meaning its own proportions, so this reduction factor (same for all plants) does not accurately represent reality. While this 80% rule is arbitrary, it serves to validate the established vascular guideline and this assumption could be adapted if relevant plant data is provided.

- Above an inosculated node, the diameter of the cross-section is expected to decrease, as discussed in Section 3.1.5. However, the extent of this reduction was not quantified. Nevertheless, since the model should adhere to the pipe model theory combined to the resistance model (previous assumption) to ensure vascular viability, it is assumed that the diameter reduction is already considered within these models.

- *Plant competition* is not mathematically accounted for in the model. A comprehensive model should establish a density-dependent mortality relationship, as mentioned in Section 3.1.4. However, no precise data was found to determine the density at which plants can be sustained. Instead of establishing a mathematical law, a logical guess will be employed to prevent over-densification of the design. Additionally, by creating a unified system, inosculated plants reduce competition, thereby motivating this simplifying.

- Only thigmotropism (see Section 3.1.2), the growth in response to touch or contact, will be accounted for in this model. Thereby plants can be guided through a temporal structure, and take the desired shape. While this assumption may seem simplistic, it aligns with the current reality of Baubotanical design. Other tropisms such as phototropism, hydrotropism, and gravitropism are not considered, noting that they can be accounted for in future more elaborate models.

- The *plant addition principle* (see Section 3.1.6) is used for the the design of ivy and willow structures.

- An idealized approach to plant characteristics is considered, assuming that each plant of the same species has identical growth patterns and mechanical properties.

- The properties of plants, as outlined in Chapter 4, serve as the basis for the design. Since information on green plant properties is not extensively documented in the literature, in cases where data is unavailable, extrapolation or calculation was employed to define missing parameters.

- Simplified models for growth are proposed based on the data gathered in Chapter 4. For ivy and white willow, a linear growth pattern will be assumed. At the scale of a few years, the period focused upon here, this approximation can be justified. However, for bamboo, a slightly more complex growth pattern is proposed based on the Logistic rule.

- Plant tissue is treated as a homogeneous isotropic material. In Chapter 4, only longitudinal properties were collected. For the sake of simplicity, while plants exhibit different properties in the radial and tangential directions, these differences will not be considered in the model. Note that they could be incorporated in a future modelling step in a straightforward fashion.

- Nodes where inosculation takes place will be modeled as rigid nodes in the numerical simulation. While the literature does not provide clear evidence regarding the strength of these nodes, a complete inosculated cross-section (see Section 3.1.5) suggests a full merging of the tissues, indicating that nodes could be rigid joints in the structure.

- Structural anchorage in represented by clamped nodes in the FE simulation. While a comprehensive model for roots is proposed in Appendix F, root incorporation would lead to a model complexity beyond the scope of this work.
- The structural analysis is carried out through FE simulation using the Karamba plugin for Rhinoceros 3D. This plugin employs linear-elastic analysis. Displacements and axial stresses within the structure are evaluated using this plugin. The axial stress assessed by Karamba is the stress resulting from the combination of normal force and bending moments.
- For the sake of simplicity and computational efficiency, 1D elastic linear beam finite elements, following the Euler Bernoulli beam theory, are utilized for the numerical simulation.
- The "utilization" component from Karamba is employed to determine the maximum loading for each structure. This component considers both the peak axial stress and buckling [170].
- Verification for the maximum structural displacement is conducted using the criteria outlined in Eurocode EN 1992-2. Although this code is designed for concrete structures, the following criterion, was chosen to be applied (no criterion exist for living plant structures):

$$\delta \leq \frac{L}{250} \tag{5.2}$$

With δ the largest structural displacement (in cm) and L the largest structural dimension (in cm).

Chapter 6

Baubotanical modeling - 3 Living Architecture Applications

Based on the established assumptions in the previous Chapter 5, a growth and a structural model are developed for each plant. Additionally, an application of each of these models is demonstrated through 3 living architecture proposals.

6.1 Application 1 - Living Moso Bamboo pavilion

Nestled within the park's lush surroundings, the Moso ice cream pavilion stands as a testament to sustainable architecture, showcasing the feasibility of building with living elements. Constructed from living bamboo, this pavilion seamlessly blends functionality with natural beauty, offering a unique experience for visitors. The ground level hosts technical facilities and a welcoming counter, providing a convenient space for patrons to indulge in their favorite treats. Above, a bamboo platform offers a picturesque setting for enjoying ice cream while soaking in panoramic views of the park.

Figure 6.1: Living Moso bamboo pavilion

Since there is no evidence suggesting that bamboo is graftable, it will be assumed that it is not. Human-made metallic rigid joints are assumed to be linking each plants at the connecting nodes (moments are transferred). The project entails constructing a pavilion using living Moso bamboo. Bamboo will be assumed to grow straight[1] (not upward) and will serve as a support onto which a platform will be attached. To align with the characteristics of bamboo, it was decided to shape the pavilion following a ruled surface. A ruled surface is one that can be generated by moving a straight line (generator) along a path. In this project, the path will be a circle, where bamboo will be planted, and the bamboo itself will serve as the generator. This approach will result in the creation of a hyperboloid structure.

The challenge of this project lies in attaching the platform to the bamboo while the bamboo is still growing. It is necessary to determine when the bamboo will stop growing at the desired height of the platform. Additionally, it must be established when the bamboo will be sufficiently strong to support the platform. Therefore, a proper growth model is required, a specific ingredient that must be accounted for in computational Baubotanical design.

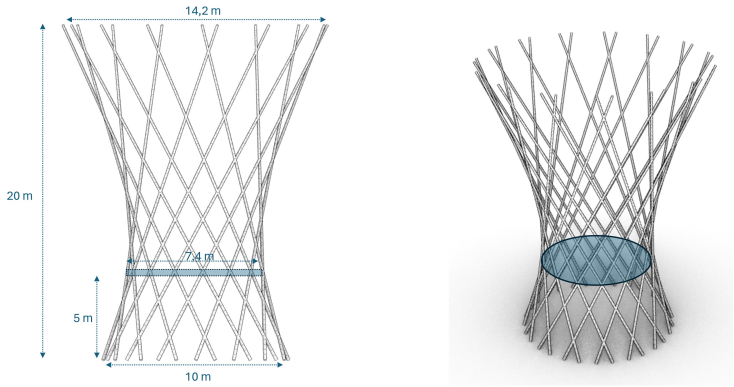

Figure 6.2: Target bamboo pavilion geometry

6.1.1 Growth model

Logistic rule adapted to Belgian climate

Moso bamboo growth follows the Logistic rule (cf Sec.4.1). According to the collected data, Moso bamboo grows 20 meters in 13 years (4745 days) in Belgium.

After testing the equations, it was observed that the growth parameter c could be adjusted for a new growing time T' while maintaining the same curve shape as in the original equation used for bamboo located in Asia. With c' and T' the new parameters corresponding to the Belgian climate.

$$c' = c \cdot \frac{T}{T'} \tag{6.1}$$

[1]Straight growth is an assumption to simplify the model. In reality, while bamboo does exhibit relatively straight growth, it tends to bend, especially at the top, due to gravity.

To adapt the Logistic rule to Belgium, the following parameters are used[2]: H' = H = 2000 cm, T' = 4745 days, and c' = 0.00405.

The resulting growth evolution for Belgium is plotted in the following graph:

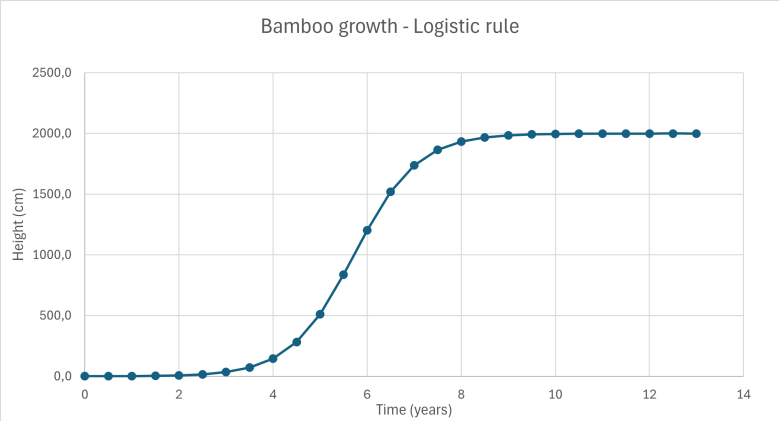

Figure 6.3: Proposed bamboo growth model in Belgian climate according to the Logistic rule

Internode Logistic adaptation

The Logistic model provides the total plant height as a function of time. However, to determine when it is possible to attach the platform, we need to determine when the bamboo will cease growing at the platform height. The model has then to be improved taking into account the telescopic growth of bamboo. The following assumptions will be taken into account to improve the model:

- An internode reaches a length of 30 cm at maturity (see Section 4.1). Therefore, approximately 67 internode elements are required to reach 20 m total stem length.
- Internode growth is supposed to take around half of the total bamboo growth time, therefore the assumption is made that the **growth time of an internode** T_{int} in our model should be around 6.5 years.
- Internodes follow the Logistic growing rule and they do not all start growing simultaneously. The lowest internode will commence growth first, followed by the second lowest internode, and so on. The last internode should begin growing approximately 6.5 years before the end of the plant's growth cycle, as it is the final growing segment. We will assume that internodes begin growing at constant intervals of time within these 6.5 years.

  The **trigger time** τ_i at which internode i starts to grow (internodes numbered from bottom to top) is expressed as:

$$\tau_i = \frac{i}{n} \cdot (T - T_{int}) \tag{6.2}$$

[2]As reminder: H is the stem length at maturity, T the time needed to reach maturity, c the growth parameter

With τ_i representing the trigger time expressed (in days), i the number assigned to each internode, n the total number of internodes, T the time needed for the plant to reach maturity (in days) and T_{int} the time required for internodes to reach maturity in days.

The **lived time** t_i (in days) of internode i is given by:

$$t_i = \begin{cases} 0 & \text{if } t \leq \tau_i \\ t - \tau_i & \text{if } t > \tau_i \end{cases} \tag{6.3}$$

The **length** h_i of internode i is then determined:

$$h_i = \frac{H_{\text{int}}}{1 + T_{\text{int}} \cdot e^{-c_{int} \cdot t_i}} \tag{6.4}$$

With h_i indicating the length of internode i (in cm). H_{int} is the internodes length at maturity (in cm), and c_{int} the internodes growth parameter.

For Moso bamboo in Belgium, the following values were used: $n = 67$, $T = 4745$ days, $T_{int} = 2372.5$ days, $H_{int} = 30$ cm, $c_{int} = 0.00810$. The internode growth parameter c_{int} is determined with Eq.(6.1) as follows: $c_{int} = c' \cdot \frac{T'}{T_{int}}$.

The height of the bamboo is determined by summing the heights of all internodes: $H' = \sum h_i$. Fig.6.4 plots the bamboo's height over time using this method. The red curves represent the growth of each internode, while the blue curve depicts the overall bamboo growth as the cumulative sum of all the red curves.

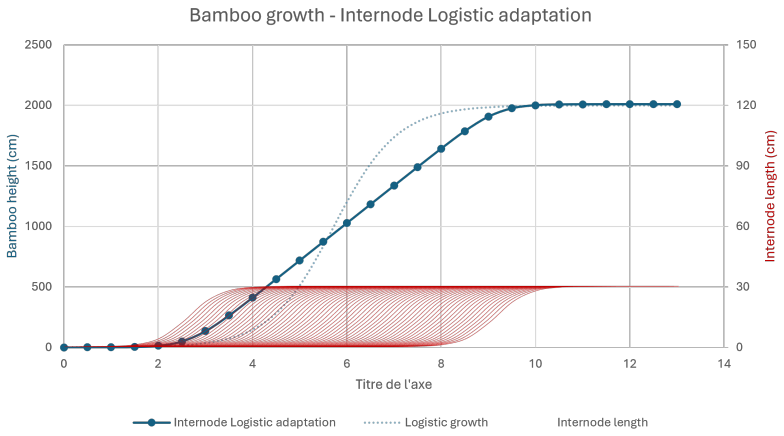

Figure 6.4: Adapted bamboo growth following Logistic rules for internodes

Note that the Internode Logistic adaptation model produces slightly different results compared to the standard Logistic model. During the first 5.5 years, it overestimates growth, while from 5.5 to 10 years, it underestimates growth. However, the overall difference is accepatable.

The platform is designed to be attached to the third series of bamboo crossings, located at approximately 5 meters height. Using the mathematical definition provided above, it is possible to determine when there will be no further growth at this height. Due to the geometry of the structure, a height of 5 meters corresponds to a bamboo length of 5.42 meters. As each internode has a length of approximately 30 cm, reaching 5.42 meters requires approximately 18 internodes. Therefore, the platform could be attached when the growth of the 18th internode ceases.

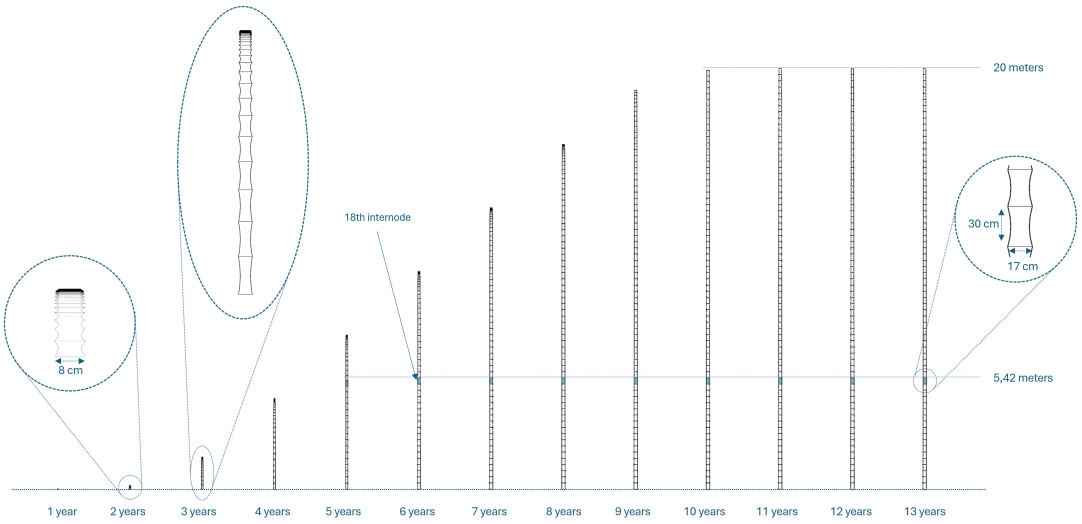

Figure 6.5: Growth of a bamboo following the proposed internode Logistic adaptation

From Eq.(6.2), it is determined that the 18th internode will start growing approximately $\tau_{18} \approx 1.74$ years after planting. An internode reaches approximately 99.6% (29.9 cm) of its final length in 4.5 years (see Fig.6.4). Therefore, it is estimated that the platform can be attached at 5 meter height after **6.24 years** of growth, based purely on the longitudinal plant growth model.

Note that at 6.24 years, we are underestimating growth (see Fig.6.4). As a result, there might still be unaccounted growth in the 18th internode, at this time.

Radial growth

Determining radial growth is crucial to characterize the geometrical properties of a bamboo cross-section over time. For the sake of simplicity, radial and wall thickness growth evolution are assumed to be uniform across the entire bamboo culm. Future work could develop a more precise model that accounts for these growth factors at each individual internode. From the collected data, Moso Bamboo starts with a diameter of 8 cm when young and reaches a diameter of 17 cm at maturity. Since no specific data on radial growth was collected, the general allometric rule is used (see Tab.3.1) that relates height growth to diameter growth:

$$\frac{dh}{dt} \propto \left(\frac{d\varnothing}{dt}\right)^{2/3} \tag{6.5}$$

With h the height (in cm), $\varnothing$ the diameter (in cm) and t the time (in days). Starting from this equation, a relationship is derived between the stem diameter and time:

$$\iff \varnothing \propto h^{5/2} + k \tag{6.6}$$

With k an integration constant. The height at instant 0 is null, h(0) = 0.

$$\iff \begin{cases} \varnothing_f &= \alpha \cdot H^{5/2} + \varnothing_0 \\ \varnothing_0 &= k \end{cases} \tag{6.7}$$

With $\varnothing_f$ the final diameter at maturity (in cm), $\varnothing_0$ the initial diameter (in cm), α a proportionality factor and H the height of the plant reached at maturity (in cm).

$$\iff \begin{cases} \alpha &= \frac{\varnothing_f - \varnothing_0}{H^{5/2}} \\ k &= \varnothing_0 \end{cases} \tag{6.8}$$

$$\iff \varnothing(t) = \frac{\varnothing_f - \varnothing_0}{H^{5/2}} \cdot h(t)^{5/2} + \varnothing_0 \tag{6.9}$$

With t the time elapsed (in days). By specifying $h(t)$, the diameter as a function of time can be expressed:

$$\iff \varnothing(t) = \frac{\varnothing_f - \varnothing_0}{H^{5/2}} \cdot \left(\frac{H}{1 + T' \cdot e^{-c't}} \right)^{5/2} + \varnothing_0 \tag{6.10}$$

With T' the time needed for the plant to reach maturity in Belgium (in days), c' the growing parameter in Belgium.

The following graph is obtained using the parameters: $\varnothing_f = 17$ cm, $\varnothing_0 = 8$ cm, $T' = 4745$ days, $H = 2000$ cm, $c' = 0.00405$.

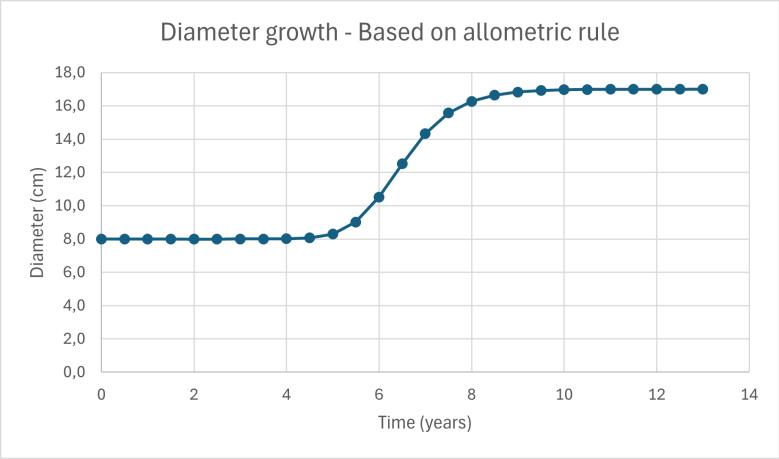

Figure 6.6: Diameter growth of Moso bamboo following allometric rules

Note that the assumption of starting with an 8 cm diameter might not be an issue, as the results of interest occur after several years (at least 6.24 years).

Growth in thickness

Another important parameter for characterizing the stem cross-section is the wall thickness. Based on the collected data, Moso bamboo reaches a wall thickness of 1.2 cm at maturity. In the absence of additional information on thickness, we will assume a linear relationship with the diameter (note that this assumption could be easily lifted provided the necessary data becomes available).

$$e(t) = \alpha \cdot \varnothing(t) + k \tag{6.11}$$

With e the thickness (in cm), $\varnothing$ the diameter (in cm), α and k constants.

The initial diameter $\varnothing_0 = 8$ cm, the final diameter $\varnothing_f = 17$ cm, and the final thickness $e_f = 1.2$ cm. The initial thickness e_0 will be determined as follow:

$$e_0 = e_f \cdot \frac{\varnothing_0}{\varnothing_f} \tag{6.12}$$

The equations yield: k = -0.00471 and $\alpha = 0.07059$. With these values, the evolution of the wall thickness of Moso bamboo is drawn:

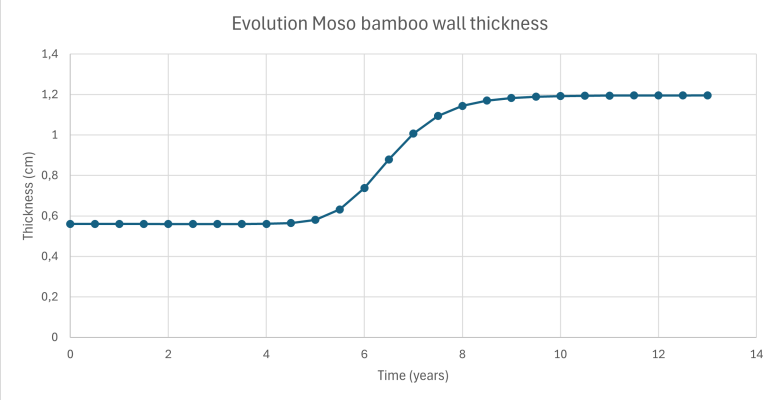

Figure 6.7: Evolution of the Bamboo wall thickness

Geometrical model

A script has been implemented in Grasshopper, providing two outputs: the bamboo geometry as a function of time and a structural model as a function of time implemented using the Karamba plugin.

The geometrical model is fed by the mathematical growth model detailed earlier. An illustration of the growing structure is provided in the following drawing:

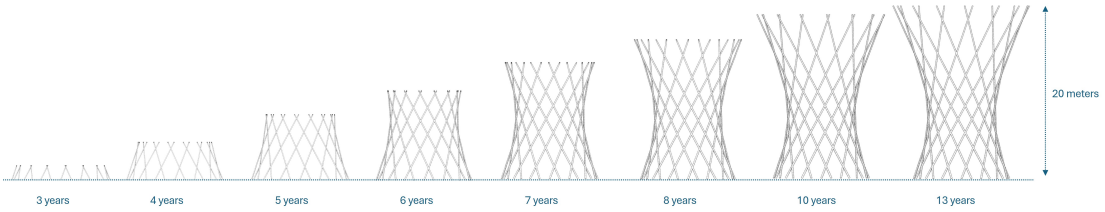

Figure 6.8: Evolution of the structural geometry as a function of time

Note that in reality a coupling between the applied mechanical loads and the plant growth exist, but is often neglected in Baubotanik [28]. It could be incorporated in future efforts for a coupled growth-structural problem.

6.1.2 Structural model

The structural model was constructed using 1D beam elements (1 per internode), with each internode maintaining a constant diameter along its length and evolving with time. Each bamboo is assumed to be anchored to the soil with fully clamped boundary conditions, and connections between bamboos are rigid. While this modeling approach may result in a stiffer structure compared to reality, it avoids delving into root or connection details for the sake of simplicity considering the main objective of addressing the feasibility of Baubotanical finite element modeling accounting for plant growth.

The self-weight of the bamboo and the weight of the platform are the considered loads. The platform weight encompasses both its self-weight and the additional load from service (e.g., people, furniture). According to Eurocode EN1991-1-1, the operating load for a cafe (which an ice cream pavilion can be assimilated to) is specified as 3 kN/m^2, while the self-weight of the platform itself is assumed to be 2 kN/m^2. Therefore, the total load transmitted by the platform to the bamboo structure is $Q_{platform} = 5$ kN/m^2. In the model, the weight of the platform is represented as vertical nodal loads pointing downwards distributed as follows:

$$f_{\text{connection}} = \frac{A_{\text{platform}}}{n_{\text{connections}}} \times Q_{\text{platform}} = 14kN \tag{6.13}$$

With, $f_{\text{connection}}$ the nodal load resulting from the platform's weight at each bamboo-platform connection, A_{platform} is the area of the platform, and $n_{\text{connection}}$ the total number of connections to the platform.

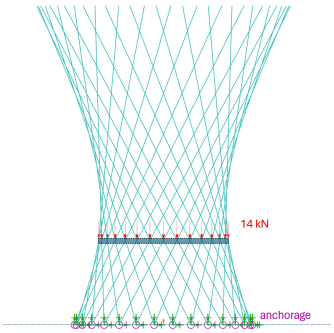

Figure 6.9: Moso pavilion structural model implemented in Karamba. Vertical point loads with a value of 14 kN are applied at the platform height. Anchorage (clamped nodes) is highlighted in purple.

The structural model allows for the determination of both stiffness and load bearing capacity of the structure over time. In this project, stiffness is defined as the maximum structural displacement under a load of 5kN/m^2 on the platform. While the load bearing capacity is defined as the maximum admissible load on the platform, determined when the critical beam element reaches a utilization of 100%, calculated by the "utilization component" in Karamba (see Ch.5).

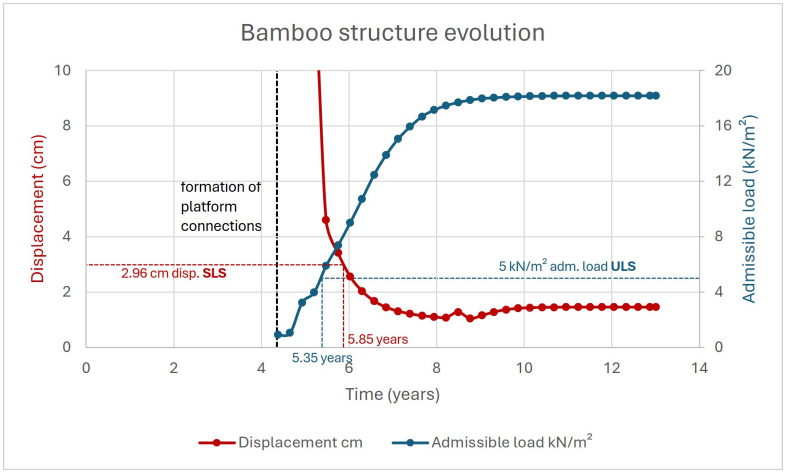

Figure 6.10: Evolution of stiffness and bearing capacity of the living bamboo structure as a function of time. The red curve represents the maximum structural displacement under a loading of 5 kN/m^2 on each platform, the blue curve represents the admissible load on each platform.

In Fig.6.10, the maximum displacement ranges from 0 to 10 cm. However, this range fails to capture the initial stage: specifically, at 4.4 years, it is 65.9 cm, under a loading of 5 kN/m^2. This significant difference is due to the less rigid structure at early stages, particularly before the first connection above the platform is formed. The structure is able to support a load of 5 kN/m^2 on the platform from 5.35 years onward.

The span-deflection ratio (see Eq.5.2) from Eurocode EN 1992-2 is utilized to verify if the resulting deformation is within acceptable limits. By using a span of L = 740 cm (see figure 6.2), the admissible deflection is about 2.96 cm. It requires approximately 5.85 years of growth to achieve

acceptable deformation (see Fig.6.10).

Fig.6.11 illustrates the deformation of the structure under the loads given in Fig.6.9. The scale of deformation is intentionally exaggerated to aid visualizing it. Note that the platform is only represented in the model as point loads; its proper integration using shell FE would have added more rigidity to the structure, which is particularly relevant since the platform is located near the areas with the most significant deformation.

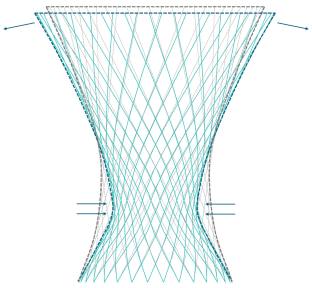

Figure 6.11: Living bamboo pavilion: initial and deformed shape in grey and blue, respectively. Arrows indicate the deformation direction (displacements are magnified for visibility)

Finally, two graphs are presented to illustrate the behavior of the structure over time. Fig.6.12 depicts the axial stress in the beams under a loading equivalent to 5 kN/m^2 on the platform and Fig.6.13 illustrates the maximum displacement of the structure under the same loading conditions. These graphs show the reduction in both stress and deformation over time.

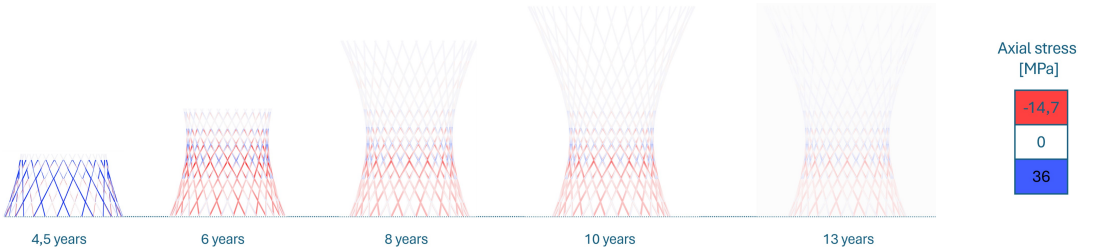

Figure 6.12: Evolution of the axial stress under a loading equivalent to 5kN/m^2 vertical load on the platform

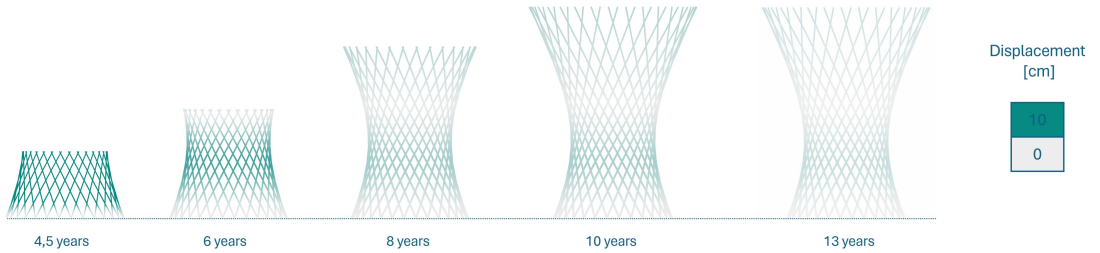

Figure 6.13: Evolution of the deformation under a loading equivalent to 5kN/m^2 vertical load on the platform

According to the Fig.6.10 the structure should be able to carry a 5kN/m^2 load after approximately 5.35 years of growth. However, it was determined that the structure required 6.24 years of growth for there to be no further growth below the platform. The following values were evaluated at 6.24 years:

$$\begin{cases} \text{Maximum displacement} & = & 4.6 \text{ cm} \\ \text{Vertical displacement} & = & 0.86 \text{ cm} \\ \text{Maximum axial compressive stress} & = & 22.24 \text{ MPa} \\ \text{Maximum axial tensile stress} & = & 21.59 \text{ MPa} \end{cases} \tag{6.14}$$

Both SLS (5.85 years) and ULS (5.35 years) are satisfied for the living bamboo pavilion, the constraint was to wait the end of growth at 6.24 years.

6.2 Application 2 - Living White Willow observatory tower

Perched gracefully atop a cliff, towering eighteen meters high over the sea, the ten-meter structure offers breathtaking vistas of both the ocean and Helsinki's cityscape. Located on Korkeasaari Island, its transparent design seamlessly integrates with the natural environment, drawing inspiration from the island's surroundings. Mirroring the soft contours of the nearby stone wall and gracefully embracing a picturesque birch grove, the tower enriches the scenic allure of the landscape. [171]

This project replicates the design of the existing observation tower, Kupla, located in Korkeasaari Zoo and designed by Avanto Architects. It features a glulam gridshell structure with three levels [171].

Figure 6.14: Helsinki observation tower Kupla ©Jussi Tiainen

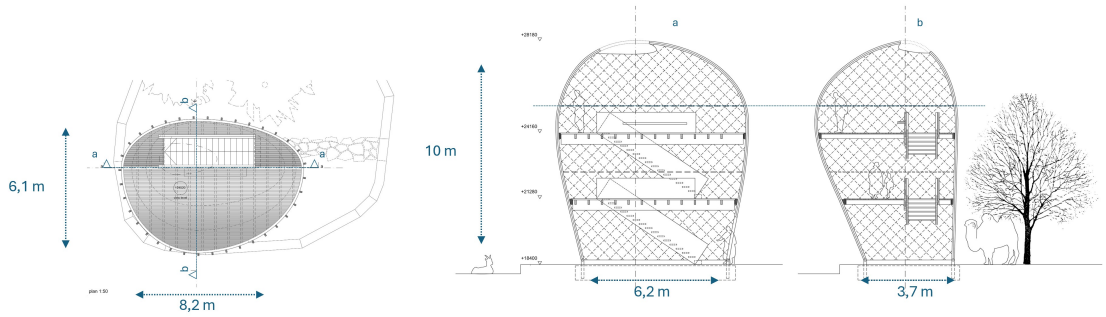

Figure 6.15: Helsinki observation tower Kupla dimensions [172]

The idea behind replicating an existing project is to assess whether living architecture design can reproduce what is already proposed in the construction industry. The challenge here lies in adapting an existing geometry to Baubotanik, whereas in general, the approach would be the inverse: the geometry should be designed according to Baubotanical design rules. The *plant addition principle* (see Section 3.1.6), combined with a temporary scaffolding, as utilized for the Baubotanik tower (see Section 2.2), will be employed. Since inosculation is utilized in this project, one of the main challenges is to ensure the proper vascularization of the plants. The following drawing illustrates the concept of temporary scaffolding to support plant growth. Once the structure is strong enough, the scaffolding can be removed.

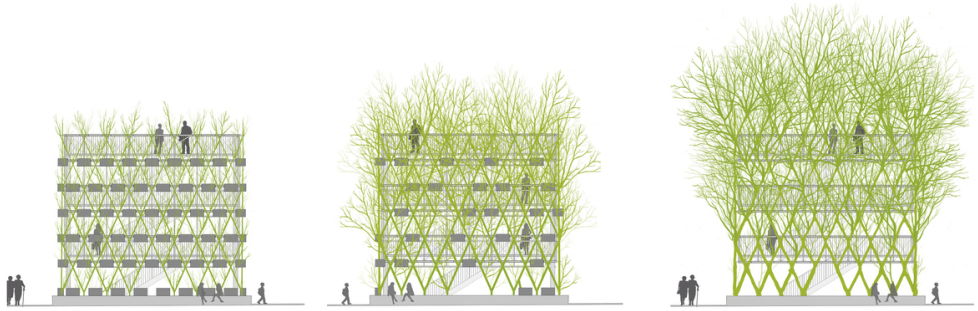

Figure 6.16: Temporary scaffolding to support growth. Image drawn by Ludwig and Schönle to illustrate the development of the Plane Tree Cube project

6.2.1 Growth model

From the literature on Salix alba L., a longitudinal growth rate of 60 cm/year was obtained. Additionally, a measured diameter of approximately 8 cm was recorded after 8 years (2920 days) of growth.

Before delving into the willow growth model, it's important to note that a constant longitudinal growth rate is not ideal. This approach not only fails to reflect the reality of plants experiencing different growth stages, but it can also lead to incoherent results. In fact constant growth

rate could potentially lead to endless growth which is not the case in nature. The idea here is to focus on the early stages of growth for which the linear growth assumption is less questionable.

With the given data, we lack information on the radial growth rate, which might prompt us to consider employing allometric rules for its determination (as done here to showcase the excessive results it provides). Given the initial diameter of 0 cm ($\varnothing_w(0) = 0$) and a diameter of 8 cm after 8 years ($\varnothing_w(2920)) = 8$ cm), a development similar to that in Eq.6.9 (which is based on an allometric rules) can be applied, yielding the following relationship (plotted in Fig.6.17):

$$\varnothing_w(t) = 1.736 \cdot 10^{-8} \cdot t^{5/2} \tag{6.15}$$

With t the time (in days) and $\varnothing_w$ the stem diameter (in cm).

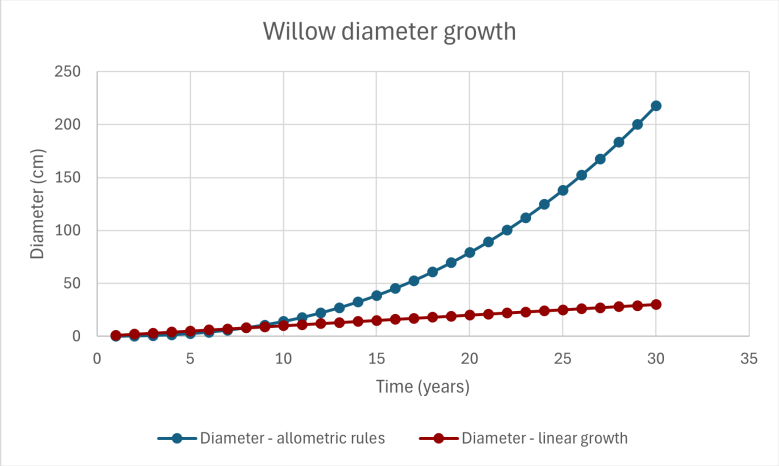

Figure 6.17: Willow stem diameter evolution: blue curve resulting from the allometric rules, red one from a linear growth rate.

Fig.6.17 depicts the evolution of willow stem diameter resulting from the allometric rules in blue and a linear growth rate in red. The validity of the blue curve is limited: at a certain point (20 years onward), the diameter becomes unrealistically significant. This arises from the assumption of a constant longitudinal growth rate, taken due to the absence of precise data on it. It's worth noting that capping the diameter growth with an allometric rule at the peak diameter could also be considered. When accurate data becomes available, the growth model can be easily adjusted. However, the linear diameter is taken for now (red curve in Fig.6.17).

In our assumptions (see Ch.5), a thinning of the stem cross section was assumed, where the top stem diameter is represented as u times the basal diameter, with u the reduction factor. The following equations reflect this assumption:

$$\begin{cases} \text{Base diameter:} & \varnothing_{w,base}(t) = \frac{d\varnothing_w}{dt} \cdot t \\ \text{Top diameter:} & \varnothing_{w,top}(t) = u \cdot \varnothing_{w,base}(t) \end{cases} \tag{6.16}$$

With t the time (in days), $\varnothing_{w,base}$ the willow stem basal diameter (in cm), $\varnothing_{w,top}$ the willow stem top diameter (in cm), $\frac{d\varnothing_w}{dt}$ the willow radial growth rate (in cm/day), u the reduction factor. The following drawing illustrates the nomenclature used for Eq.(6.16).

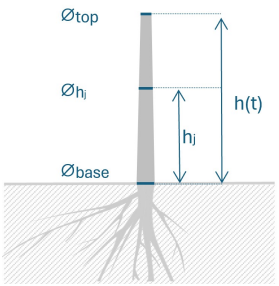

Figure 6.18: Illustration of the stem diameter reduction factor. With h_j a certain height withing the stem, h the total height of the stem, $\varnothing_{h_j}$ and $\varnothing_{top}$ are the corresponding diameter at these heights along the stem, and $\varnothing_{base}$ the basal diameter

By combining these equations, and assuming a linear diameter evolution for the willow stem with time, the diameter can be determined at any height h_j within the plant:

$$\varnothing_{w,h_j}(t) = \varnothing_{w,base}(t) \cdot (1 - \frac{h_{w,j}(1-u)}{h_w(t)}) \tag{6.17}$$

With $\varnothing_{w,h_j}$ the stem diameter (in cm) at a certain height $h_{w,j}$ (in cm) within the stem , h_w the total length of the stem (in cm).

Finally, the following equations are used to describe the growth of Salix alba L.:

$$\begin{cases} \text{Longitudinal growth:} & h_w(t) = \frac{dh_w}{dt} \cdot t \\ \text{Diameter growth at height } h_{w,j}\text{:} & \varnothing_{w,h_{w,j}}(t) = \varnothing_{w,base}(t) \cdot (1 - \frac{h_{w,j}(1-u)}{h_w(t)}) \end{cases} \tag{6.18}$$

With $\frac{dh_w}{dt}$ the willow longitudinal growth rate (in cm/day).

The following parameter values are used for the willow model: $\frac{dh_w}{dt} = 0.1644$ cm/day , $\frac{d\varnothing_w}{dt} = 0.0014$ cm/day and u = 0.8.

6.2.2 Vascular condition

The structure will be assembled by joining different plants together through inosculation. It is essential to adhere to the vascular condition (see Eq.5.1) to ensure the viability of the system. This condition will define the construction sequence for this structure.

Connections are grouped into series of points located at the same level (see Fig.6.19). It is assumed that at each crossing, a plant will be planted on a scaffold, resulting in each inter-crossing element being a single stem plant (no plant will join more than two crossing points). To ensure the vascular condition is met, the section of the lower plant has to be superior or equal to the section of the plant above at the moment they join. To achieve this, a trigger time should be determined for each plant to start growing on the initially supporting scaffold, with plants above starting to grow later than those below.

Let us call i a level of connections in the structure, with the lowest level of connections being $i = 0$. A plant starting to grow at a level i will be defined by subscript i. For instance l_i is the length between a connection i at levels and $i + 1$.

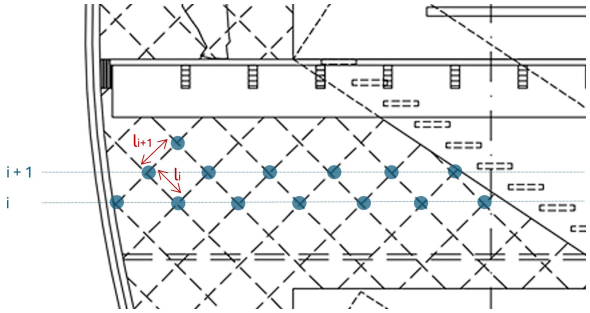

Figure 6.19: Scheme of the connection levels. Plant crossings (highlighted by blue dots) are aligned at a level. The lengths between crossings at level i and crossings at level $i+1$ is defined as l_i

The stem element i will reach the connection $i+1$ within the time $t_{l_i} = \frac{l_i}{\frac{dh}{dt}}$. A trigger parameter τ_i will be established, and each plant on level i will start to grow at the time τ_i. Note that this is an idealized approach where all plants are considered to grow equally.

$$\begin{cases} \varnothing_{top,i}(t_{l_i}) & = & u \cdot \varnothing_{base,i}(t_{l_i}) \\ \varnothing_{base,i+1}(t_{l_i} - \tau_{i+1}) & = & \varnothing_{top,i}(t_{l_i}) \end{cases} \tag{6.19}$$

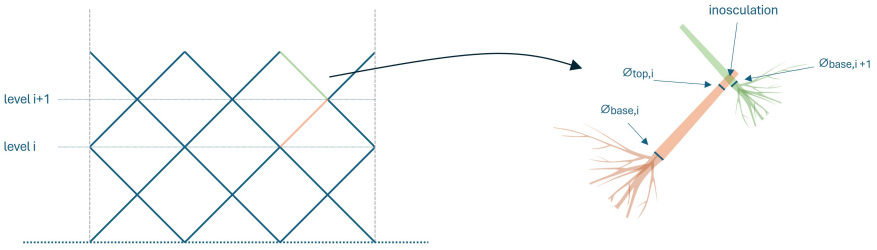

Figure 6.20: Nomenclature used for the equation 6.19

Based on Eqs.(6.19), the trigger time τ_i for each plant to begin growing can be determined. In a way that when a plant on level i meets plant on level $i+1$, the top diameter of plant i ($\varnothing_{top,i}$) matches the basal diameter of plant $i+1$ ($\varnothing_{base,i+1}$).

$$\iff \varnothing_{base,i+1}(t_{l_i} - \tau_{i+1}) = u \cdot \varnothing_{base,i}(t_{l_i}) \tag{6.20}$$

$$\iff \frac{d\varnothing}{dt}(t_{l_i} - \tau_{i+1}) = u \cdot \frac{d\varnothing}{dt} \cdot t_{l_i} \tag{6.21}$$

$$\iff \tau_{i+1} = (1-u) \cdot t_{l_i} \tag{6.22}$$

$$\iff \tau_i = (1-u) \cdot t_{l_{i-1}} \tag{6.23}$$

Note that the trigger time of element $i-1$ should also be considered when defining the trigger time of element i:

$$\iff \tau_i = (1-u) \cdot t_{l_{i-1}} + \tau_{i-1} \tag{6.24}$$

Plants at level i are thus intended to start growing at the trigger time τ_i. To conclude this mathematical definition, it should be added that when an element reaches length l_i, its longitudinal growth ceases because their tips will be cut:

$$\begin{cases} h(t) = \frac{dh}{dt} \cdot t & \text{if } \frac{dh}{dt} \cdot t \leq l_i \\ h(t) = l_i & \text{if } \frac{dh}{dt} \cdot t > l_i \end{cases} \tag{6.25}$$

The mathematical growth model described above was implemented into Grasshopper to generate a parametric geometrical model of this structure. The evolution of the geometry of the structure over time, is illustrated in Fig.6.21:

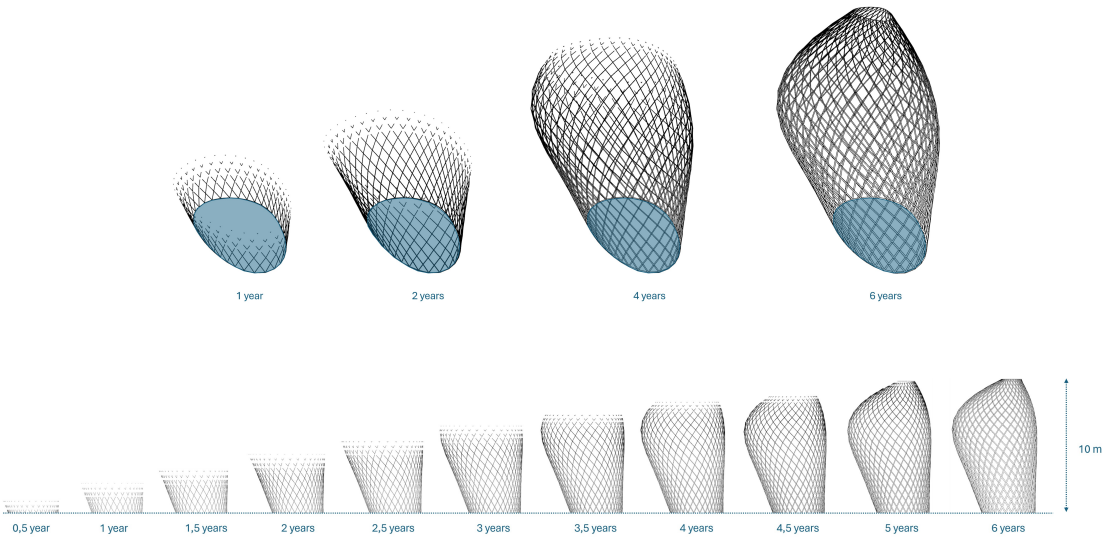

Figure 6.21: Evolution of the geometry of the living willow observation tower structure

Thanks to this model, it is estimated that it will take approximately 6 years for the structure to form. Additionally, it allows for the verification that the vascular condition is satisfied. Fig.6.22 illustrates that a section in the lower part of the structure results in a larger area than a section in a higher part.

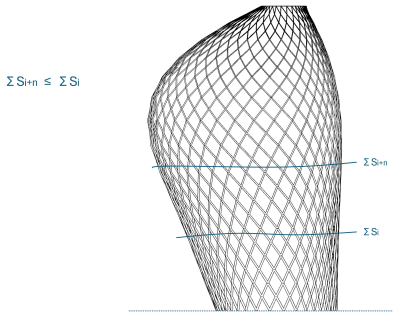

Figure 6.22: Vascular condition verified for the willow structure at 6 years growth time

6.2.3 Structural model

The previous geometrical model has been adapted to construct an evolving structural (FE) model. The assumption is made that the diameter along one element remains constant; it is equal to the diameter at the position of the end connection. Note that while there is no diameter reduction along a beam element, the diameter still changes with time. As we take the lowest diameter in the element, this approach is conservative. This decision is primarily made to simplify the implementation into the Karamba FE model.

The model adheres to the hypotheses established in chapter 5: 1D FE elements are utilized for beams (each segement is 1 FE), connections between plants are considered rigid, and plants at ground level are anchored through clamped nodes.

The self-weight of the willow ($\rho_w = 529$ kg/m^3) and the weight of the platforms (5 kN/m^2, as in Section 6.1.2) are the considered loads. The same approach as the one used for the living bamboo pavilion represents the platforms only as loads in the model. The loading and boundary conditions are illustrated in Fig.6.23.

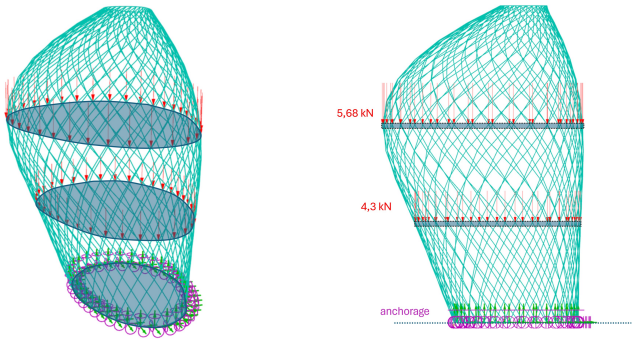

Figure 6.23: Structural model of the living willow structure implemented in Karamba. Vertical point loads with a value of 5.68 kN and 4.3 kN are applied respectively to the upper platform and the lower platform connecting nodes. Anchorages are highlighted in purple.

Stiffness and load bearing capacity are defined as in Section 6.1.2. The structure is estimated to form in about 6 years, therefore the structural analysis commences at this time.

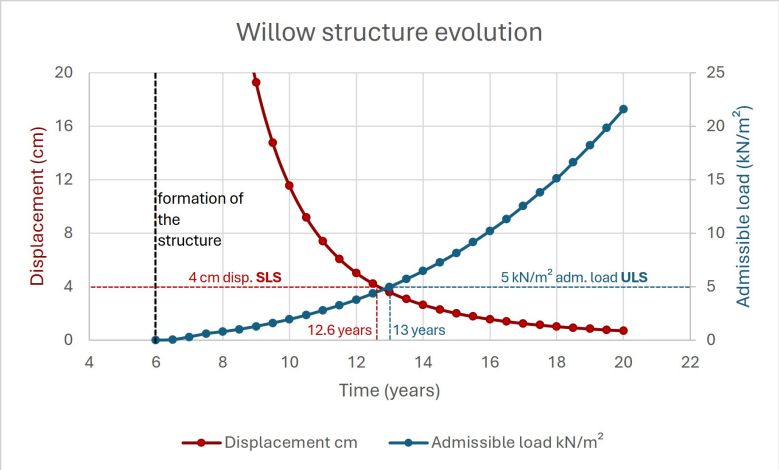

Figure 6.24: Evolution of stiffness and bearing capacity of the living willow structure as a function of time. The red curve represents the maximum structural displacement under a loading of 5 kN/m^2 on each platform, the blue curve represents the admissible load applied on each platform.

In Fig.6.24, the maximum structural displacement at 8 years is 35.65 cm under a loading of 5 kN/m^2 on each platform. The load bearing capacity reaches 5kN/m^2 at 13 years.

The span-deflection ratio from Eurocode EN 1992-2 (see Eq.5.2) is utilized to verify if the resulting deformation is within acceptable limits. By using a span of L = 1000 cm, the admissible deflection is about 4 cm. The willow structure requires 12.6 years of growth to have admissible displacement.

Fig.6.25 illustrates the deformation of the structure under the loads given in Fig.6.23. The deformation is intentionally magnified to ease visibility. The structure deforms as expected, primarily in the direction of the larger off-center portion. It's important to note that the platforms are only included in the model as loads, like in the previous model, having similar implications (lower stiffness).

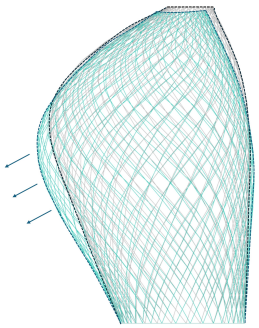

Figure 6.25: Initial and deformed shape of the living willow structure in grey and blue, respectively. Arrows indicate the deformation direction (displacements are magnified for visibility)

Finally, Fig.6.26 and Fig.6.27 are presented to illustrate the behavior of the structure over time. Fig.6.26 depicts the axial stress in the beams under a loading of 5 kN/m^2 on each platform and Fig.6.27 illustrates the maximum structural displacement of the structure under the same loading conditions. The reduction in both stress and deformation over time can be clearly observed, as expected.

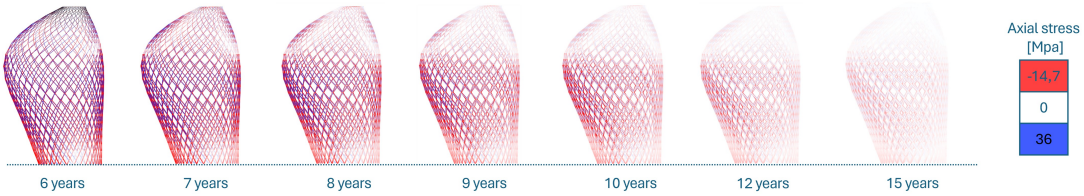

Figure 6.26: Evolution of the axial stress under a load of 5kN/m^2 on each platform

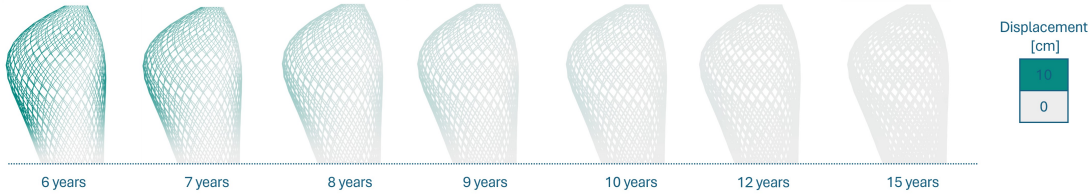

Figure 6.27: Evolution of the maximum displacement under a load of 5kN/m^2 on each platform

Based on the model built, the structure is projected to become functional after approximately 13 years of growth. The following values were evaluated at this stage:

$$\begin{cases} \text{Maximum displacement} & = & 3.59 \text{ cm} \\ \text{Vertical displacement} & = & 2.25 \text{ cm} \\ \text{Maximum axial compressive stress} & = & 9.66 \text{ MPa} \\ \text{Maximum axial tensile stress} & = & 8.83 \text{ MPa} \end{cases} \tag{6.26}$$

Both SLS (12.6 years) and ULS (13 years) are satisfied for the living willow structure. The ULS is the limiting constraint, and the structure is estimated to be functional after 13 years.

6.3 Application 3 - Living Ivy footbridge

The Living Ivy Foot Bridge is a 15-meter span structure designed to cross a river. Serving as both a pedestrian thoroughfare and an ecological asset, the bridge minimizes environmental impact while enhancing biodiversity. Through innovative design and sustainable practices, it harmonizes with the surrounding environment, embodying a synergy between human infrastructure and nature.

This project aims to design a 15-meter footbridge constructed using living ivy. Ivy was chosen as a solution to avoid creating a large temporary installation to support plant growth. Cables

will be attached from both sides of the ditch, serving as support for the ivy to grow upon. Ivy's flexibility and grafting ability are two elements that are harnessed for this project. This project uses inosculation and thus is a plant addition based Baubotanical application. This structure is shaped using catenaries pointing downwards for two main reasons. First because the Ivy's resistance in tension is larger than its resistance in compression (see Tab.4.3). Also due to the large span, cables, which are efficient and easy to implement, are used to guide ivy growth; and the natural hanging shape of a cable is a catenary. This is not the main focus of this paper, but to create a more efficient structure, a form-finding process using the Kangaroo plugin was conducted to generate the 2D geometry. The final project geometry is illustrated in Fig.6.28:

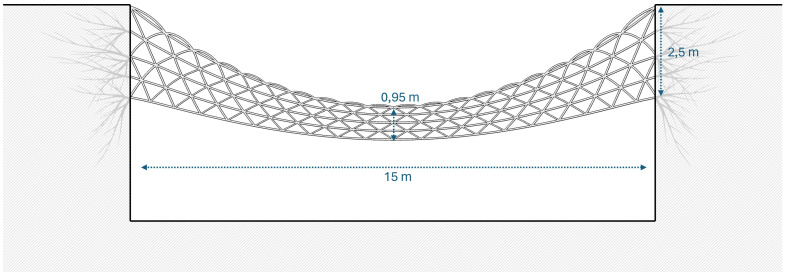

Figure 6.28: Living Ivy footbridge geometry side view

The structure will be constructed using the *plant addition principle* (see Section 3.1.6). The process involves three steps. Initially, cables will be placed to guide the growth of the plants. Next, primary elements will grow along the cables. Finally, secondary elements will be grown, aiming to unify the structure into one cohesive entity. To ensure proper vascularity, sections of the elements closer to the center should be smaller than those at the sides. Consequently, the plants closer to the center should be planted later.

The growth construction process is illustrated in Fig.6.29. In step 3, the red elements are planted earlier than the yellow elements in order to ensure a proper vascularity within the structure. Additionally, containers for growing plants are attached to the cable structure in this step. These containers will be removed once inosculation is effective, allowing the structure to stand as a unified entity.

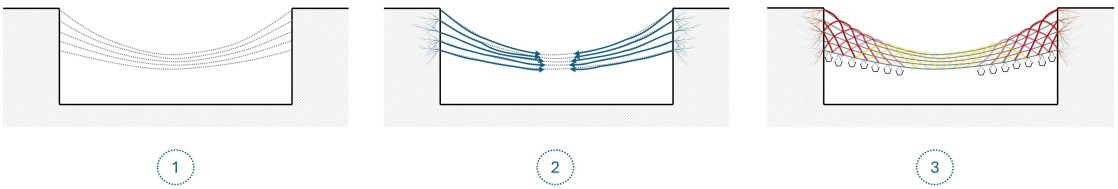

Figure 6.29: Living Ivy footbridge growth process. 1) Establishment of the temporary cable structure, 2) Growth of primary elements, 3) Growth of secondary elements; red elements are planted the earliest in this step

6.3.1 Growth model

From the literature on Hedera helix L., a longitudinal growth rate of 100 cm/year has been observed, along with a radial growth rate of 0.15 cm/year. No additional data has been found to

develop a more precise growth model. The allometric rules are not applied in this case, because we already have the specific growth rates. While using linear growth may not result in the most accurate model, it should be sufficient to draw first conclusions for this structure.

The following parameter values were used in Eqs.(6.18) to represent ivy growth with a linear growth model: $\frac{dh}{dt} = 0.274$ cm/day , $\frac{d\varnothing}{dt} = 4.11 \times 10^{-4}$ cm/day and u = 0.8.

6.3.2 Vascular condition

The structure will be assembled by joining different plants together through inosculation. It is essential to adhere to the vascular condition to ensure the viability of the system. This condition will define the construction sequence for this structure.

The principal elements will be grown first. As these elements don't depend on other elements, they will be planted at time t = 0. The same applies for secondary elements planted in the ground on both sides of the structure. On the contrary, the secondary elements planted on containers hanging from the temporary structure should have a trigger time to ensure that total area of the cross section on the structure diminishes when closer to the center to ensure satisfying the vascular condition. The trigger time depends on the development of previously existing elements.

Fig.6.30 illustrates the concept of trigger times for each plant.

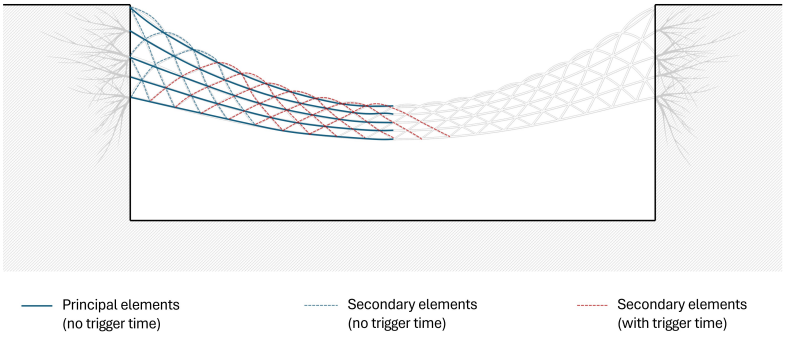

Figure 6.30: Ivy footbridge triggered growth. The elements in blue do not require a trigger time; they start growing at t = 0. The red elements, however, require a trigger time. Each red element must wait for the preceding dotted blue element to grow sufficiently before it can begin to grow.

In Fig.6.30 red dotted elements depend on the blue dotted elements, following Eq.(6.24):

$$\tau_{red} = (1 - u) \cdot t_{l_{blue}} \tag{6.27}$$

With τ_{red} the trigger time for red elements, $t_{l_{blue}}$ the time needed for the blue element to reach the point where it would encounter the red element to be able to form a common node.

The model was designed to ensure the vascular condition, as illustrated in the Fig.6.31.

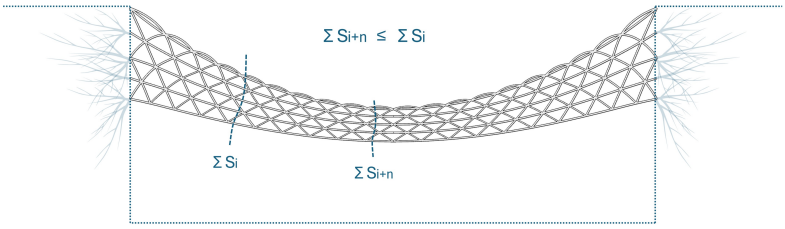

Figure 6.31: Verification of the vascular condition

Resulting growth

The mathematical definition described above was implemented in Grasshopper to create the growing geometry. Fig.6.32 illustrates the growth of the living ivy bridge over a period of 10 years following the implemented model.

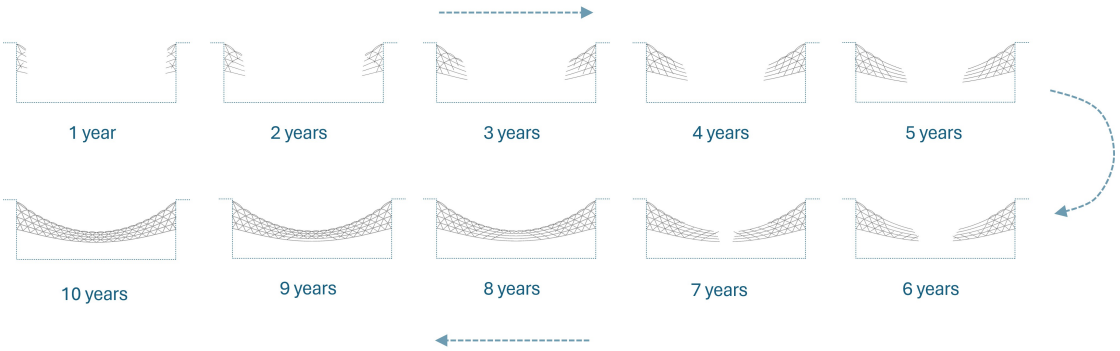

Figure 6.32: Ivy footbridge growth evolution

6.3.3 Structural model

The previously established geometry was adapted with slight modifications to construct an evolving structural FE model in Karamba. Curved elements were discretized into straight elements between each intersection. Additionally, the curved elements at the top were not included in the model. These changes were made to simplify the implementation in Karamba (the differences are highlighted in Fig.6.33).

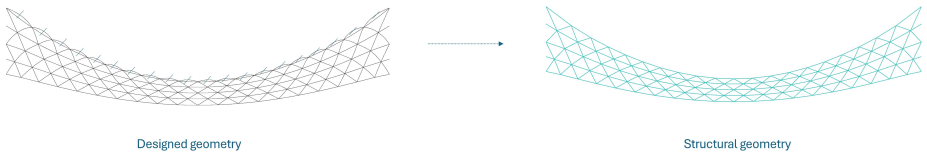

Figure 6.33: Living ivy footbridge designed geometry vs discretized structural geometry

1D FE elements are utilized (1 per segment), connections between beams are considered rigid, and plants are anchored through clamped nodes at the roots (left and right boundaries) as shown

in Fig.6.34.

According to NBN EN 1991-2, the service load q on a footbridge should be calculated as follows:

$$q = 2 + \frac{120}{L + 30} \quad [kN/m^2] \tag{6.28}$$

With L the span of the footbridge (in meters).

The living ivy footbridge spans 15 meters, resulting in a service load of approximately $q = 4.7\,\mathrm{kN/m^2}$. For simplicity, the deck of the bridge is not modeled. Instead, the loads will be distributed and carried by the modeled elements. The deck itself should be made of ivy covered by wooden planks. As for other projects, we will consider a self-weight of 2 $\mathrm{kN/m^2}$. Therefore, the resulting design load is $Q_{deck} = 6.7\,\mathrm{kN/m^2}$.

Loads will be represented by vertical nodal loads pointing downwards applied at the lowest connections (see Fig.6.34). The load on each node is calculated as follows:

$$f_{\text{connection}} = \frac{A_{\text{deck}}}{n_{\text{connections}}} \times Q_{\text{deck}} \tag{6.29}$$

With, $f_{\text{connection}}$ the nodal load resulting from the deck, A_{deck} the area of the deck, and $n_{\text{connection}}$ the total number of connections to the deck (bottom nodes). The length of the deck, measured in the Rhinoceros model, is approximately 15.3 meters, and the width is supposed to be 1.3 meters. The number of connections (considering both sides) is $n_{\text{connections}} = 38$. Therefore, the load on each connection is estimated to be $f_{\text{connection}} = 3.5\,\mathrm{kN}$.

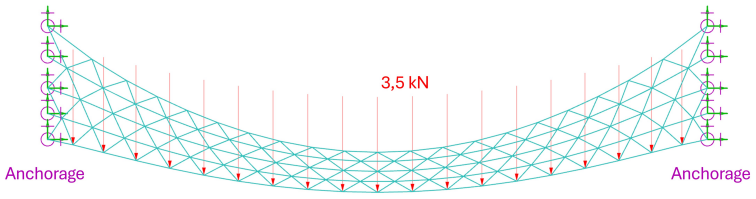

Figure 6.34: 2D FE model of the living ivy footbridge implemented in Karamba. Vertical point loads with a value of 3.5 kN are applied to the footbridge deck. Anchorages are highlighted in purple.

In this project, stiffness is quantified through the maximum displacement under a load of 6.7 $\mathrm{kN/m^2}$ on the deck, while strength is defined as the maximum admissible load on the deck when the critical beam element reaches a utilization of 100%, calculated with the "utilization component" in Karamba.

The structure is estimated to form in about 10 years, therefore the structural analysis commences at this time.

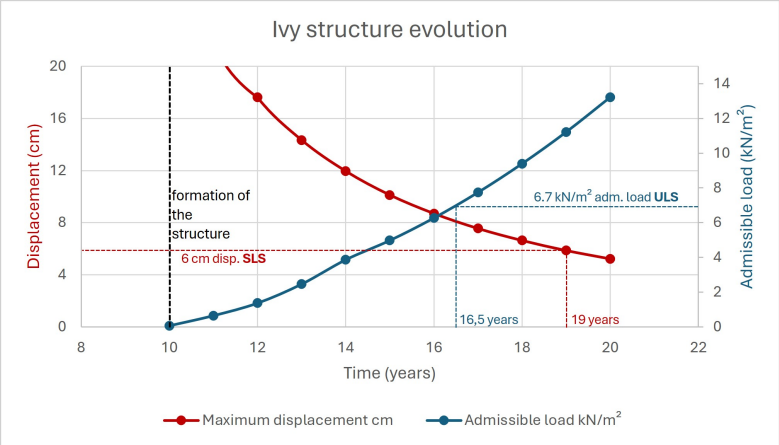

Figure 6.35: Evolution of stiffness and bearing capacity of the living ivy structure as a function of time. The red curve represents the maximum structural displacement under a loading of 6.7 kN/m^2 on each platform, the blue curve represents the admissible load on each platform.

Fig.6.36 illustrates the deformation of the structure under the loads. The 2D structure deforms as expected. It's important to note that a full 3D representation of this bridge could be set up in a straightforward manner in future work.

The span ratio from Eurocode EN 1992-2 is utilized to verify if the resulting deformation is within acceptable limits. By using a span of L = 1500 cm, the admissible deflection is about 6 cm. Therefore the deflection at 17 years of growth is not acceptable. The deflection become acceptable after 19 years of growth with a value of approximately 6 cm.

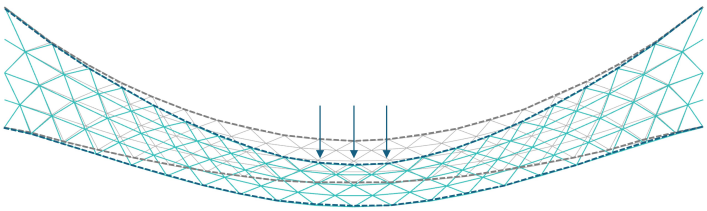

Figure 6.36: Initial and deformed shape in grey and blue, respectively. Arrows indicate the deformation direction. (Displacements magnified by a scale factor for visibility

Finally, Fig.6.37 and Fig.6.38 illustrate the behavior of the structure over time. Fig.6.37 depicts the axial stress in the beams under a loading of 6.7 kN/m^2 on the deck and Fig.6.38 illustrates the maximum structural displacement of the structure under the same loading conditions. The reduction in both stress and displacement over time can be observed.

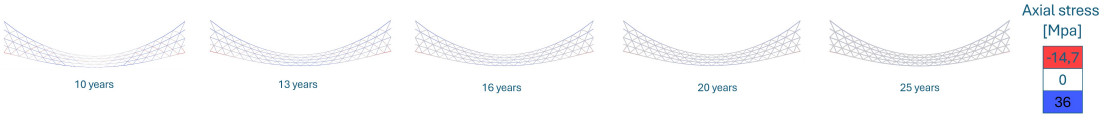

Figure 6.37: Evolution of the axial peak stress under a loading of 6.7 kN/m^{2}on the deck

Figure 6.38: Evolution of the maximum displacement under a loading of 6.7 kN/m^2

Based on the model built, the structure should be able to carry the applied load after approximately 17 years of growth. The following values were evaluated at 17 years:

$$\begin{cases} \text{Maximum displacement} & = & 7.56 \text{ cm} \\ \text{Maximum axial compressive stress} & = & 6.34 \text{ MPa} \\ \text{Maximal axial tensile stress} & = & 11.14 \text{ MPa} \end{cases} \tag{6.30}$$

Both SLS (19 years) and ULS (16.5 years) are satisfied for the living willow structure. The SLS is the limiting constraint, and the structure is estimated to be functional after 19 years.

6.4 Discussion

Based on the developed modeling approach, the proposed projects appear feasible from a structural strength and stiffness points of view. The Living Moso Bamboo pavilion should be functional after 6.5 years of growth, the Living White Willow observatory tower should be functional after 13 years of growth and the Living Ivy footbridge should be functional after 19 years of growth.

The growth model plays a determinant role in assessing the feasibility of Baubotanical designed projects. In this work, the approach is to derive the geometry from the growth model and then apply a finite element analysis to this geometry. In future work, both models could be combined in an iterative process, as loads applied to living, growing plants influence their growth.

Although a similar design approach was used across all three projects, the utilization of different plant species tailored to different applications resulted in distinct limiting constraints for each project. The bamboo pavilion project is not a Baubotanical design since it does not utilize inosculation. For this project, it was necessary to estimate the point at which there would be no more significant growth below the platform height (this was the limiting constraint), so that the platform could be properly attached to the bamboo structure. On the other hand, the willow observatory tower and the ivy footbridge represent Baubotanical applications. These projects required the development of a specific construction process to ensure the vascular viability of plants. For the living willow structure, the limiting constraint was the admissible load (ULS),

while for the living ivy footbridge, the limiting constraint was the admissible maximum displacement (SLS).

Assuming the administrative and design stage duration is the same for Baubotanical and conventional projects, the point of comparison would be the construction time. Based on a brief review of current projects, the estimated construction time for such conventional projects can be estimated 1 to 2 years at most. The long growing phase required for Baubotanical designs is a significant concern for their practical application. Additionally, while not in use, these living structures require constant attention and maintenance. However, throughout their lifespan, they provide the benefit of CO2 absorption (see section 6.4.1).

It is important to emphisize that the growth models in this work were simplified. While clearly not constituting an exhaustively complete model, the goal here was to focus on the structures until they become serviceable (early growth). Assumptions, such as linear growth for Salix alba L. and Hedera helix L., were made due to a lack of data. Consequently, these models may not accurately reflect reality on larger time scales. Allometric rules were essential for complementing missing data based on the gathered information. However, specifically, with a linear longitudinal growth assumption, using allometric rules to determine radial growth has proven to be unrealistic (willow example). This also underscores the necessity of collecting accurate and sufficient data to build a proper growth model.

Because the projects made for each plant are different, making a proper comparison between them is challenging. To ease the discussion, a comparison for the same toy example is provided here. The comparison extends over a period of 20 years, a time range within which the results are potentially valid. The behavior for each plant species once it reaches a length of 1 meter is focused upon for a long clamped-free beam subject to bending by a 0.1 kN force applied at the free end.

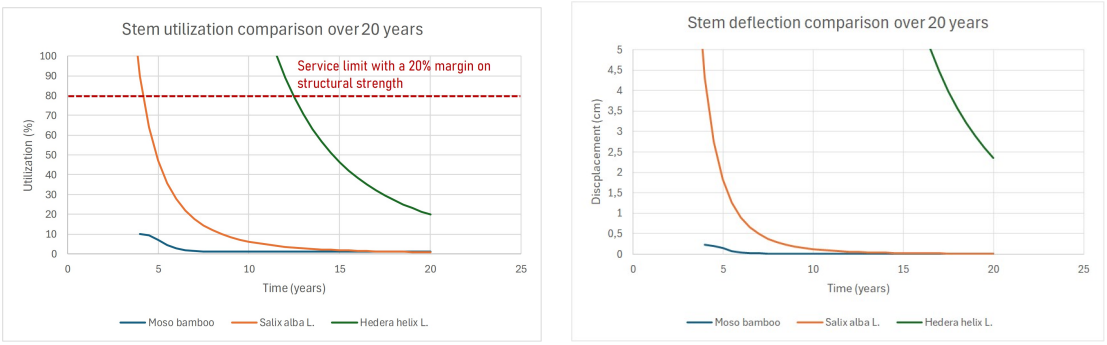

(a) (b)

Figure 6.39: Mechanical behavior evolution for a cantilever beam made of plant stem loaded with a 0.1 kN nodal load at its extremity for bending. Comparison between Moso bamboo (blue), Salix alba L. (orange) and Hedera helix L. (green). (a) compares the stem utilization (stress to strength ratio) over time (see Chapter 5), (b) compares the stem free end displacement over time.

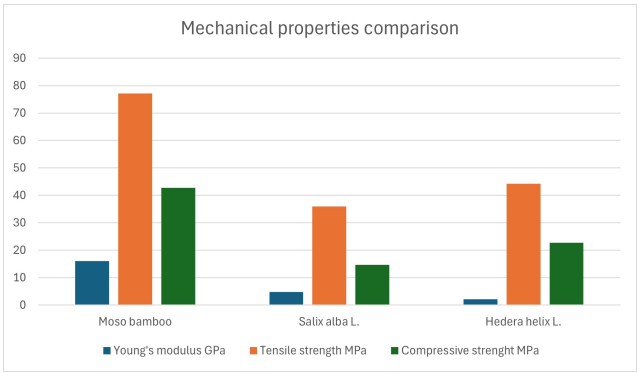

Figure 6.40: Mechanical properties comparison between Moso bamboo, Salix alba L. and Hedera helix L.

Moso bamboo exhibits superior overall mechanical behavior compared to Salix alba L., followed by Hedera helix L. (see Fig.6.40). For bamboo the assumption that it starts with a diameter of 8 cm and the adaptation of the model for Belgium should be refined.

To complement this comparison, the evolution of stem length, diameter and volume over time is assessed for each plant:

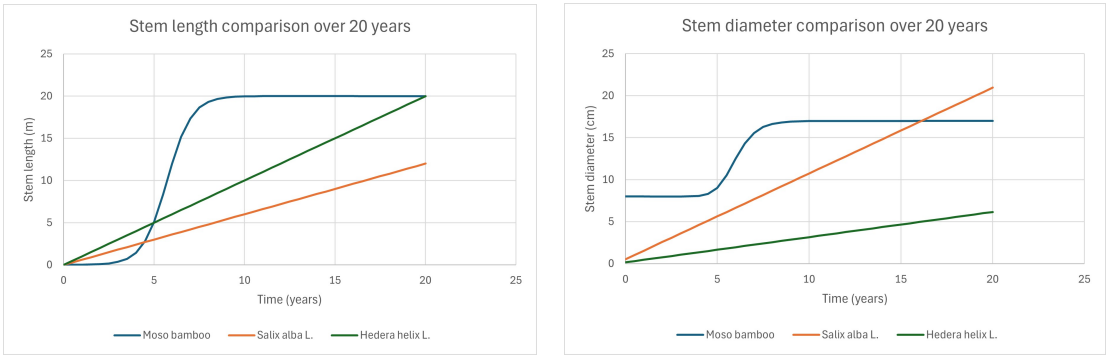

(a) (b)

Figure 6.41: Growth comparison between Moso bamboo (blue), Salix alba L. (orange) and Hedera helix L. (green). (a) compares the stem length over time, (b) compares the stem diameter over time.

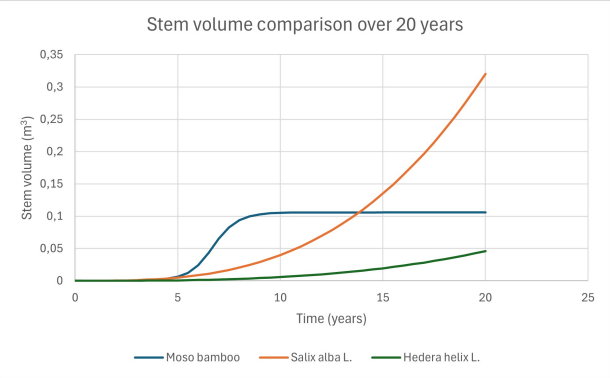

Figure 6.42: Stem volume evolution over time comparison between Moso bamboo (blue), Salix alba L. (orange) and Hedera helix L. (green)

Figure 6.43 highlights the rapid growth of bamboo in its early stages. However, over the long term, the other species eventually reach and even surpass bamboo in volume (computed from diameter, wall thickness - for bamboo - and length stem).

According to these graphs, Salix alba L. appears very promising for Baubotanical design. However, it has the shortest lifespan, approximately 30 years which means that the willow application project could potentially have 17 years of service. In comparison, Moso bamboo has a lifespan of about 50 years (bamboo application project $\sim$ 43 years of service), while Hedera helix L. can live for more than a hundred years and can actually grow horizontally. These lifespans are comparatively shorter than those of traditional buildings, which are typically designed to last for more than 50 or even 100 years [173].

6.4.1 Sustainability - Carbon sequestration

Sustainability is a crucial strength of these living structures and should be considered when evaluating their disadvantages and advantages for real-world applications. The introduction (Ch.1) highlighted they can contribute to reducing runoff water, cooling urban areas, and boosting biodiversity. Here, the carbon sequestration potential of these structures is considered to estimate crude order of magnitudes.

CO_2 is a greenhouse gas that significantly contributes to global warming. Trees are widely recognized for their crucial role in mitigating CO_2 levels in the atmosphere, primarily by sequestering carbon in biomass (living mass of a plant). Plants utilize carbon from the atmosphere to produce glucose through photosynthesis. However, not all the carbon transformed into glucose can be considered removed from the atmosphere. Some of the glucose is converted into starch and cellulose, essential components of biomass. Yet, another portion of the carbon is not stored and is released into the atmosphere, particularly during plant respiration. To estimate the amount of carbon each plant can store, a rough estimate typically assumes that 50% of the biomass consists of carbon [174].

The biomass comprises many parts of the plant (e.g., roots, leaves, branches) while in developed models only the stem is considered. As a conservative estimates, the stem volume determined in Fig.6.43 is utilized for the carbon that could be sequestered. By knowing the volume (Fig.6.43)

and density (Ch.4) for each plant, the carbon mass can be determined straightforwardly. The amount of CO_2 absorbed can then be calculated by considering that carbon constitutes approximately 27.3% of the total mass of CO_2 [175].

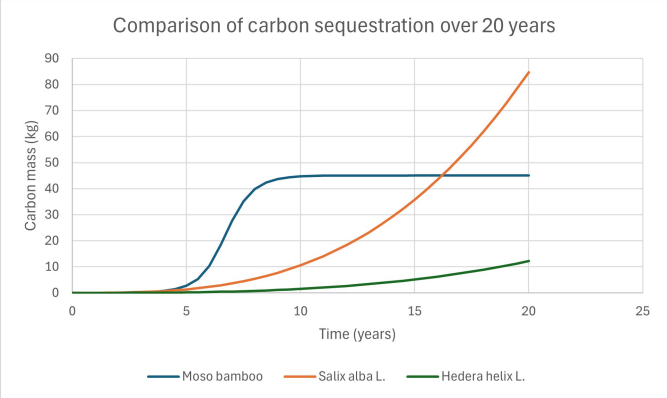

Figure 6.43: Carbon absorption over time. Comparison between on stem of Moso bamboo, Salix alba L. and Hedera helix L.

It's important to note that the approach of using only stem mass is particularly disadvantageous for ivy, as it possesses a significant amount of secondary branches and leaves. With this approach, the amount of carbon absorbed by each of the proposed projects over 20 years is calculated as follows:

- Moso bamboo pavilion: 4.08 tons of CO_2 absorbed over 20 years
- Willow observatory tower: 47.8 tons of CO_2 absorbed over 20 years
- Living ivy footbridge (2D assumption): 0.73 tons[3] of CO_2 absorbed over 20 years

For comparison, in Belgium, the average estimated CO_2 emissions per person per year is around 9 tons [176]. While the CO_2 absorbed by each project provides a rough estimation, a more thorough analysis is necessary to refine the results. However, the CO_2 absorption appears relatively low in comparison to current emissions. To better estimate the environmental benefits of living constructions, a further comparison could involve considering the CO_2 emissions during the construction of both a traditional building and a Baubotanical structure.

[3]Note that the deck, which also consists of ivy, was not modeled and thus is not taken into account in this calculation

Chapter 7

Conclusions and outlook

This work was structured into two main parts: the foundational framework for Baubotanical design, which defined the key principles governing the growth of living plants and their mechanical characteristics; and the implementation of growth and structural models with their application for three specific projects: one living architecture project from Moso bamboo (Phyllostachys edulis), and two Baubotanik projects following the *plant addition principle* from white willow (Salix alba L.) and ivy (Hedera helix L.) .

The growth and mechanical properties were gathered from literature. When data were unavailable, the missing properties were estimating using the determined principles governing living plants such as the allometric rules, the correlation between plants mechanical properties and their density, plant tissues mechanical properties or the correlation between green wood and dry wood mechanical properties. Moreover, a set of simplifying assumptions was established to build the models with the specific aim to serve for Baubotanical design. An evolving finite element model was implemented for each project from their plant growth models using the Karamba parametric finite element plugin for Rhinoceros 3D. With these models three applications were developed: a living bamboo pavilion, a living willow observatory tower and a living ivy footbridge. The main conclusions drawn are listed below:

- The considered Baubotanik structures are feasible from a structural strength and stiffness point of view.
- The use of trees or plants in construction offers numerous benefits, including enhancing air quality in cities, mitigating the urban heat island effect, reducing the risk of flooding, promoting biodiversity, and enriching local ecosystems.
- Baubotanical structures have the capacity to absorb CO_2 from the atmosphere; however, the quantity absorbed by the projects examined in this work appears to be low compared to the global emissions released by human activity.
- Compared to classical constructions, these projects require significantly more time for implementation and may not be suited for our fast-paced society.
- In comparison to conventional buildings, these structures have a shorter service duration. This duration depends on both the lifespan of the plant, which might be short depending on the species, and the initial serviceability time (when the structure first meets serviceability criteria). Throughout the entire lifespan of the plants (even before the structure is put

into service), maintenance is necessary to ensure the integrity and targeted growth of the structure.

Specific applications could be adapted for Baubotanical design, providing the potential to cleanse from CO_2. However, to assess feasibility for real-world applications, design tools are essential. This work focused on developing such tools with a justified set of assumptions. A significant foundation of this work stems from the Baubotanik Research Group, this study aimed to complement and contribute to the field of living architecture design by proposing an original methodology for implementing growth and structural numerical models.

No imperfections were incorporated in the models. Nature's unpredictability introduces variations in material properties or growth patterns different from those predicted by the idealized models used in this work. Additionally, the models assume fully rigid connections between elements and roots are represented as clamped nodes. This rigid assumption may not truly reflect reality, especially concerning the known flexibility of roots. These assumptions could be lifted in future work in which more elaborate growth models could also be considered. The elements included in the appendix of this manuscript could serve as a foundation to further refine the structural and growing model.

Appendix A

Plant anatomy - Vascular system

Relevancy for Baubotanical design: A fundamental understanding of plant anatomy is required to understand plant functioning. It aids in comprehending other concepts explained further on, such as plant growth dynamics (Section 3.1.1), inosculation (Section 3.1.5), plants vascular systems of (Section 3.1.7), and in characterizing green wood properties (Section 3.2).

A plant can be divided into three main parts: roots, stems, and leaves.

Roots serve to anchor the plant in the soil, while also absorbing water and essential solutes necessary for the plant's survival. **Leaves**, containing chlorophyll as the primary component, play a crucial role in producing glucose, which is essential for the production of amino acids (vital for the proper functioning of plants). **Stems** act as the structural and vascular connection between the leaves and the roots [177].

A **vascular system** comprising **xylem** and **phloem** ensures the transportation of these essential elements. Both xylem and phloem consist of rows of cells forming continuous tubes that run the entire length of the plant. Xylem vessels are composed of elongated, non-living cells impermeable to water, with walls containing lignin, a complex organic polymer that lends strength and rigidity to plant cell walls. Xylem vessels ensure the movement of water and solutes in a unidirectional flow from roots to leaves. Phloem vessels, composed of living cells, facilitate the transportation of glucose and amino acids (serving crucial roles in growth and regulating metabolic processes) to various parts of the plant [177, 59].

In the stem, vascular bundles are generally positioned near the edges. Due to their better structural properties compared to other tissues (see Table 3.2), these bundles help the plant withstand bending forces. Conversely, in roots, which generally do not experience bending, these bundles are centrally located. This placement difference contributes to the differing mechanical properties between stem and root [99].

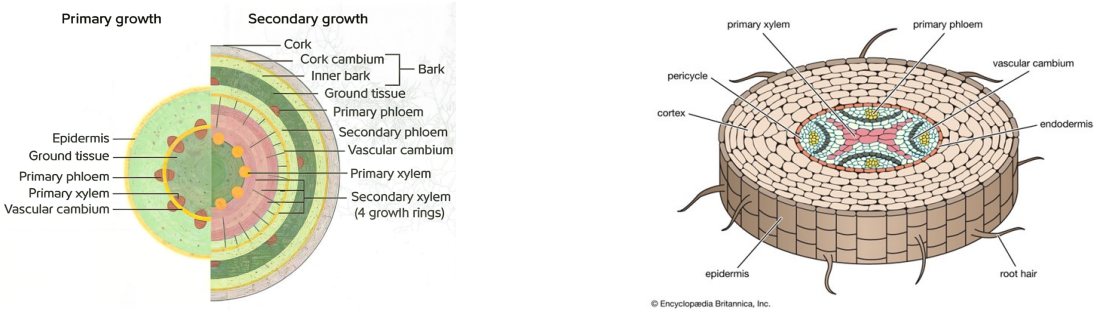

(a) stem cross section [178]

(b) root cross section [177]

Figure A.1: Plant tissues

The constituents of the composite material shown in Figure A.1 are explained as follows.

The **epidermis** constitutes the outermost cell layer of a plant stem. It serves as a protective barrier against physical damage, pathogens, and excessive water loss. In some plants, the epidermis may have specialized structures such as stomata and trichomes, which regulate gas exchange and reduce water loss, respectively [59].

The **cortex** refers to a stratum of parenchyma cells positioned beneath the epidermis within plant stems. It serves several functions, including the storage of nutrients, synthesis of compounds, and providing support. In certain plants, the cortex may also contain specialized cells such as collenchyma or sclerenchyma, which offer additional structural support [59].

Sclerenchyma is among the strongest and stiffest tissues in plants. Composed predominantly of dead cells at maturity, it forms lignified walls that impart strength and stiffness to various parts of the plant [59].

The **cambium** represents a layer of meristematic tissue situated between the xylem and phloem within the stem. Its primary role involves facilitating secondary growth, generating fresh vascular tissue (secondary xylem and phloem) that contributes to the expansion in diameter or thickness of the stem. There exist two distinct types of cambium: vascular cambium, responsible for generating secondary vascular tissue, and cork cambium (phellogen), which yields cork cells essential for the outer bark [59].

Cork constitutes the outermost protective layer of the stem, developed through the production of cork cells by the cork cambium. It serves as a waterproof barrier, protecting the inner tissues from desiccation, physical damage, and pathogens. Cork cells contain a waxy substance called suberin, which makes them impermeable to gases and water [59].

Appendix B

Functional structural plant models

Functional-structural plant modeling (FSPM) is a computational approach to describe plants by creating models of their structure and physiological processes at different levels (organ, individual plant, canopy). These models account for both the geometry and topology of plant organs and consider how local environmental factors such as temperature, radiation, CO_2 concentration, and relative humidity influence processes like photosynthesis, growth, and branching. Dynamic FSPMs simulate changes over time, while static FSPMs use a fixed structure to explain spatial variations in physiological activities. FSPMs differ from process-based models by explicitly incorporating structural feedback, where the plant's structure affects and is affected by physiological functions [179].

A plant, when viewed as a single entity, embodies an autotrophic organism; however, no single part within it can claim full autonomy. Instead, it represents a burgeoning assembly of semi-autonomous organs, each adapting to local conditions while interconnected to exchange essential resources. This interconnection facilitates coordination in development through internal signaling mechanisms and the utilization of shared genetic information [180].

Since in general there are important differences between the root system and the shoot system, it can be more convenient to model them separately [95]. In the current work the focus is set entirely on the stems as structural load bearing elements and roots aren't represented, keeping in mind that their flexibility and strength may be considered in a future, more elaborate model (see research on roots in Appendix F).

For centuries, plant scientists have constructed conceptual models to understand plant growth and development. Only in the late 1990s did quantitative models begin to emerge that comprehensively address the interaction between the modular structure of plants, the abiotic environment, and internal functioning and signaling[181, 182].

The development of Functional-Structural Plant Models (FSPMs) was driven by three overarching objectives: 1) Unraveling the operational mechanisms of plants across different scales, 2) Synthesizing knowledge from diverse fields including plant biology, biophysics, ecology, and computer science, and 3) Creating predictive models applicable in domains where plant architecture significantly influences outcomes [183].

A detailed review of FSPMs over the past two decades was conducted by Louarn and Song in 2020 [180]. While research into the development of FSPMs spans various fields of plant science, it appears that, at present, there are no FSPMs entirely dedicated to Baubotanical design. Nonetheless, these models remain of significant interest due to their capacity to simulate living plants. The appendix C compiles three tables where the main existing models for plants, roots and urban trees are described.

Appendix C

Existing models

Model name *urban trees*	**References**	**Type of model**	**Programming language**	**Availability**
UrbTree	[184]	Software tool designed for simulating and analyzing urban tree growth and development. Factors: soil composition, climate conditions, and urban infrastructure.	Python	Upon request
i-Tree	[185]	A software suite for assessing urban forests, to understand the economic, ecological, and social benefits of trees in cities. It analyzes tree canopy cover, air quality, stormwater management, and carbon storage,	GIS-extension tool	https://www.itreetools.org/
CITYgreen	[186]	Software for urban forestry and green infrastructure planning. It assesses benefits of city green spaces including environmental, social, and economic aspects. With tools for analyzing tree canopy coverage, air quality improvement, stormwater management, and energy savings,	GIS-esxtension tool	Upon request
UFORE	[187]	Urban Forest Effects is a software tool designed to quantify urban forests structure, function, and value. Help to evaluate ecological and economic benefits of urban trees. It analyzes tree species, canopy cover, air pollution removal, carbon sequestration, and energy conservation.	Not indicated	Upon request
CityTree	[188]	This growth model functions on physiological principles, simulating the individual growth of trees. It delineates the carbon and water cycles within trees, incorporating biological, physical, and chemical processes that are chiefly shaped by environmental conditions.	Not indicated	Upon request

Table C.1: Overview of major urban tree models

Appendix D

The Lindenmeyer System

In FSPM studies, the **L-system** stands out as the predominant method for simulating plant growth [14]. Numerous FSPM platforms have been built upon the foundational principles of L-systems. Among others, notable examples include: **L-Studio** [189], **GroIMP** [190], **OpenAlea** [191], and **L-Py** [192]. Descriptions of these platforms can be found in the Table **??**.

The **Lindenmayer system**, abbreviated as L-system, serves as a mathematical formalism employed to simulate plant growth processes, notably capturing the intricate branching patterns found in natural organisms such as trees and algae.

Originating from the work of Hungarian biologist Aristid Lindenmayer in 1968, L-systems utilize rewriting rules iteratively to generate strings of symbols that represent plant structures. These symbols are interpreted geometrically to generate visual representations of plant forms [193].

The process of creating geometric shapes using string commands is known as turtle interpretation. In this method, commands guide a virtual "turtle" to move forward or change its direction. The resulting path traced by the turtle represents the geometry being drawn [194].

In an L-system, there are typically two key components:

1. A set of symbols or an alphabet: These symbols denote different components of the plant, including the stem, leaves, branches , and other structural elements.
2. A set of production rules or rewriting rules: These rules describe how each symbol should be replaced in each iteration of the system. The rules are typically based on the context of the symbol and may involve parameters such as angle of branching and growth length.

The iterative application of production rules results in the generation of increasingly complex structures, mimicking the growth patterns observed in real plants. L-systems can produce a wide variety of plant forms, ranging from simple branching structures to intricate and realistic representations of trees and other vegetation.

L-systems are widely used in computer graphics, biology, and artificial life simulations for modeling and simulating plant growth, as well as in generative art for creating visually appealing and intricate patterns inspired by nature [193].

The L-system syntax presents certain limits, including:

1. The inability to define unique rotation angles and distances for each movement.
2. Challenges in integrating physiological processes related to plant growth.
3. Challenges arise in manipulating the generated geometry, rendering it incapable of accurately representing re-joined networks of branches, such as those observed in grafted tree formations.

Consequently, advancements have led to innovations like Language XL, which implements relational growth grammars (RGG). This enables the simultaneous rewriting of plant descriptions and geometry generation [195, 190].

Appendix E

Mapping Plant topology: A Comparative Examination of Imaging Methods

Topology investigates the characteristics of geometric objects that persist under continuous deformations like stretching and twisting, without tearing or gluing [196]. In the case of complex shapes, a simplified version called a topological skeleton is often used [197].This skeleton, which is equidistant to shape boundaries, is mathematically defined through various methods such as distance functions, medial axis or morphological operators [198, 199, 200]. Despite differences in construction, the skeleton and its distance to the boundary contain all necessary information for shape reconstruction, making it a valuable tool in analyzing and understanding complex geometries as of plants.

Technological advancements and increasing computational capabilities have eased the development of new tools for gathering the requisite data to reconstruct tree topologies. The following are some examples of these tools:

LiDAR (Light Detection and Ranging): This technology employs laser pulses to gauge distances to objects, producing accurate 3D models of tree canopies and structures [201, 202].

Photogrammetry: Photogrammetry involves taking overlapping photographs of trees from different angles and using software to reconstruct their 3D structure based on the visual data [22].

Terrestrial Laser Scanning (TLS): TLS involves mounting laser scanners on tripods and capturing high-resolution 3D point cloud data of trees and their surroundings [203, 204].

Ground-Penetrating Radar (GPR): GPR technology uses radar pulses to penetrate the ground and map the root systems of trees below the surface [205].

Portable X-ray CT Scanning: Portable X-ray computed tomography (CT) scanning can provide detailed cross-sectional images of tree trunks and branches, allowing for non-destructive analysis of internal structures [206].

These tools generally yield raw data. The discrete point cloud obtained needs to undergo processing to reconstruct the topology of the plant. Several methodologies have been devised for this purpose. Raumonen et al. [207] introduced a unique technique utilizing "cover sets" to rebuilt tree geometry. Similarly, PypeTree [208] employed "segments" derived from shaping curves, followed by adjustments to rectify inaccuracies. SimpleTree [209] utilized voxel-grid and Euclidean clustering in C++ to construct cylindrical tree models and developed a crown calculation tool for estimating canopy volume, demonstrating the effectiveness of cylinder fitting in accurately representing tree trunks and branches. Additionally, AdTree [210] adopted a skeleton-oriented approach, employing cylinder fitting to the point cloud model of individual trees.

Modeling plant topology is crucial for Baubotanical design. The accuracy of structural analysis is deeply linked to the representation of geometry. Finite element analysis can be performed from highly precise 3D models to simplified 1D models. However, the complexity of the model directly impacts the computational load. It's essential to recognize that a more detailed model doesn't always yield more accurate results. Therefore, representing living plants for design purposes requires striking a balance between accuracy and computational efficiency.

Appendix F

Roots

This appendix provides a detailed review of roots to facilitate their modeling for Baubotanical design purposes. It includes a description of a complex resistance model proposed by Zhu et al. [211], an overview of the mechanical properties of roots, a detailed examination of root architecture, and assumptions and elements that could be implemented to improve root system resistance.

F.0.1 Root resistance model

Roots are indispensable in Baubotanical design, serving not only for plant nutrition but also as the primary means of anchoring the structure. A recent study by Shu et al. in 2022 highlighted that the primary contributors to tree hazards are root deterioration and internal trunk decay. Given their intricate nature, current computational models are unable to accurately assess these risks." [14]. In fact, the lack of available data on roots presents a challenge in creating accurate models [212]. A robust model should establish a correlation between the stability of roots and factors such as the configuration of the root structure and the properties of the soil. [43].

In the literature, numerous models exist for root system resistance. While analytical models are available, numerical methods, particularly the finite element method, receive more attention due to their robustness in defining complex 3D geometries [45, 213, 211]. Presently, there exists no widely agreed-upon approach for effectively modeling root systems [214].

Various failure modes exist, including soil wedge failure when the soil exceeds its tensile capacity [215], root pull-out [216], root breakage [217], and combinations thereof [218].

The pull-out resistance test, conducted either in situ or in laboratories, is a commonly used method to assess the strength of a root system. In this experiment, the bottom part of the plant stem is secured in a clamp, and then the plant is pulled upwards vertically to gauge how the force applied correlates with the subsequent vertical movement [219].

Within literature, there are various models concerning root system resistance. Despite the availability of analytical models, numerical techniques, notably the finite element method, garner greater interest owing to their capacity to accurately delineate intricate 3D geometries [45, 213, 211]. Presently, there is a lack of agreement regarding the most effective approach for modeling root systems. Some researchers prefer using solid elements [43, 213], while others

opt for beam elements based on theories such as the Timoshenko beam theory or the Euler-Bernoulli elastic beam theory [220].

The focus here is set on the model proposed by Zhu et al. [211] (the interested reader can find a review on modeling also in this reference), which represents an enhancement of existing models and holds relevance for Baubotanical design .

The model is built utilizing the embedded beam element (EBE), comprising two components: the beam element representing the root itself, and a contact surface embedded with zero thickness [46].

The model enables relative displacement Δ between the soil and root, with the shared interface adhering to a perfect elastic-plastic behavior. Until reaching a critical displacement Δ_{cr}, the behavior remains elastic, with a linear correlation between the shear stress interface and the relative displacement Δ. Upon surpassing Δ_{cr}, the interface shear behavior shifts to a perfectly plastic state, inducing the root to slide at an interface shear stress τ_{max} remaining constant. This can be expressed mathematically as follows:

$$\tau = \begin{cases} k_s \Delta & \text{if } \Delta \leq \Delta_{\text{cr}} \\ \tau_{\text{max}} & \text{if } \Delta > \Delta_{\text{cr}} \end{cases} \tag{F.1}$$

With k_s representing the bond modulus of the root-soil interface and τ_{max} denoting the shear stress determined by Coulomb's friction law [221]:

$$\tau_{\text{max}} = \sigma_n \tan(\Phi) \tag{F.2}$$

σ_n denotes the normal stress in the soil failure plane, Φ represents the soil's internal friction angle, and τ_{max} signifies the soil shear strength.

Root behavior when $\Delta \leq \Delta_{\text{cr}}$

The EBE axial strain (ε_a) is composed by the root elastic strain (ε_e) and the interfacial shear strain (ε_s). It can be expressed as follows:

$$\varepsilon_a = \varepsilon_e + \varepsilon_s = \frac{\sigma_a}{E_r} + \frac{\Delta}{\bar{l}} \tag{F.3}$$

The equation provided below yields the EBE critical elastic axial strain:

$$\varepsilon_a^{cr} = \varepsilon_e^{cr} + \varepsilon_s^{cr} = \frac{\sigma_a^{\text{max}}}{E_r} + \frac{\Delta^{\text{cr}}}{\bar{l}} \tag{F.4}$$

With E_r representing the Young modulus of the root, σ_a denoting the EBE axial stress, d_r indicating the root diameter, and $\bar{l}$ representing the characteristic length of the root. The exponent cr signifies "critical".

Root behavior when $\Delta > \Delta_{cr}$

During the pulling-up process, there is a noticeable decrease in root resistance, attributed to a reduction in the root-soil interface area. In order to account for this softening behavior, the model introduces a criterion for damage initiation Eq.(F.5) alongside a linear degradation law governing material stiffness Eq.(F.6).

The damage initiation criterion:

$$F_{pf} = \left| \frac{\varepsilon_a}{\varepsilon_a^{cr}} \right| = 1 \tag{F.5}$$

The degradation law:

$$E_p^s = (1 - D_{pf}) E_p^e \tag{F.6}$$

The degradation variable:

$$D_{pf} = \frac{\varepsilon_a^f (\varepsilon_a - \varepsilon_a^{cr})}{\varepsilon_a (\varepsilon_a^f - \varepsilon_a^{cr})} \tag{F.7}$$

With F_{pf} the pulling force ratio, E_p^s the EBE Young modulus in the softening phase, E_p^e the EBE Young modulus in the linear elastic phase and D_{pf} the degradation variable. The exponent f stands for "failure" and cr for "critical".

The failure strain ε_a^f can be correlated with the dissipated energy per unit area G_p throughout the pullout failure process [222]:

$$\varepsilon_a^f = \frac{2G_p}{\sigma_a^{\max} \bar{l}} \tag{F.8}$$

Root breakage

Root breakage occurs when the stress within the root surpasses its strength. This model builds upon the work by Yang et al. [45], wherein roots were conceptualized as metal laminates, offering a closer approximation to the brittle failure behavior observed in real roots.

The damage initiation variable :

$$F_{bf} = \sqrt{\frac{\varepsilon_a^t}{\varepsilon_a^c} (\varepsilon_a)^2 + \left(\varepsilon_a^t - \frac{(\varepsilon_a^t)^2}{\varepsilon_a^c} \right) \varepsilon_a} = \sqrt{\frac{\varepsilon_a^t}{\varepsilon_a^c} \left[(\varepsilon_a)^2 + (\varepsilon_a^c - \varepsilon_a^t) \varepsilon_a \right]} \tag{F.9}$$

Damage occurs when the damage initiation variable F_{bf} reaches the ultimate tensile strength ε_a^t or the ultimate compressive strain ε_a^t. Once the damage initiates, the damage variable, D_{bf}, increases until it reaches 1 at failure. The damage variable is linked to the failure energy of the root, G_b (determined by a three-point bending test) as follows:

$$D_{bf} = 1 - \frac{\varepsilon_a^t}{F_{bf}} e^{-\frac{E_r \varepsilon_a^t (F_{bf} - \varepsilon_a^t) \bar{l}}{G_b}} \tag{F.10}$$

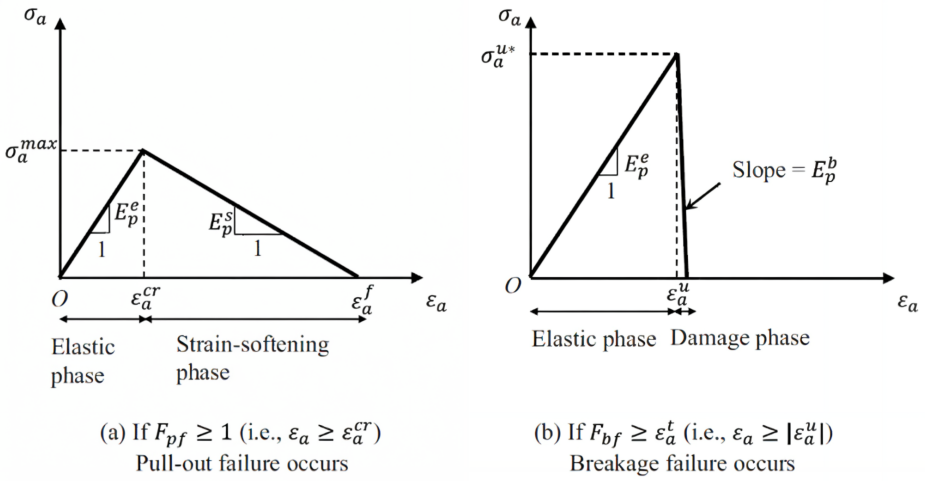

(a) If $F_{pf} \geq 1$ (i.e., $\varepsilon_a \geq \varepsilon_a^{cr}$) Pull-out failure occurs

(b) If $F_{bf} \geq \varepsilon_a^t$ (i.e., $\varepsilon_a \geq |\varepsilon_a^u|$) Breakage failure occurs

Figure F.1: Root stress-strain diagram for the modified EBE model [211]

With u representing both tension t or compression c and E_p^b the elastic modulus during the failure phase.

F.0.2 Roots mechanical properties

Root mechanical properties are closely linked to the diameter; the larger the diameter, the stronger and stiffer the root becomes [45]. Several studies assessed roots strength through mechanical tests [44, 45, 46, 49, 211]. The following range of magnitudes can be obtained from the literature:

- Root elastic modulus : 1.2 GPa - 10.1 GPa
- Root tensile strength : 31 MPa - 51.8 MPa
- Root compressive strength : 16 MPa - 25.8 MPa
- Root Poisson coefficient : 0.3

Liang et al. conducted laboratory tests on analog roots made of ABS plastic and correlated the Young's modulus E_r and tensile strength σ_a^t with the root diameter d_r [223]:

$$E_r = 3.24(d_r)^{-0.55} \tag{F.11}$$

$$\sigma_a^t = 57.89(d_r)^{-0.52} \tag{F.12}$$

F.0.3 Root architecture

Root architecture or geometry is required to conduct a finite element analysis. Schnepf et al. classified root growth models into three main categories: the root depth model, characterized by an exponential distribution of root length with depth; the density-based model; and the 3D root architecture model, which considers the dynamic evolution of root structure [224]. The challenge in creating such models lies in integrating genotype with phenotype to develop an architecture

that can effectively respond to various environmental factors, including water conditions, nutrient availability, radiation exposure, and others [225].

F.0.4 Assumption and beyond the scope

Root modeling presents significant challenges, prompting some researchers to simplify the problem, particularly when it's not the primary focus of their research (e.g. using an equivalent stiffness[57]).

Recent studies have demonstrated the effectiveness of guiding root growth to shape them into desired forms. These research efforts have been notably undertaken in the domains of art and the creation of new biomaterials based on roots. However, there is potential interest in Baubotanik to explore this technique for optimizing the anchorage of such structures [17, 18].

Appendix G

Declaration of Generative AI and AI-assisted technologies in the writing process

During the preparation of this work the author used ChatGPT 3.5 in order to edit, translate or correct some elements of the core text. After using this tool/service, the author reviewed and edited the content as needed and takes full responsibility for the content of the publication.

Bibliography

[1] E. Mackres, T. Wong, S. Null, R. Campos, and S. Mehrotra, "The future of extreme heat in cities: What we know — and what we don't," *www.wri.org*, 11 2023. [Online]. Available: https://www.wri.org/insights/future-extreme-heat-cities-data

[2] U. Environment, "Nations must go further than current paris pledges or face global warming of 2.5-2.9°c," 11 2023. [Online]. Available: https://www.unep.org/news-and-stories/press-release/nations-must-go-further-current-paris-pledges-or-face-global-warming

[3] D. Dodman, B. Hayward, M. Pelling, V. Castan Broto, W. Chow, E. Chu, R. Dawson, L. Khirfan, T. Mcphearson, A. Prakash, Y. Zheng, G. Ziervogel, H.-O. Pörtner, D. Roberts, M. Tignor, E. Poloczanska, K. Mintenbeck, A. Alegría, M. Craig, S. Langsdorf, S. Löschke, V. Möller, A. Okem, and B. Rama, "Cities, settlements and key infrastructure," *Climate Change 2022: Impacts, Adaptation and Vulnerability. Contribution of Working Group II to the Sixth Assessment Report of the Intergovernmental Panel on Climate Change*, 2022. [Online]. Available: https://www.ipcc.ch/report/ar6/wg2/downloads/report/IPCC_AR6_WGII_Chapter06.pdf

[4] IPCC, "Synthesis report of the ipcc sixth assessment report (ar6) summary for policymakers," IPCC, 2023. [Online]. Available: https://www.ipcc.ch/report/ar6/syr/downloads/report/IPCC_AR6_SYR_SPM.pdf

[5] F. Heisel and D. E. Hebel, "Pioneering construction materials through prototypological research," *Biomimetics*, vol. 4, p. 56, 08 2019.

[6] UNEP, "Building materials and the climate: Constructing a new future," *UNEP - UN Environment Programme*, 09 2023. [Online]. Available: https://www.unep.org/resources/report/building-materials-and-climate-constructing-new-future#:~:text=The%20buildings%20and%20construction%20sector

[7] T. Rötzer, A. Moser-Reischl, M. Rahman, R. Grote, S. Pauleit, and H. Pretzsch, "Modelling urban tree growth and ecosystem services: Review and perspectives," *Progress in Botany*, vol. 82, pp. 405–464, 01 2020.

[8] M. Weeden, "The 9 oldest, tallest, and biggest trees in the world," One Tree Planted, 08 2023. [Online]. Available: https://onetreeplanted.org/blogs/stories/oldest-tallest-biggest-trees

[9] B. Bioproducts, "10 things you didn't know about bamboo," 11 2020. [Online]. Available: https://www.bamboobioproducts.com/post/10-things-you-didn-t-know-about-bamboo

[10] S. Youssefian and N. Rahbar, "Molecular origin of strength and stiffness in bamboo fibrils," *Scientific Reports*, vol. 5, 06 2015. [Online]. Available: https://www.ncbi.nlm.nih.gov/pmc/articles/PMC4459167/

[11] P. of Green Technologies in Landscape Architecture TUM School of Engineering and D. T. U. of Munich, "Baubotanik," www.arc.ed.tum.de. [Online]. Available: https://www.arc.ed.tum.de/en/gtla/research/baubotanik/

[12] A. Wiechula, *Wachsende Häuser aus lebenden Bäumen entstehend*, 1926.

[13] B. Gale, "The potential of living willow structures in the landscape," Ph.D. dissertation, 12 2011.

[14] Q. Shu, T. Rötzer, A. Detter, and F. Ludwig, "Tree information modeling: A data exchange platform for tree design and management," *Forests*, vol. 13, p. 1955, 11 2022.

[15] O. O. Smolina, "Arborsculpture theme park," *IOP Conference Series: Materials Science and Engineering*, vol. 962, pp. 032 059–032 059, 11 2020.

[16] R. Reames, *Arborsculpture : Solutions for a Small Planet.* Williams, Or. Arborsmith Studios, 2007.

[17] J. Zhou, B. Barati, J. Wu, D. Scherer, and E. Karana, "Digital biofabrication to realize the potentials of plant roots for product design," *Bio-Design and Manufacturing*, 09 2020.

[18] I. A. Carrete, S. Ghodrat, D. Scherer, and E. Karana, "Understanding the effects of root structure on the mechanical behaviour of engineered plant root materials," *Materials Design*, vol. 225, p. 111521, 01 2023. [Online]. Available: https://www.sciencedirect.com/science/article/pii/S0264127522011443

[19] O. Smolina, "Variability of approaches to arborsculptures," *IOP Conference Series: Materials Science and Engineering*, vol. 687, pp. 055 035–055 035, 12 2019.

[20] M. Ripani, "Living fences: Using plants to define your boundaries," *Sanctuary: Modern Green Homes*, p. 86–91, 2021. [Online]. Available: https://www.jstor.org/stable/27094288

[21] G. Khan, "Surreal photos of india's living root bridges," Travel, 03 2018. [Online]. Available: https://www.nationalgeographic.com/travel/article/living-root-bridges-clean-village-mwalynnong-india

[22] W. Middleton, Q. Shu, and F. Ludwig, "Photogrammetry as a tool for living architecture," *The International Archives of the Photogrammetry, Remote Sensing and Spatial Information Sciences*, vol. XLII-2/W17, pp. 195–201, 11 2019.

[23] F. Ludwig, W. Middleton, F. Gallenmüller, P. Rogers, and T. Speck, "Living bridges using aerial roots of ficus elastica – an interdisciplinary perspective," *Scientific Reports*, vol. 9, 08 2019. [Online]. Available: https://www.nature.com/articles/s41598-019-48652-w

[24] W. Middleton, A. Habibi, S. Shankar, and F. Ludwig, "Characterizing regenerative aspects of living root bridges," *Sustainability*, vol. 12, p. 3267, 04 2020.

[25] W. Middleton, Q. Shu, and F. Ludwig, "Representing living architecture through skeleton reconstruction from point clouds," *Scientific Reports*, vol. 12, 01 2022.

[26] F. Ludwig, "Baubotanik - designing growth processes," *University of Insbruck (Conference Paper)*, 01 2014.

[27] F. Ludwig, H. Schwertfreger, and O. Storz, "Living systems: Designing growth in baubotanik," *Architectural Design*, vol. 82, pp. 82–87, 03 2012.

[28] F. Ludwig, "Botanische grundlagen der baubotanik und deren anwendung im entwurf," 01 2012.

[29] OLA, "Ola office for living architecture · architekten und stadtplaner partgmbb · stuttgart, germany," www.o-l-a.eu. [Online]. Available: https://www.o-l-a.eu/home/

[30] F. Ludwig and D. Schönle, *Growing Architecture*. Birkhäuser, 12 2022.

[31] K. J. Niklas, "Applications of finite element analyses to problems in plant morphology," *Annals of Botany*, vol. 41, p. 133–153, 1977. [Online]. Available: https://www.jstor.org/stable/42770132

[32] H. Oliveri, J. Traas, C. Godin, and O. Ali, "Regulation of plant cell wall stiffness by mechanical stress: a mesoscale physical model," *Journal of Mathematical Biology*, vol. 78, pp. 625–653, 09 2018.

[33] M. D. Mylo, A. Hoppe, L. Pastewka, T. Speck, and O. Speck, "Elastic property and fracture mechanics of lateral branch-branch junctions in cacti: A case study of opuntia ficus-indica and cylindropuntia bigelovii," *Frontiers in plant science*, vol. 13, 09 2022.

[34] B. Wang, X. Zhao, H. Peng, H. Meng, L. Wang, and C. Li, "Evaluation of biomechanical properties of jujube branches and analysis of prediction accuracy based on multi-scale artificially simplified model," *AIP Advances*, vol. 11, 04 2021.

[35] A. J. Bidhendi and A. Geitmann, "Tensile testing of primary plant cells and tissues," *Springer eBooks*, pp. 321–347, 01 2018.

[36] S. A. Belteton, W. Li, M. Yanagisawa, F. A. Hatam, M. I. Quinn, M. K. Szymanski, M. W. Marley, J. A. Turner, and D. B. Szymanski, "Real-time conversion of tissue-scale mechanical forces into an interdigitated growth pattern," *Nature Plants*, vol. 7, pp. 826–841, 06 2021.

[37] T. Guillon, Y. Dumont, and T. Fourcaud, "Numerical methods for the biomechanics of growing trees," *Computers Mathematics with Applications*, vol. 64, pp. 289–309, 08 2012.

[38] A. J. Bidhendi and A. Geitmann, "Finite element modeling of shape changes in plant cells," *Plant Physiology*, vol. 176, pp. 41–56, 01 2018.

[39] T. Fourcaud and P. Lac, "Numerical modelling of shape regulation and growth stresses in trees," *Trees*, vol. 17, pp. 23–30, 09 2002.

[40] A. Öchsner, L. F. da Silva, and H. Altenbach, *Analysis and Design of Biological Materials and Structures*. Springer Science Business Media, 01 2012, vol. 14.

[41] E. Kuhl, "Growing matter: a review of growth in living systems," *Journal of the Mechanical Behavior of Biomedical Materials*, vol. 29, pp. 529–543, 01 2014.

[42] M. Eskandari and E. Kuhl, "Systems biology and mechanics of growth," *Wiley Interdisciplinary Reviews: Systems Biology and Medicine*, vol. 7, pp. 401–412, 09 2015.

[43] L. Dupuy, T. Fourcaud, and A. Stokes, "A numerical investigation into factors affecting the anchorage of roots in tension," *European Journal of Soil Science*, vol. 56, pp. 319–327, 06 2005.

[44] L. X. Dupuy, T. Fourcaud, P. Lac, and A. Stokes, "A generic 3d finite element model of tree anchorage integrating soil mechanics and real root system architecture," *American Journal of Botany*, vol. 94, pp. 1506–1514, 09 2007.

[45] M. Yang, P. Défossez, F. Danjon, and T. Fourcaud, "Tree stability under wind: Simulating uprooting with root breakage using a finite element method," *Annals of Botany*, vol. 114, p. 695–709, 2014. [Online]. Available: https://www.jstor.org/stable/43579638

[46] M. Yang, P. Défossez, F. Danjon, S. Dupont, and T. Fourcaud, "Which root architectural elements contribute the best to anchorage of pinus species? insights from in silico experiments," *Plant and Soil*, vol. 411, pp. 275–291, 2017. [Online]. Available: https://doi.org/10.1007/s1110401629920

[47] H. Rahardjo, F. Harnas, E. Leong, P. Tan, Y. Fong, and E. Sim, "Tree stability in an improved soil to withstand wind loading," *Urban Forestry Urban Greening*, vol. 8, pp. 237–247, 01 2009.

[48] M. Yang, P. Defossez, and T. Fourcaud, "Improving finite element models of roots-soil mechanical interactions," HAL Archives Ouvertes, p. np, 06 2013. [Online]. Available: https://hal.science/hal-01189998

[49] T. Liang, J. A. Knappett, A. Leung, A. Carnaghan, A. G. Bengough, and R. Zhao, "A critical evaluation of predictive models for rooted soil strength with application to predicting the seismic deformation of rooted slopes," *Landslides*, vol. 17, pp. 93–109, 08 2019.

[50] T. Jackson, A. Shenkin, A. Wellpott, K. Calders, N. Origo, M. Disney, A. Burt, P. Raumonen, B. Gardiner, M. Herold, T. Fourcaud, and Y. Malhi, "Finite element analysis of trees in the wind based on terrestrial laser scanning data," *Agricultural and Forest Meteorology*, vol. 265, pp. 137–144, 02 2019.

[51] Y. Kim, H. Rahardjo, and D. L. Tsen-Tieng, "Mechanical behavior of trees with structural defects under lateral load: a numerical modeling approach," *Urban Forestry Urban Greening*, vol. 59, p. 126987, 04 2021.

[52] J. R. Moore and D. A. Maguire, "Simulating the dynamic behavior of douglas-fir trees under applied loads by the finite element method," *Tree Physiology*, vol. 28, pp. 75–83, 01 2008.

[53] J. A. J. Huber, O. Broman, M. Ekevad, J. Oja, and L. Hansson, "A method for generating finite element models of wood boards from x-ray computed tomography scans," *Computers Structures*, vol. 260, p. 106702, 02 2022. [Online]. Available: https://www.sciencedirect.com/science/article/pii/S0045794921002248

[54] C. J. Stubbs, R. Larson, and D. D. Cook, "Mapping spatially distributed material properties in finite element models of plant tissue using computed tomography," *Biosystems Engineering*, vol. 200, pp. 391–399, 12 2020.

[55] J. Henriques, J. Xavier, and A. Andrade-Campos, "Identification of orthotropic elastic properties of wood by digital image correlation and finite element model updating techniques," *Procedia Structural Integrity*, vol. 37, pp. 25–32, 2022.

[56] L. Morav˘cík, R. Vincúr, and Z. Rózová, "Analysis of the static behavior of a single tree on a finite element model," *Plants*, 2021.

[57] W. Middleton, H. Erdal, A. Detter, P. D'Acunto, and F. Ludwig, "Comparing structural models of linear elastic responses to bending in inosculated joints," *Trees*, vol. 37, pp. 891–903, 02 2023.

[58] mintupi6b4, "Geeksforgeeks — a computer science portal for geeks," GeeksforGeeks, 2024. [Online]. Available: https://www.geeksforgeeks.org/

[59] R. F. Evert, S. E. Eichhorn, and K. Esau, *Esau's Plant Anatomy : meristems, cells, and Tissues of the Plant Body : Their structure, function, and Development.* J. Wiley, 2006.

[60] M. Sassi, O. Ali, F. Boudon, G. Cloarec, U. Abad, C. Cellier, X. Chen, B. Gilles, P. Milani, J. Friml, T. Vernoux, C. Godin, O. Hamant, and J. Traas, "An auxinmediated shift toward growth isotropy promotes organ formation at the shoot meristem in arabidopsis," *Current Biology*, vol. 24, pp. 2335–2342, 2014. [Online]. Available: https://www.sciencedirect.com/science/article/pii/S0960982214010495

[61] M. Sassi and J. Traas, "New insights in shoot apical meristem morphogenesis: Isotropy comes into play," *Plant Signaling Behavior*, vol. 10, p. e1000150, 11 2015.

[62] M. Baucher, M. E. Jaziri, and O. Vandeputte, "From primary to secondary growth: Origin and development of the vascular system," *Journal of Experimental Botany*, vol. 58, p. 3485–3501, 2007. [Online]. Available: https://www.jstor.org/stable/24036861

[63] D. F. Cutler, C. E. J. Botha, and D. Wm Stevenson, *Plant Anatomy : an Applied Approach.* Blackwell Pub, 2008.

[64] K. J. Niklas and H.-C. Spatz, *Plant Physics.* The University of Chicago Press, 2012.

[65] C. Mattheck, *Design in Nature.* Springer Science Business Media, 12 2012.

[66] D. E. Moulton, H. Oliveri, and A. Goriely, "Multiscale integration of environmental stimuli in plant tropism produces complex behaviors," *Proceedings of the National Academy of Sciences of the United States of America*, vol. 117, p. 32226–32237, 2020. [Online]. Available: https://www.jstor.org/stable/27005790

[67] L. Taiz, E. Zeiger, I. M. Møller, and A. S. Murphy, *Plant Physiology and Development*, 6th ed. Sinauer Associates, Inc., Publishers, 2015.

[68] K. T. Yamamoto, *Phototropism.* Humana Press, 01 2019.

[69] L. Poorter, "Growth responses of fifteen rain forest tree species to a light gradient : the relative importance of morphological and physiological traits," *Functional Ecology*, vol. 13, 06 1999.

[70] H. Pretzsch, *ReEvaluation of Allometry: StateoftheArt and Perspective Regarding Individuals and Stands of Woody Plants*, 09 2010, vol. 71, pp. 339–369.

[71] J. Gayon, "History of the concept of allometry," *American Zoologist*, vol. 40, pp. 748–758, 10 2000.

[72] L. Von Bertalanffy, *theoretische biologie: ii. band: stoffwechsel, wachstum. : 2. aufl.* A. FRANCKE AG, BERN, 1951.

[73] B. Enquist and K. Niklas, "Invariant scaling relations across treedominated communities," *Nature*, vol. 410, pp. 655–60, 05 2001.

[74] G. West, J. Brown, and B. Enquist, "A general model for the origin of allometric scaling laws in biology," *Science (New York, N.Y.)*, vol. 276, pp. 122–6, 05 1997.

[75] H. Pretzsch, P. Biber, and J. Ďurský, "The single treebased stand simulator silva: Construction, application and evaluation," *Forest Ecology and Management*, vol. 162, pp. 3–21, 06 2002.

[76] B. Enquist, J. Brown, and G. West, "Allometric scaling of plant energetics and population density," *Nature*, vol. 395, pp. 163–165, 01 1998.

[77] M. Mccarthy and B. Enquist, "Consistency between an allometric approach and optimal partitioning theory in global patterns of plant biomass allocation," *Functional Ecology*, vol. 21, pp. 713–720, 06 2007.

[78] M. Westoby, "The self-thinning rule," *Advances in Ecological Research*, pp. 167–225, 1984.

[79] E. Britannica, *Graft — Description, Types, Uses — Britannica*, 2020. [Online]. Available: https://www.britannica.com/topic/graft

[80] M. J. Harrington, O. Speck, T. Speck, S. T. Wagner, and R. Weinkamer, "Biological archetypes for self-healing materials," *POLYMER*, vol. 273, pp. 307–344, 01 2015.

[81] T. Link, "Arborsculpture: An emerging art form and solutions to our environment," *University of California, Davis Department of Environmental Sciences Landscape Architecture Program*, 06 2008.

[82] M. D. Mylo, F. Ludwig, M. A. Rahman, Q. Shu, C. Fleckenstein, T. Speck, and O. Speck, "Conjoining trees for the provision of living architecture in future cities: a long-term inosculation study," *Plants*, vol. 12, p. 1385, 01 2023. [Online]. Available: https://www.mdpi.com/2223-7747/12/6/1385/htm

[83] M. Olson, J. Rosell, S. Muñoz, and M. Castorena, "Carbon limitation, stem growth rate and the biomechanical cause of corner's rules," *Annals of botany*, vol. 122, 06 2018.

[84] D. D. Smith, "Even when the seasons change our allometry stays the same. a commentary on: 'corner's rules pass the test of time: Little effect of phenology on leaf-shoot and other scaling relationships'," *Annals of Botany*, vol. 126, pp. iii–iv, 10 2020.

[85] P.-E. Lauri, "Corner's rules as a framework for plant morphology, architecture and functioning – issues and steps forward," *The New Phytologist*, vol. 221, p. 1679–1684, 2019. [Online]. Available: https://www.jstor.org/stable/26874132

[86] K. Shinozaki, K. Yoda, K. Hozumi, and T. Kira, "A quantitative analysis of plant form-the pipe model theory : I.basic analyses," *The Ecological Society of Japan*, vol. 14, pp. 97–105, 06 1964.

[87] K. Rennolls, "Pipe-model theory of stem-profile development," *Forest Ecology and Management*, vol. 69, pp. 41–55, 11 1994.

[88] R. Lehnebach, R. Beyer, V. Letort, and P. Heuret, "The pipe model theory half a century on: a review," *Annals of Botany*, vol. 121, p. 1427, 06 2018.

[89] C. Godin, "Representing and encoding plant architecture: a review," *Annals of Forest Science*, vol. 57, pp. 413–438, 06 2000.

[90] P. Schopfer and A. Brennicke, *Pflanzenphysiologie*. Springer-Verlag, 08 2016.

[91] P. Prusinkiewicz, M. T. Allen, G. Louarn, and T. M. DeJong, "Numerical methods for transport-resistance source–sink allocation models," *Functional-Structural Plant Modelling in Crop Production*, pp. 123–137, 01 2007.

[92] G. Boenisch and J. Kattge, "Try plant trait database," www.try-db.org. [Online]. Available: https://www.try-db.org/TryWeb/Home.php

[93] "Plant database search," pfaf.org. [Online]. Available: https://pfaf.org/user/plantsearch.aspx

[94] C. Nixon and W. Ziegler, "National tree growth rate database," *trid.trb.org*, 2021. [Online]. Available: https://trid.trb.org/view/1903455

[95] C. Godin and Y. Caraglio, "A multiscale model of plant topological structures," *Journal of Theoretical Biology*, vol. 191, pp. 1–46, 03 1998.

[96] K. J. Niklas, *Plant Biomechanics : an Engineering Approach to Plant Form and Function*. University of Chicago, Imp, 1992.

[97] D. E. Kretschmann, *Wood Handbook : Wood as an Engineering Material*, centennial edition ed. Forest Products Society, 2010.

[98] C. J. Stubbs, N. S. Baban, D. J. Robertson, L. Alzube, and D. D. Cook, "Bending stress in plant stems: Models and assumptions," *Springer eBooks*, pp. 49–77, 01 2018.

[99] S. WolffVorbeck, O. Speck, M. Langer, T. Speck, and P. Dondl, "Charting the twisttobend ratio of plant axes," *Journal of the Royal Society, Interface*, vol. 19, p. 20220131, 06 2022.

[100] T. Speck and M. Schmitt, "Mechanische werte," *Lexikon der Biologie – Biologie im Überblick*, pp. 244 – 247, 1992.

[101] G. Bold, M. Langer, L. Börnert, and T. Speck, "The protective role of bark and bark fibers of the giant sequoia (sequoiadendron giganteum) during high-energy impacts," *International Journal of Molecular Sciences*, vol. 21, p. 3355, 01 2020. [Online]. Available: https://www.mdpi.com/1422-0067/21/9/3355

[102] H. Ambronn, *Über die Entwickelungsgeschichte und die mechanischen Eigenschaften des Collenchyms: Ein Beitrag zur Kenntniss des mechanischen Gewebesystems*, jahrbücher für wissenschaftliche botanik ed. G. Bernstein., 1881, vol. 12.

[103] O. Speck, M. Schlechtendahl, F. Borm, T. Kampowski, and T. Speck, "Humidity-dependent wound sealing in succulent leaves of delosperma cooperi – an adaptation to seasonal drought stress," *Beilstein Journal of Nanotechnology*, vol. 9, pp. 175–186, 01 2018.

[104] M. D. Mylo, L. Hesse, T. Masselter, J. Leupold, K. Drozella, T. Speck, and O. Speck, "Morphology and anatomy of branch–branch junctions in opuntia ficus-indica and cylindropuntia bigelovii: A comparative study supported by mechanical tissue quantification," *Plants*, vol. 10, pp. 2313–2313, 10 2021. [Online]. Available: https://www.ncbi.nlm.nih.gov/pmc/articles/PMC8618873/

[105] H. Bargel, H. Spatz, T. Speck, and C. Neinhuis, "Two-dimensional tension tests in plant biomechanics - sweet cherry fruit skin as a model system," *Plant Biology*, vol. 6, pp. 432–439, 07 2004.

[106] K. Denman, G. Brasseur, A. Chidthaisong, P. Ciais, P. Cox, R. Dickinson, D. Haugustaine, C. Heinze, E. Holland, D. Jacob, U. Lohmann, R. S, S. Dias, S. Wofsy, and X. Zhang, *Couplings Between Changes in the Climate System and Biogeochemistry*, ser. Climate Change 2007: The Physical Science Basis, 01 2007, vol. 2007, pp. 499–587.

[107] J. Chave, D. Coomes, S. Jansen, S. L. Lewis, N. G. Swenson, and A. E. Zanne, "Towards a worldwide wood economics spectrum," *Ecology Letters*, vol. 12, pp. 351–366, 04 2009.

[108] K. J. Niklas and H. Spatz, "Worldwide correlations of mechanical properties and green wood density," *American Journal of Botany*, vol. 97, pp. 1587–1594, 10 2010.

[109] F. Ludwig, d. Bruyn, M. Thielen, and T. Speck, "Plant stems as building material for living plant constructions," *Proceedings of the 6th Plant Biomechanics Conference*, pp. 398–405, 01 2009.

[110] K. Keito, N. Nishiyama, H. Kashiwagi, and S. Shibata, "Massflowering of cultivated moso bamboo, phyllostachys edulis (poaceae) after more than a halfcentury of vegetative growth," *Journal of Japanese Botany*, vol. 97, pp. 145–155, 06 2022.

[111] M. Lobovikov, L. Ball, M. Guardia, and L. Russo, *World bamboo resources : a thematic study prepared in the framework of the Global Forest Resources Assessment.* Food And Agriculture Organization Of The United Nations, 2007.

[112] A. Emamverdian, Y. Ding, F. Ranaei, and Z. Ahmad, "Application of bamboo plants in nine aspects," *The Scientific World Journal*, vol. 2020, pp. 1–9, 09 2020. [Online]. Available: https://www.ncbi.nlm.nih.gov/pmc/articles/PMC7555460/

[113] L. Bambous, "Lil'ô bambous - bambouseraie belgique — une bambouseraie et un jardin exotique à namur spécialisé en bambous non-envahissants, fargesia, bananiers, palmier, graminées et statues asiatiques." [Online]. Available: https://lilobambous.be/

[114] P. Hamblenne, "Pépinières hamblenne - pépinière bambous - pépiniériste namur belgique," *www.hamblenne.be*. [Online]. Available: https://www.hamblenne.be/Cat_bambous.htm

[115] J. Fu, "Chinese moso bamboo: Its importance," *BAMBOO · the Magazine of the American Bamboo Society*, vol. 22, 11 2000.

[116] H. Archila, S. Kaminski, D. Trujillo, E. Zea Escamilla, and K. A. Harries, "Bamboo reinforced concrete: a critical review," *Materials and Structures*, vol. 51, 07 2018. [Online]. Available: https://link.springer.com/article/10.1617/s11527-018-1228-6

[117] M. O. Sanni-Anibire, B. Abiodun Salami, and N. Muili, "A framework for the safe use of bamboo scaffolding in the nigerian construction industry," *Safety Science*, vol. 151, p. 105725, 07 2022.

[118] G.-Y. Tao, M. Ramakrishnan, K. K. Vinod, K. Yrjälä, V. Satheesh, J. Cho, Y. Fu, and M. Zhou, "Multi-omics analysis of cellular pathways involved in different rapid growth stages of moso bamboo," *Tree Physiology*, vol. 40, pp. 1487–1508, 07 2020.

[119] Tao, Y. Fu, and Zhou, "Advances in studies on molecular mechanisms of rapid growth of bamboo species." *Journal of Agricultural Biotechnology*, vol. 26, p. 871–887, 2018.

[120] L. Li, Z. Cheng, Y. Ma, Q. Bai, X. Li, Z. Cao, Z. Wu, and J. Gao, "The association of hormone signalling genes, transcription and changes in shoot anatomy during moso bamboo growth," *Plant Biotechnology Journal*, vol. 16, pp. 72–85, 06 2017.

[121] C. Wu, Z. Cheng, and J. Gao, "Mysterious bamboo flowering phenomenon: A literature review and new perspectives," *Science of The Total Environment*, vol. 911, pp. 168 695–168 695, 02 2024.

[122] X. Zheng, S. Lin, H. Fu, Y. Wan, and Y. Ding, "The bamboo flowering cycle sheds light on flowering diversity," *Frontiers in Plant Science*, vol. 11, 04 2020.

[123] C. Veller, M. A. Nowak, and C. C. Davis, "Extended flowering intervals of bamboos evolved by discrete multiplication," *Ecology Letters*, vol. 18, pp. 653–659, 05 2015.

[124] D. H. Janzen, "Why bamboos wait so long to flower," *Annual Review of Ecology and Systematics*, vol. 7, pp. 347–391, 11 1976.

[125] X. Song, C. Peng, G. Zhou, H. Gu, Q. Li, and C. Zhang, "Dynamic allocation and transfer of non-structural carbohydrates, a possible mechanism for the explosive growth of moso bamboo (phyllostachys heterocycla)," *Scientific Reports*, vol. 6, 05 2016.

[126] A. M. Gilard, "Bambou géant moso phyllostachys edulis: Guide complet 2024," Bambou en France, 02 2020. [Online]. Available: https://bambouenfrance.fr/bambou-geant-moso-edulis-pubescens/

[127] S. Amada, Y. Ichikawa, T. Munekata, Y. Nagase, and H. Shimizu, "Fiber texture and mechanical graded structure of bamboo," *Composites Part B: Engineering*, vol. 28, pp. 13–20, 01 1997.

[128] T. Chen, D. Wang, and S. Wang, "The trend of growth characteristics of moso bamboo (phyllostachys pubescens) forests under an unmanaged condition in central taiwan," *Taiwan Journal of Forest Science*, vol. 31, pp. 75–88, 06 2016.

[129] P. G. Dixon and L. J. Gibson, "The structure and mechanics of moso bamboo material," *Journal of The Royal Society Interface*, vol. 11, p. 20140321, 10 2014.

[130] C. Shen, Z. Feng, P. Chen, S. Chen, and T. Ullah, "Research and evaluation of growth rate model for native chinese moso bamboo," *Applied Ecology and Environmental Research*, vol. 18, pp. 1459–1470, 2020.

[131] Q. Wei, L. Guo, C. Jiao, Z. Fei, M. Chen, J. Cao, Y. Ding, and Q. Yuan, "Characterization of the developmental dynamics of the elongation of a bamboo internode during the fast growth stage," *Tree Physiology*, vol. 39, pp. 1201–1214, 07 2019.

[132] M. Chen, L. Guo, M. Ramakrishnan, Z. Fei, K. Kurungara Vinod, Y. Ding, C. Jiao, Z. Gao, R. Zha, C. Wang, Z. Gao, F. Yu, G. Ren, and Q. Wei, "Rapid growth of moso bamboo (¡i¿phyllostachys edulis¡/i¿): Cellular roadmaps, transcriptome dynamics, and environmental factors," *The plant cell*, vol. 34, pp. 3577–3610, 06 2022. [Online]. Available: https://academic.oup.com/plcell/article-abstract/34/10/3577/6619569

[133] R. Lorenzo, M. Godina, L. Mimendi, and H. Li, "Determination of the physical and mechanical properties of moso, guadua and oldhamii bamboo assisted by robotic fabrication," *Journal of Wood Science*, vol. 66, 03 2020.

[134] L. Sanchez, A. G. Mullins, J. A. Cunningham, and J. Mihelcic, "Mechanical properties of bamboo: a research synthesis of strength values and the factors influencing them," *American Bamboo Society*, vol. 29, pp. 1–21, 10 2019.

[135] J. Zhu, H. Peng, J. Lyu, and T. Zhan, "Evaluation of orthotropic elasticity of gradient-structured bamboo by microtensile testing combined with digital image correlation technique," *Industrial crops and products*, vol. 203, pp. 117 097–117 097, 11 2023.

[136] P. Huang, W.-S. Chang, M. P. Ansell, Y. J. Chew, and A. Shea, "Density distribution profile for internodes and nodes of phyllostachys edulis (moso bamboo) by computer tomography scanning," *Construction and Building Materials*, vol. 93, pp. 197–204, 09 2015.

[137] J. Isebrands and J. Richardson, Eds., *Poplars and willows : trees for society and the environment*. The Food and Agriculture Organization of the United Nations and Cabi, 2014.

[138] L. Engels, "How to grow and care for white willow," *The Spruce*, 11 2023. [Online]. Available: https://www.thespruce.com/white-willow-salix-alba-guide-5211968

[139] A. Praciak and C. International, *The CABI encyclopedia of forest trees*. Cabi, 2013.

[140] PictureThis, "Quelle est la température optimale pour saule blanc (plage de température, effets et anomalies) ?" [Online]. Available: https://www.picturethisai.com/fr/care/temperature/Salix_alba.html

[141] T. Durrant, D. de Rigo, and G. Caudullo, "Salix alba in europe: distribution, habitat, usage and threats," *European Atlas of Forest Tree Species*, vol. Tree species, 03 2016.

[142] P. R. Greene, "Weeping willow growth rates compare with salix babylonica re-rooted branch cuttings," *Research Reviews: Journal of BotanicalSciences*, 02 12.

[143] T. U. N. . Lab, "Weeping willow - salix alba," *University of Minnesota — Urban Forestry Outreach Research*. [Online]. Available: https://trees.umn.edu/weeping-willow-salix-alba

[144] D. J. Metcalfe, "Hedera helix l." *Journal of Ecology*, vol. 93, p. 632–648, 2005. [Online]. Available: https://www.jstor.org/stable/3599428

[145] A. Okerman, "Combating the "ivy desert": the invasion of hedera helix (english ivy) in the pacific northwest united states," *conservancy.umn.edu*, vol. 6, 2000. [Online]. Available: https://hdl.handle.net/11299/59738

[146] M. Strelau, D. Clements, J. Benner, and R. Prasad, "The biology of canadian weeds: 157.hedera helixl. andhedera hibernica(g. kirchn.) bean," *Canadian Journal of Plant Science*, vol. 98, pp. 1005–1022, 10 2018.

[147] P. Q. Rose, *The Gardener's Guide to Growing Ivies*. Timber Press (OR), 1996.

[148] L. Mortensen and G. Larsen, "Effects of temperature on growth of six foliage plants," *Scientia Horticulturae*, vol. 39, pp. 149–159, 05 1989.

[149] H. Bauer and R. Kofler, "Photosynthesis in frost-hardened and frost-stressed leaves of hedera helix l." *Plant, Cell and Environment*, vol. 10, pp. 339–346, 06 1987.

[150] M. Murai, "Understanding the invasion of pacific northwest forests by english ivy (hedera spp., araliaceae)." Ph.D. dissertation, 1999.

[151] H. Hoflacher and H. Bauer, "Light acclimation in leaves of the juvenile and adult life phases of ivy (hedera helix)," *Physiologia Plantarum*, vol. 56, pp. 177–182, 10 1982.

[152] B. Melzer, R. Seidel, T. Steinbrecher, and T. Speck, "Structure, attachment properties, and ecological importance of the attachment system of english ivy (hedera helix)," *Journal of Experimental Botany*, vol. 63, pp. 191–201, 09 2011.

[153] B. Badre, P. Nobelis, and M. Trémolières, "Quantitative study and modelling of the litter decomposition in a european alluvial forest. is there an influence of overstorey tree species on the decomposition of ivy litter (hedera helix l.)?" *Acta Oecologica*, vol. 19, pp. 491–500, 11 1998.

[154] M. A. Waggy, "Hedera helix. in: Fire effects information system," www.fs.usda.gov, 2010. [Online]. Available: https://www.fs.usda.gov

[155] M. E. Millner, "Natural grafting in hedera helix," *New Phytologist*, vol. 31, pp. 2–25, 02 1932.

[156] N. Stavretovic, "Biological characteristics of the species hedera helix l. and its use in controlling erosion in shady places," *Archives of Biological Sciences*, vol. 59, pp. 139–143, 2007.

[157] P. Heuzé, J.-L. Dupouey, and A. Schnitzler, "Radial growth response ofhedera helixto hydrological changes and climatic variability in the rhine floodplain," *River Research and Applications*, vol. 25, pp. 393–404, 05 2009.

[158] F. E. Putz and H. A. Mooney, *The Biology of Vines*. Cambridge University Press, 1991.

[159] A. Schnitzler and P. Heuzé, "Ivy (hedera helix l.) dynamics in riverine forests: Effects of river regulation and forest disturbance," *Forest Ecology and Management*, vol. 236, pp. 12–17, 11 2006.

[160] F. Milard, "Domptez le lierre," www.gerbeaud.com, 03 2010. [Online]. Available: https://www.gerbeaud.com/jardin/fiches/lierre.php

[161] L. chemin de la nature, "Le lierre grimpant, une plante qui vous veut du bien." 2016. [Online]. Available: https://www.lechemindelanature.com/articles/a/lierre

[162] K. L. Larocque, "Blurred park boundaries and the spread of english ivy (hedera helix l.): case studies from greater victoria, british columbia," Ph.D. dissertation, 1999. [Online]. Available: http://hdl.handle.net/1828/2383

[163] D. Castagneri, M. Garbarino, and P. Nola, "Host preference and growth patterns of ivy (hedera helix l.) in a temperate alluvial forest," *Plant Ecology*, vol. 214, pp. 1–9, 11 2012.

[164] P. Nola, "Interactions between fagus sylvatica l. and hedera helix l.: a dendroecological approach," *Dendrochronologia*, vol. 15, pp. 23–37, 1997. [Online]. Available: https://hdl.handle.net/11571/571105

[165] Heijnen, "Lierre plantes - feuillage persistant — plantes heijnen," *Heijnen*. [Online]. Available: https://www.plantesdehaies-heijnen.fr/plantes-de-haie/lierre

[166] MeillandRichardier, "Lierre d'irlande ou hedera helix 'hibernica'," *MeillandRichardier*. [Online]. Available: https://www.meillandrichardier.com/lierre-d-irlande-hedera-hibernica.html#description

[167] P. Wiedemann and C. Neinhuis, "Biomechanics of isolated plant cuticles," *Botanica Acta*, vol. 111, pp. 28–34, 02 1998.

[168] S. Vogel, "Twist-to-bend ratios of woody structures," *Journal of Experimental Botany*, vol. 46, p. 981–985, 1995. [Online]. Available: https://www.jstor.org/stable/23694956

[169] T. Hattermann, L. Petit-Bagnard, C. Heinz, P. Heuret, and N. P. Rowe, "Mind the gap: Reach and mechanical diversity of searcher shoots in climbing plants," *Frontiers in Forests and Global Change*, vol. 5, 04 2022.

[170] C. Preisinger, "Karamba 3d manual," *Karamba3D*, 2013. [Online]. Available: https://manual.karamba3d.com/

[171] A. A. Helsinki, "Lookout tower." [Online]. Available: https://avan.to/works/lookout-tower/

[172] F. A. Navigator, "Helsinki zoo observation tower kupla ·," *finnisharchitecture.fi*. [Online]. Available: https://finnisharchitecture.fi/helsinki-zoo-observation-tower-kupla/

[173] travaux.eco, "Quelle est la durée de vie des maisons ? selon le matériau," 11 2023. [Online]. Available: https://travaux.eco/architecture-materiaux/quelle-est-la-duree-de-vie-des-maisons/

[174] S. C. Thomas and A. R. Martin, "Carbon content of tree tissues: A synthesis," *Forests*, vol. 3, p. 332–352, 06 2012. [Online]. Available: https://www.mdpi.com/1999-4907/3/2/332

[175] W. C. Portal, "Masse molaire co2(g)," *fr.webqc.org*. [Online]. Available: https://fr.webqc.org/molecular-weight-of-CO2%28g%29.html

[176] J. Moerman, "Combien de co2 émettons-nous en belgique ?" *écoconso - du conseil à l'action*, 01 2019. [Online]. Available: https://www.ecoconso.be/fr/content/combien-de-co2-emettons-nous-en-belgique

[177] T. E. of Encyclopedia Britannica, *Phloem — plant tissue*, 10 2016. [Online]. Available: https://www.britannica.com/science/phloem

[178] ck12info, "Curriculum materials license — ck-12 foundation," *www.ck12info.org*, 2021. [Online]. Available: https://www.ck12info.org/curriculum-materials-license/

[179] G. Buck-Sorlin, "Functional-structural plant modeling," *Encyclopedia of Systems Biology*, pp. 778–781, 2013.

[180] G. Louarn and Y. Song, "Two decades of functional–structural plant modelling: Now addressing fundamental questions in systems biology and predictive ecology," *Annals of Botany*, vol. 126, pp. 501–509, 07 2020.

[181] T. M. DeJong, D. Da Silva, J. Vos, and A. J. Escobar-Gutiérrez, "Using functional–structural plant models to study, understand and integrate plant development and ecophysiology," *Annals of Botany*, vol. 108, pp. 987–989, 10 2011.

[182] P. Prusinkiewicz, "Modeling plant growth and development," *Current Opinion in Plant Biology*, vol. 7, pp. 79–83, 02 2004.

[183] C. Godin and H. Sinoquet, "Functional-structural plant modelling," *New Phytologist*, vol. 166, pp. 705–708, 05 2005.

[184] H. Kramer and J. Oldengarm, "Urbtree: a tree growth model for the urban environment," *Carbon Balance and ManagementCarbon Balance Manage*, 01 2010.

[185] D. Nowak, D. Crane, J. Stevens, R. Hoehn, J. Walton, and J. Bond, "A ground-based method of assessing urban forest structure and ecosystem services," *Arboriculture Urban Forestry*, vol. 34, pp. 347–358, 11 2008.

[186] L. Peng, S. Chen, Y. Liu, and J. Wang, "Application of citygreen model in benefit assessment of nanjing urban green space in carbon fixation and runoff reduction," *Frontiers of Forestry in China*, vol. 3, pp. 177–182, 04 2008.

[187] S. Saunders, E. Dade, and V. Niel, "An urban forest effects (ufore) model study of the integrated effects of vegetation on local air pollution in the western suburbs of perth, wa," *19th International Congress on Modelling and Simulation*, 2011.

[188] T. Rötzer, M. Rahman, A. Moser-Reischl, S. Pauleit, and H. Pretzsch, "Process based simulation of tree growth and ecosystem services of urban trees under present and future climate conditions," *Science of The Total Environment*, vol. 676, pp. 651–664, 08 2019.

[189] R. Karwowski and P. Prusinkiewicz, "The lsystembased plantmodeling environment lstudio 4.0," *Presented at 4th International Workshop on Functional and Structural Plant Models*, 12 2008.

[190] R. Hemmerling, O. Kniemeyer, D. Lanwert, W. Kurth, and G. Buck-Sorlin, "The rule-based language xl and the modelling environment groimp illustrated with simulated tree competition," *Functional Plant Biology*, vol. 35, pp. 739–739, 12 2008.

[191] C. Fournier, C. Pradal, G. Louarn, D. Combes, J. Soulié, D. Luquet, F. Boudon, and M. Chelle, "Building modular fspm under openalea: concepts and applications," *Proc. of the 6th International Workshop on FunctionalStructural Plant Models*, 09 2010.

[192] F. Boudon, C. Pradal, T. Cokelaer, P. Prusinkiewicz, and C. Godin, "L-py: an l-system simulation framework for modeling plant architecture development based on a dynamic language," *Frontiers in Plant Science*, vol. 3, 2012.

[193] P. Prusinkiewicz and A. Lindenmayer, *The Algorithmic Beauty of Plants*. Springer-Verlag, 1996.

[194] *Graphical Applications of L-Systems*. Canadian Man-Computer Communications Society, 1986. [Online]. Available: http://graphicsinterface.org/wp-content/uploads/gi1986-44.pdf

[195] O. Kniemeyer, G. Buck-Sorlin, and W. Kurth, "Groimp as a platform for functional-structural modelling of plants," *Functional-Structural Plant Modelling in Crop Production*, pp. 43–52, 2007.

[196] M. Armstrong, *Basic Topology*. Springer Science Business Media, 04 2013.

[197] R. Jain, R. Kasturi, and B. Schunck, *Machine Vision*, 01 1995, vol. 5.

[198] Y. Zhou, A. Kaufman, and A. W. Toga, "Three-dimensional skeleton and centerline generation based on an approximate minimum distance field," *The Visual Computer*, vol. 14, pp. 303–314, 12 1998.

[199] M. Tănase and R. C. Veltkamp, "A straight skeleton approximating the medial axis," *Lecture Notes in Computer Science*, pp. 809–821, 01 2004.

[200] *Mathematical Morphological Analysis of Typical Cyclone Eyes on Ocean SAR.* IEEE Geoscience and Remote Sensing Symposium, 2014.

[201] M. Disney, "Terrestrial lidar: a three-dimensional revolution in how we look at trees," *The New Phytologist*, vol. 222, p. 1736–1741, 2019. [Online]. Available: https://www.jstor.org/stable/26675927

[202] A. Lau, L. P. Bentley, C. Martius, A. Shenkin, H. Bartholomeus, P. Raumonen, Y. Malhi, T. Jackson, and M. Herold, "Quantifying branch architecture of tropical trees using terrestrial lidar and 3d modelling," *Trees*, vol. 32, pp. 1219–1231, 05 2018.

[203] P. Raumonen, E. Casella, K. Calders, S. Murphy, M. Åkerblom, and M. Kaasalainen, "Massive-scale tree modelling from tls data," *ISPRS Annals of the Photogrammetry, Remote Sensing and Spatial Information Sciences*, vol. II-3/W4, pp. 189–196, 03 2015.

[204] M. Maimaitijiang, V. Sagan, H. Erkbol, J. Adrian, M. Newcomb, D. LeBauer, D. Pauli, N. Shakoor, and T. C. Mockler, "Uav-based sorghum growth monitoring: A comparative analysis of lidar and photogrammetry," *ISPRS Annals of Photogrammetry, Remote Sensing and Spatial Information Sciences*, vol. V-3-2020, pp. 489–496, 08 2020.

[205] J. Hruska, J. Cermak, and S. Sustek, "Mapping tree root systems with ground-penetrating radar," *Tree Physiology*, vol. 19, pp. 125–130, 02 1999.

[206] A. Piovesan, V. Vancauwenberghe, T. Van, P. Verboven, and B. Nicolai, "X-ray computed tomography for 3d plant imaging," *Trends in Plant Science*, vol. 26, pp. 1171–1185, 11 2021.

[207] P. Raumonen, M. Kaasalainen, M. Åkerblom, S. Kaasalainen, H. Kaartinen, M. Vastaranta, M. Holopainen, M. Disney, and P. Lewis, "Fast automatic precision tree models from terrestrial laser scanner data," *Remote Sensing*, vol. 5, pp. 491–520, 01 2013.

[208] S. Delagrange, C. Jauvin, and P. Rochon, "Pypetree: a tool for reconstructing tree perennial tissues from point clouds," *Sensors*, vol. 14, pp. 4271–4289, 03 2014.

[209] Markku, P. Raumonen, M. Kaasalainen, and E. Casella, "Analysis of geometric primitives in quantitative structure models of tree stems," *Remote Sensing*, vol. 7, pp. 4581–4603, 04 2015.

[210] S. Du, R. Lindenbergh, H. Ledoux, J. Stoter, and L. Nan, "Adtree: Accurate, detailed, and automatic modelling of laser-scanned trees," *Remote Sensing*, vol. 11, p. 2074, 01 2019. [Online]. Available: https://www.mdpi.com/2072-4292/11/18/2074#

[211] J. Zhu, A. K. Leung, and Y. Wang, "Modelling root–soil mechanical interaction considering root pull-out and breakage failure modes," *Plant and Soil*, vol. 480, pp. 675–701, 07 2022.

[212] C. Saint Cast, C. Meredieu, P. Défossez, L. Pagès, and F. Danjon, "Modelling root system development for anchorage of forest trees up to the mature stage, including acclimation to soil constraints: the case of pinus pinaster," *Plant and Soil*, vol. 439, pp. 405–430, 03 2019.

[213] T. Fourcaud, J. Ji, Z. Zhang, and A. Stokes, "Understanding the impact of root morphology on overturning mechanisms: a modelling approach," *Annals of Botany*, vol. 101, pp. 1267–1280, 08 2007.

[214] J. Pokorny, j. obrien, R. Hauer, G. Johnson, j. albers, p. bedker, and m. mielke, *Urban Tree Risk Management: A Community Guide to Program Design and Implementation*, 09 2003.

[215] H. Rahardjo, F. R. Harnas, I. Indrawan, E. Choon Leong, P. Tan, Y. L. Fong, and L. Fern Ow, "Understanding the stability of samanea saman trees through tree pulling, analytical calculations and numerical models," *Urban for Urban Green*, vol. 13, pp. 355–364, 01 2014.

[216] A. Stokes, "An experimental investigation of the resistance of model root systems to uprooting," *Plant Soil*, vol. 78, pp. 415–421, 10 1996.

[217] X. Ji, L. Chen, and A. Zhang, "Anchorage properties at the interface between soil and roots with branches," *Journal of Forestry Research*, vol. 28, pp. 83–93, 2017. [Online]. Available: https://doi.org/10.1007/s1167601602942

[218] F. Giadrossich, M. Schwarz, D. Cohen, F. Preti, and D. Or, "Mechanical interactions between neighbouring roots during pullout tests," *Plant and Soil*, vol. 367, pp. 391–406, 2013. [Online]. Available: https://doi.org/10.1007/s1110401214751

[219] B. Docker and T. Hubble, "Quantifying root-reinforcement of river bank soils by four australian tree species," *Geomorphology*, vol. 100, pp. 401–418, 08 2008.

[220] G. J. Meijer, D. Muir Wood, J. Knappett, A. Glyn Bengough, and T. Liang, "Analysis of coupled axial and lateral deformation of roots in soil," *International Journal for Numerical and Analytical Methods in Geomechanics*, vol. 43, pp. 684–707, 12 2018.

[221] M. Schwarz, D. Cohen, and D. Or, "Root-soil mechanical interactions during pullout and failure of root bundles," *Journal of Geophysical Research*, vol. 115, 12 2010.

[222] I. Lapczyk and J. A. Hurtado, "Progressive damage modeling in fiber-reinforced materials," *Composites Part A: Applied Science and Manufacturing*, vol. 38, pp. 2333–2341, 11 2007.

[223] T. Liang, J. A. Knappett, and N. Duckett, "Modelling the seismic performance of rooted slopes from individual root–soil interaction to global slope behaviour," *Géotechnique*, vol. 65, pp. 995–1009, 12 2015.

[224] A. Schnepf, D. Leitner, M. Landl, G. Lobet, T. Hieu Mai, S. Morandage, C. Sheng, M. Zörner, J. Vanderborght, and H. Vereecken, "Crootbox: a structural–functional modelling framework for root systems," *Annals of Botany*, vol. 121, pp. 1033–1053, 04 2018.

[225] D. Leitner, S. Klepsch, G. Bodner, and A. Schnepf, "A dynamic root system growth model based on lsystems," *Plant and Soil*, vol. 332, pp. 177–192, 2010. [Online]. Available: https://doi.org/10.1007/s1110401002847

ECOLE
POLYTECHNIQUE
DE BRUXELLES

DOCUMENT TO BE INCLUDED IN THE MASTER THESIS

CONSULTATION OF THE MASTER THESIS

I, the undersigned

NAME ~~Pierre~~ GUILLEMOT

FIRST NAME PIERRE-MARIE, BERNARD

MASTER PROGRAM ARCHITECTURAL ENGINEERING

MASTER THESIS TITLE COMPUTATIONAL STUDY OF THE FEASIBILITY OF BAUBOTANICAL STRUCTURES

AUTHORIZE*

~~**REFUSE***~~

(IN CASE OF REFUSAL, THIS DOCUMENT MUST BE COUNTERSIGNED BY THE MASTER THESIS SUPERVISOR)

(Delete as appropriate)*

Consultation of this master thesis by users of the libraries of the Université libre de Bruxelles.

If consultation is authorised, the undersigned hereby grants the Université libre de Bruxelles a free and non-exclusive licence, for the duration of the legal term of protection of the work, to reproduce and communicate to the public the above-mentioned work, on graphic or electronic media, in order to enable users of the libraries of the ULB and other institutions to consult it within the framework of inter-library loan.

Brussels, 24/05/2024

Signature of the student

Signature of the supervisor
(only if consultation is refused)